Transcriptional Analysis of CCR5 upon Cytokine Stimulation of Prostate Cancer Cells

Ameera Sabrina Amran

MSc (by Research)

University of York

Biology

28th November 2024

Abstract

C-C Chemokine Receptor type 5 (CCR5) is a G-Coupled Protein Receptor, and bound to its main ligand CCL5, the CCR5/CCL5 axis is known to mediate immune responses. The CCL5/CCR5 axis has been found to be associated in multiple diseases including Prostate Cancer (PCa), where it has been postulated to be a target for cancer therapy. Despite published findings that CCR5 antagonist interfere with PCa cells, the transcriptional mechanisms underlying the CCL5/CCR5 axis in PCa are ill defined, especially regarding the genetic and transcriptional regulation of the receptor.

The work presented in this thesis focuses on the transcriptional regulation of CCR5 in PCa cell lines, LNCaP and PC3. I investigated whether a long-term cytokine stimulation using CCL5 and/or IL-6 would induce autocrine loops to their respective receptors, activating a cascade of signalling pathways, and whether these cytokines act in synergy at a transcriptional level. My results indicate that, although there is lack of evidence for direct CCL5/CCR5 engagement, long term IL-6 stimulation induced upregulation of STAT3 for LNCaP at the mRNA and protein level, with no differences upon dual IL-6 and CCL5 stimulation. Dual cytokine stimulation increased EIF4EBP1 transcriptional expression in PC3. I also show that long term CCL5 stimulation of LNCaP cells induced transcriptional expression of the CCR5-specific chemokine CCL4 compatible with the idea of a receptor-ligand feedback loop. These findings confirm that although LNCaP and PC3 are models of metastatic PCa, they are vastly different phenotypically and genetically.

Further work using cancer cells originating from the tumour microenvironment would be required to confirm my observations and enhance our current understanding of chemokine receptors in cancer biology.

Declaration

I declare that this thesis is a presentation of original work, and I am the sole author. This work has not previously been presented for an award at this, or any other, University. All sources are acknowledged as references.

Table of Contents

List of Figures

List of Tables

Acknowledgements

Dr. Nathalie Signoret (supervisor) I would like to give huge thanks to Nathalie for taking me under her wing for this project: for her perseverance, her unwavering support, and her expansive scientific prowess. From desperate emails on a weekend morning, to pep talks when I was at a low, I am truly honoured to have worked alongside you, within such a welcoming and supportive lab environment. I could not have evolved so much this year without you!

Afzaal Tufail Your ability to seamlessly absorb, apply and communicate science is awe-inspiring. Massive thank you to Afzaal for passing on his invaluable knowledge about almost every new lab technique I've learnt during my Master's! I cannot thank you enough for running a handful of my Western Blot samples for me as well. You brought rays of sunshine to Q2, not just to me, but for everyone lucky enough to be sat near you!

Prof. Dimitris Lagos (TAP Member) Thank you to Dimitris for his guidance and scrutiny during my TAP meetings. I greatly appreciate all the feedback you have provided me, as it has pushed me to not only improve the quality of my work, but to think more like a scientist of high standard. I hope this piece of work reflects my responses to your feedback aptly.

Esme Hutton I would like to thank Esme for their steadfast support, providing me with fastidious advice on tissue culture and flow cytometry. Massive thank you as well for setting up the GEO analysis, which I have quoted in this thesis. Your relentless passion in the work you do is an inspiration to me.

Dr. Dave Boucher I give thanks to Dave for providing me with primary cells isolated from patients, which I have used in this project. I appreciate and will fondly remember your kind reassurances while working late in Tissue Culture.

Chloe Legge Shout out to Chloe for being an absolute gem in Q block. Thank you for spreading your contagious cheerfulness, for all the fun chats and laughs. Your persistent support eased the weight of the master's off my shoulders!

Callum Robson Callum, as the acting lab technician of the Boucher lab, has always been happy to help anyone in need with his endless technical expertise. Thank you for your aid in troubleshooting my assays. Working with you has been a privilege.

Dr. Sally James, Dr. Lesley Gilbert and Samantha Donninger from the Genomic Lab at the Technology Facility. As qPCR was a major focus in this project, I thank you for your patience and attentiveness with my constant flurry of questions on everything there is to know about this technique! My knowledge and understanding about qPCR have improved immensely thanks to Sally and her team.

Nikki Savvas and Deborah Malley from Teaching Block. Thank you for cooperating with me around the use of the qPCR machine and for your helpful advice with primer validation.

Dr. Alastair Droop Thanks to Alastair for coaching me on R to help better analyse my qPCR data. I've never met a more enthusiastic data scientist!

Dr. James Fox Thank you for acting as a great starting point in this project; designing a handful of the primers I have used and leaving a fully comprehensible lab book I could pick up and work from.

1. Introduction

1.1. CCR5: An overview

The C-C Chemokine Receptor type 5 (CCR5) is known to encompass many functions in the human body mainly through immune responses and has been found to be associated in multiple diseases including prostate cancer (PCa). Recent research has shifted from its mechanistic response upon ligand binding, to the effect of its genetic and transcriptional regulation within the nucleus.

1.1.1. Structure and activation of CCR5

CCR5 is a G-protein Coupled Receptor (GPCR) and part of the most common family of cell membrane receptors in eukaryotes, transmitting signals from the external cellular environment. GPCRs are made of a single polypeptide chain, which folds and spans the phospholipid bilayer membrane 7 times (Alberts *et al*., 2022). CCR5 contains 7 transmembrane α helices, connected to each other by 3 extracellular loops as well as 4 intracellular loops. The fourth intracellular loop is created due to acylation, securing the carboxyl tail to the plasma membrane (Oppermann, 2004). The amino acid organisation of CCR5 is summarised in **Figure 1**.

GPCRs are coupled to heterotrimeric GTP-binding proteins (G-proteins), consisting of an alpha (G_α), beta (G_β) and gamma (G_γ) subunit. During ligand binding of CCR5, an interaction between the core structure, N-terminal tail, and the second extracellular loop of CCR5. The second extracellular loop determines ligand specificity (Samson *et al*., 1997). Conformational changes are induced, where rapid phosphorylation of the CCR5 cytoplasmic tail on specific residues by a G-protein receptor kinase causes the G-protein to dissociate into G_α and G_β/G_γ, each subunit activating their own signalling pathways. Thus, a cascade of intracellular events ensues. The phosphorylated CCR5 then interacts with β-arrestin, which acts as a scaffold to target receptors for internalisation (Bennett, Fox and Signoret, 2011).

cAMP (cyclic adenosine monophosphate) is an essential second messenger for signalling pathways, facilitating the cascade of intracellular events. Another way GPCRs can be activated is by cross activation via cyclic AMPs (cAMPs). Through the effects of other GPCRs, there can be an increase or decrease of cAMP levels, which can further activate new GPCRs. An increase of cAMP concentration will activate GPCRs associated with G stimulatory protein (G_s), while a decrease of cAMP concentration will activate GPCRs with G inhibitory protein (G_i) (Alberts *et al*., 2022). CCR5 is predominantly associated with G_i (Zhao *et al*., 1998).

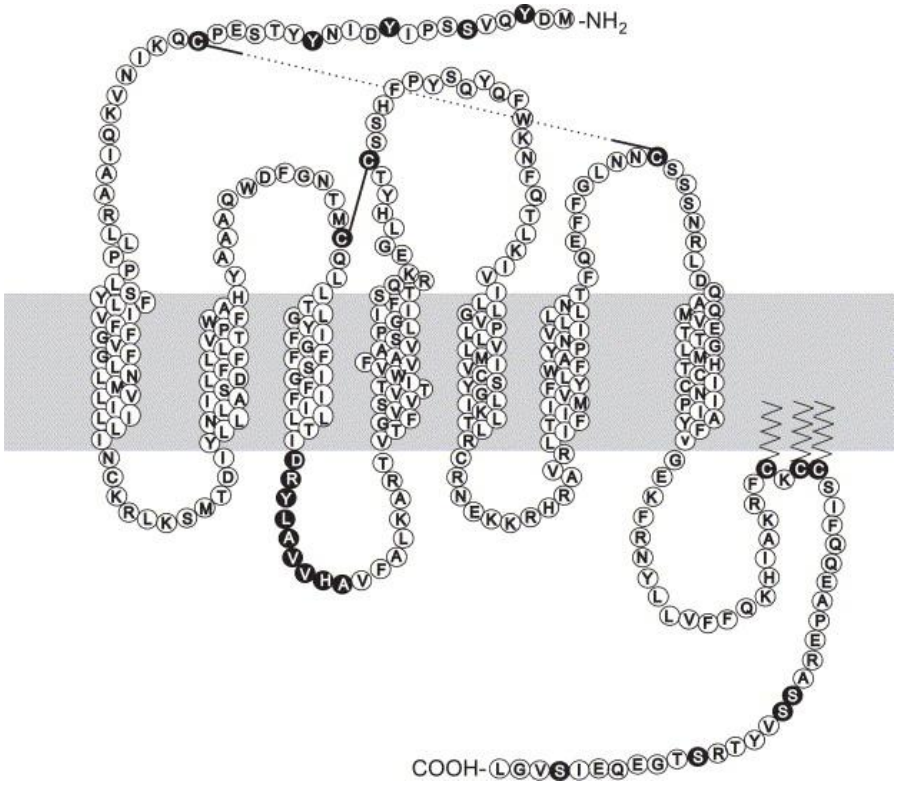

Figure 1: Human CCR5 amino acid organisation sourced from Oppermann, 2004. The amino acids filled in black have been shown to be important in CCR5 functionality. The grey box represents the approximate location of the lipid bilayer membrane. Above the grey box is the extracellular region, and below the grey box is the intracellular region. The three zig-zag lines represent acylation of the carboxyl tail. The lines in between C residues represent disulphide bridges.

1.1.2. CCR5 and agonistic ligands in immunity

Chemokine receptors such as CCR5 typically bind to chemotactic cytokines or chemokines, which are small, secreted proteins (8-12kDa) (Zlotnik and Yoshie, 2000, Kufareva, 2016). This interaction is mainly known to trigger chemokine-mediated cell-directed migration towards an increasing concentration gradient of chemokines, a process called chemotaxis. There are four subfamilies of chemokines, known as CXC, CC, XC and CX3C, which are classified based on the arrangement of their cysteine residues closest to the N-terminus. CC, CXC and CX3C chemokines contain either no amino acid, a single amino acid or three amino acids between their first two cysteine residues respectively. XC chemokines lack a second cysteine residue (Kufareva, 2016). Chemokines exert their function by binding both specifically and promiscuously to chemokine receptors. For example, CCR5 interacts with multiple CC chemokines: CCL3, CCL4, CCL5, and CCL8 (Zlotnik and Yoshie, 2000). CCR5 is basally expressed by immune cells, including T cells, macrophages, dendritic cells, eosinophils and microglia. The main effect of CCR5 stimulation on immune cells is chemotaxis (Aldinucci, Borghese and Casagrande, 2020).

1.2. CCR5 in cancer

Although CCR5 has been well documented in immune cells, it has also been found to be expressed endogenously by many cancer cell lines, including prostate (Vaday *et al*., 2006), colorectal (Liu *et al*., 2020) and breast cancer (Velasco-Velázquez *et al*., 2012). CCR5 has been reported to contribute to several ‘hallmarks of cancer’, including but not limited to promoting metastasis (Urata *et al*., 2018), immune cell escape (Xiong *et al*., 2024), immune suppression (Hawila *et al*., 2017) and cell proliferation (Vaday *et al*., 2006). Therefore, due to its contribution to tumourigenesis, CCR5 is considered a potential target for cancer therapy.

The literature has looked at blocking the tumourigenic effects of CCL5 stimulation in cancer cells with the CCR5 specific antagonist Maraviroc, which is a small molecule developed for the prevention of HIV-1 infection, as CCR5 plays a principal role as viral co-receptor. Maraviroc interferes with the binding of CCR5 to HIV-1, by specifically and competitively binding to CCR5, a process known as antagonism (Qi

et al., 2020). Cancer studies using Maraviroc failed to demonstrate CCR5 receptor function unambiguously (Vaday *et al*., 2006; Velasco-Velázquez *et al*., 2012). In a mouse study, Maraviroc was able to block CCR5 signalling via CCL5/CCR5 axis, preventing the homing of cancer cells to develop metastasis in the bone of mice, in v-Src oncogene-transformed metastatic PCa (Sicoli *et al*., 2014). However, it has been established that Maraviroc binds human but not murine CCR5, deeming mouse studies on Maraviroc untranslatable to humans (Ochoa-Callejero *et al*., 2013).

1.3. Prostate Cancer Overview

Prostate Cancer (PCa) is the second most common type of carcinoma diagnosed in males; about 1 in 6 UK males born in 1961 are estimated to be diagnosed with PCa in their lifetimes (Sung *et al*., 2021, Cancer Research UK, 2023). PCa is a heterogenous disease whereby most cases are indolent, meaning slow-growing and localised, and consequently 5% of PCa cases develop into metastatic PCa (mPCa) (Helgstrand *et al*., 2018). When detected early, PCa can be successfully treated with surgery or radiation therapy (Sakellakis, Jacqueline Flores and Ramachandran, 2022). PCa development begins at a localised level, as low-grade prostatic intraepithelial neoplasia (PINs), which is characterised by hyperplasia of the luminal epithelial cells of the prostate. PINs then transition into aggressive adenocarcinoma.

1.3.1. Challenges in the treatment of mPCa

Normal and early-stage carcinogenic prostate tissue relies on androgen receptor (AR) signalling for growth, development and maintenance (Massie *et al*., 2011). Androgens such as testosterone are primarily produced by the testis. Removal of the testis by castration is one method of reducing AR signalling, known as Androgen Deprivation Therapy (ADT), which practitioners use to treat PCa. If castration fails to subdue the carcinoma, PCa transitions to castration resistant prostate cancer (CRPC), which finally advances to mPCa (Shen and Abate-Shen, 2010). ADT is generally effective in prolonging the overall survival of PCa patients, but is not considered a cure, with 5-10% of patients surviving within 10 years of treatment (Tangen *et al*., 2003). Although androgen is depleted upon castration, AR signalling is maintained independent of androgen ligand as a result of genetic mutations, cross

talk of signalling pathways, and AR gene amplification in mPCa, switching from a paracrine-dependent to an autocrine-dependent mechanism for AR signalling (Massie *et al*., 2011, Gao, Arnold and Isaacs, 2001).

Additionally, mPCa is known for giving rise to 'cold tumours' due to their immunosuppressive tumour microenvironments (TME). Several factors which influence the immunosuppressive TME including the presence of regulatory T cells, M2-like Tumour Associated Macrophages (TAMs) and myeloid-derived suppressor cells (MDSCs), which all act to secrete molecules which mediate immunosuppression, such as IL-8, vascular endothelial growth factor (VEGF) and IL-23 (Stultz and Fong, 2021).

AR independence and immunosuppressive TME are some of the factors which make mPCa particularly challenging to treat, and therefore identifying a target for treatment is in high demand. Publications have reported CCL5/CCR5 as a potential target for treatment of mPCa (Culig *et al*., 2005).

1.4. Molecular mechanisms underpinning CCR5 activity

All established molecular mechanisms underpinning chemokine-mediated CCR5 activation have been investigated in transfected cells and primary immune cells such as T cells and monocytes/macrophages (Mack *et al*., 1998; Signoret *et al*., 2000, 2005; Bennett, Fox and Signoret, 2011; Fox *et al*., 2015). However, these same mechanisms have been difficult to validate for cancer cells, which do not behave the same way as in transfected and immune cells, possibly due to low expression of CCR5.

1.4.1. Evidence of CCR5 and its activity in PCa

1.4.1.1. Published literature

Several publications claim that the CCL5/CCR5 axis plays a tumorigenic role in PCa. As reported in Vaday *et al*. 2006, CCL5 stimulation of PCa cell lines induced proliferation and invasion, which was blocked by the CCR5 antagonist TAK-779, implicating ligand specificity. The group also reported varied CCL5 mRNA and protein

expression, as well as cell surface and intracellular CCR5 found for all PCa cell lines. Huang *et al*. found that CCL5 secreted by Tumour Associated Macrophages (TAMs) stimulated PCa cell proliferation via CCR5 (Huang *et al*., 2020). Markers for epithelial-mesenchymal transition (EMT), a contributor to tumour progression, were found upon CCL5 stimulation. This was reversed through treatment with CCL5 siRNA, which acts to silence CCL5 mRNA and gene expression (Huang *et al*., 2020). Zhao *et al*. found that the CCL5/CCR5 axis may induce autophagy by decreasing AR expression in CRPC, further aggravating the condition. This group also confirmed an increase of secretory CCL5 in media and CCL5 mRNA (Zhao *et al*., 2018). These publications imply a possible CCL5/CCR5 autocrine/paracrine loop, which propagates PCa progression.

1.4.1.2. Findings from the lab

Unpublished findings from the Signoret lab do not show much in common with the published literature as mentioned. CCR5 was found barely detectable on LNCaP (Lymph Node Carcinoma of the Prostate) and PC3 cells with very low cell surface levels by flow cytometry and ELISA on total cell lysates (A. Tufail ongoing PhD). Additionally, detection of CCR5 protein via Western Blotting failed to confirm its expression. As for cell proliferation, our lab observed a small but transient increase in the rate of cell proliferation upon CCL5 stimulation after 24 hours (A. Tufail ongoing PhD). PCa cell lines also co-express other CC chemokine receptors such as CCR1 and CCR2 (Lu *et al*., 2007; Kato *et al*., 2013). These receptors are capable of interacting with CCR5 ligands and are involved in cancer (Shin *et al*., 2017; Xu *et al*. 2021), thus this could account for effects described in published works.

Nevertheless, the work from the Signoret lab indicates that CCR5 is not inert on these cells, since we have evidence for CCR5 binding site occupancy as well as initiation of weak and transient CCR5, MAPK and CREB-1 phosphorylation events upon CCL5 stimulation, which result in the secretion of inflammatory chemokines within 24h (A. Tufail ongoing PhD). These findings raise the question as to how CCR5/CCL5 activation mechanistically responds in PCa cells, which I will investigate in this project. A summary of what has been found in the literature compared to what has been found in the lab in **Table 1:1**.

Table 1: Summary of findings on the CCR5/CCL5 axis. PCa cell type, publication claims, dose of stimulation used by said publication, references, and findings in the Signoret lab are listed.

PCa Cell Line	Publication claim	Dose of stimulation	Reference to publication	Signoret Lab findings
LNCaP and PC3	CCL5 binding to CCR5	100 ng/ml CCL5		Unpublished
LNCaP	CCL5 induced CCR5 phosphorylation	100 ng/ml CCL5		Unpublished
LNCaP	CCL5/CCR5 induces ERK phosphorylation	100 ng/ml CCL5		Unpublished
DU-145, LNCaP and PC3	CCL5 secretion detected by ELISA	N/A	(Vaday *et al*., 2006)	Confirmed
DU-145, LNCaP and PC3	CCR5 on cell surface by FC	N/A	(Vaday *et al*., 2006)	Low levels for LNCaP and PC3
DU-145 and PC3	CCR5 protein detected by WB	40 ng/ml CCL5	(Huang *et al*., 2020)	Not detectable for LNCaP and PC3
PC3 and LNCaP	CCR5/CCL5 axis promotes invasion	10-100 ng/ml CCL5	(Vaday *et al*., 2006)	N/A
DU-145 and PC3	CCR5/CCL5 axis promotes metastasis	5-40 ng/ml CCL5	(Huang *et al*., 2020)	N/A
DU-145 and PC3	CCR5 promotes migration	20-40 ng/ml CCL5	(Huang *et al*., 2020)	N/A
DU-145 and LNCaP	CCR5/CCL5 axis stimulates proliferation	10-100 ng/ml CCL5	(Vaday *et al*., 2006)	Small increase in LNCaP

NS - No significant ; N/A – Not applicable ; WB – Western Blot ; FC – Flow Cytometry ; ELISA – Enzyme Linked Immunosorbent Assay

1.4.2. CCR5 and transcriptional regulation

1.4.2.1. CCR5 transcripts

The transcriptional regulation of CCR5 is not often considered, since the main mechanism to control the functional activity of this receptor involves the process of desensitisation (Bennett, Fox and Signoret, 2011).

The CCR5 gene is located on Chromosome 3, part of a chemokine locus nearby CCR1 and CCR2, specifically on 3p21.3-p24 (Ensembl, no date). When CCR5 is transcribed, RNA Polymerase II converts it from DNA to pre-mRNA. When this occurs, introns are spliced out by spliceosomes, which are made from small nuclear RNA (snRNA) and small nuclear Ribonucleoproteins (snRNPs). What remains are exons as well as Untranslated Regions (UTRs), which form a mature mRNA. The mature mRNA is then translated by ribosomes into polypeptide chains. Introns are classically 'non-coding' parts of the sequence, which do not code for amino acids. Exons are 'coding' parts of the sequence which code for amino acids. UTRs aid in mature mRNA localisation (Alberts *et al*., 2022).

CCR5 has multiple transcripts or isoforms of different lengths, two types of which are defined as 'truncated' and 'full length' as described in Mummidi *et al*.,1997. The group described two 'full length' transcripts for CCR5 and several truncated transcripts, arising differentially due to alternative splicing patterns and multiple transcription start sites. The 'full length' isoforms are thought to be responsible for the expression of the CCR5 protein and are named CCR5A and CCR5B. 'Truncated' isoforms are shorter than 'full length' isoforms, and contain exon 2A, 2B and 3. These isoforms are truncated at the Exon 2A and 2B region, while Exon 3 along with the entire ORF are unchanged. They are thought to be involved in CCR5 transcriptional regulation. CCR5A and CCR5B contain Exon 1, 2B and 3, differing in the presence (CCR5A) or absence (CCR5B) of Exon 2A. These transcripts encode the same amino acid sequence, which leads to the CCR5 protein - summarised in **Figure 2**.

Later in 2007, Mummidi *et al*. found that full length transcripts, which contained exon 1 (including CCR5A and CCR5B) were associated with increased cell surface

presence of CCR5 in activated T cells, whereas the truncated transcripts did not lead to cell surface expression (Mummidi *et al*., 2007). Other than the studies mentioned, CCR5 transcription has barely been investigated beyond immune or transfected cells; one aim to further address in this project.

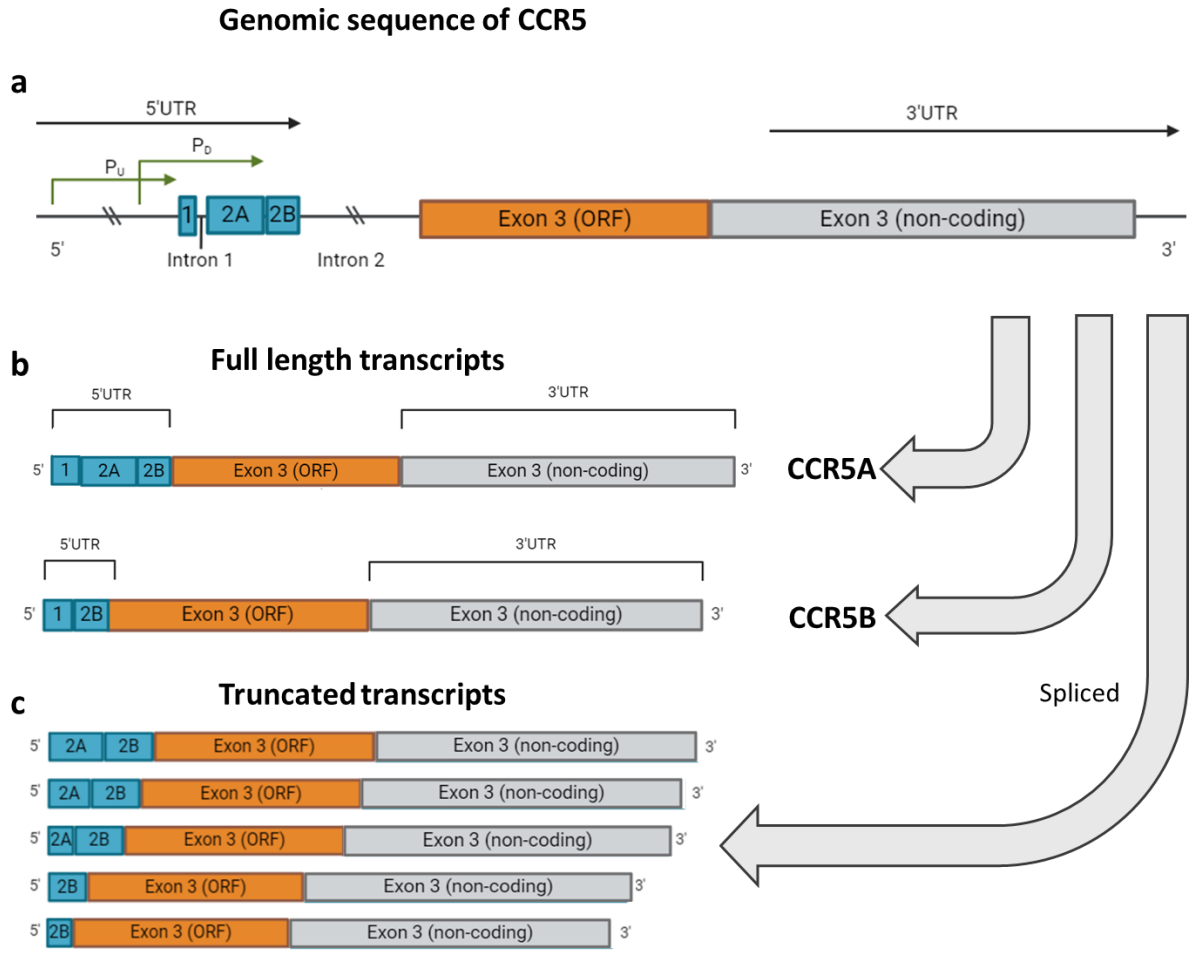

Figure 2: Genomic sequence, full length and truncated transcript isoforms of human CCR5, adapted from Mummidi *et al*., 1997: Genomic sequence (**a**) of human CCR5. Green arrows mark regions corresponding to P_U and P_D. Boxes with numbers represent exons with exon numbers. Lines connecting boxes show introns. Slashes show gaps in the sequences. (**b**): The two full length transcripts are labelled CCR5A and CCR5B respectively. Boxes show the spliced exons and correspond with the gene map (**a**). Truncated transcripts of CCR5 (**c**).

1.4.2.2. **CCR5AS**

Non-coding RNA (ncRNA), which was an area of unknown until recently, adds another layer of complexity on the gene regulation of CCR5. ncRNAs arise from spliced intron sequences and do not code for protein. Researchers have identified many types of ncRNA with varying roles – one type is long non-coding RNA (lncRNAs). In the form of antisense RNA, lncRNA can act like guide sequences, where they can form complementary base pairs with mRNA, thus blocking protein translation. Antisense RNA can be formed from protein-coding genes but are transcribed in an antiparallel direction. (Alberts *et al*., 2022).

Kulkarni *et al* found that a CCR5 antisense RNA (CCR5AS) could control the expression of CCR5 by interfering with the RNA-binding protein Raly, which binds to the 3' UTR of CCR5 transcript triggering its degradation (Kulkarni *et al*., 2019). This way, CCR5AS prevents CCR5 mRNA turnover and favours CCR5 protein expression. In this project, I aim to detect the presence of CCR5AS and investigate whether it influences CCR5 expression in PCa cells. **Figure 4** summarises the pathway mentioned.

1.4.2.3. **CCR5 associated downstream signalling proteins**

Activation of CCR5 can lead to downstream effects including changes in the transcription of mRNA, leading to changes in protein expression, and therefore cellular responses. Overactivation of CCR5 in PCa, as implicated in studies mentioned (Vaday *et al*., 2006, Huang *et al*. 2020) could lead to dysregulation of transcription of proteins. Recent studies indicate that dysregulated transcription of proteins implicated in cell metabolism and signalling drive various cancers (Kant *et al*., 2022). Targeting signalling proteins downstream of CCR5 may therefore offer a potential therapeutic strategy for PCa.

Some examples of signalling proteins associated with CCR5 are as follows. The CREB pathway, activated by secondary messenger cAMP (see **Section 1.1.1**) has been found to regulate CCR5 expression in activated T cells (Kuipers *et al*., 2008). Additionally, Garcia *et al.* observed activated CREB in PCa cells, which, when inhibited, induced apoptosis (Garcia *et al*. 2006). NF-κB has been found to be activated in response to increased CCL5 and IL-6 production, leading to CCR5 binding which stimulated cell proliferation via the STAT5-Cyclin D1 pathway (Colombatti *et al*., 2009). Huang *et al.* differentially analysed mRNA expression for metastatic and stemness-related genes in PCa stem cells, finding that STAT3 had the greatest increase in gene response to CCL5 stimulation. β-catenin was also found to associate closely with metastatic and stemness related genes, as well as other genes involved in the STAT3 pathway. Consequently, Huang *et al*. found that CCL5 acts upon CCR5 via the β-catenin/STAT3 pathway, and this effect was abrogated using CCR5 siRNA. The same study also observed lower E-cadherin – a known tumour suppressor (Na *et al*., 2020) - upon CCL5 stimulation (Huang *et al*., 2020). Thus, these findings confirmed CCR5 specificity to signal transduce tumour associated genes.

Murooka *et al.* observed that the CCL5/CCR5 axis promotes proliferation in breast cancer cells via the mTOR pathway (Murooka, Rahbar and Fish, 2009). On the other hand, Pencik *et al.* found that human PCa mice models with upregulated STAT3 led to the upregulation of its associated target proteins LKB1/AMPK, which act to inhibit the mTOR pathway. This leads to the inhibition of CREB-1, resulting in no transcription of oncogenes (Pencik *et al*., 2023). This finding is in contradiction to Huang and

Murooka *et al.* who found that the activation of STAT3 and mTOR respectively is pro-tumorigenic. A summary of these signalling protein interactions can be found in **Figure 3**.

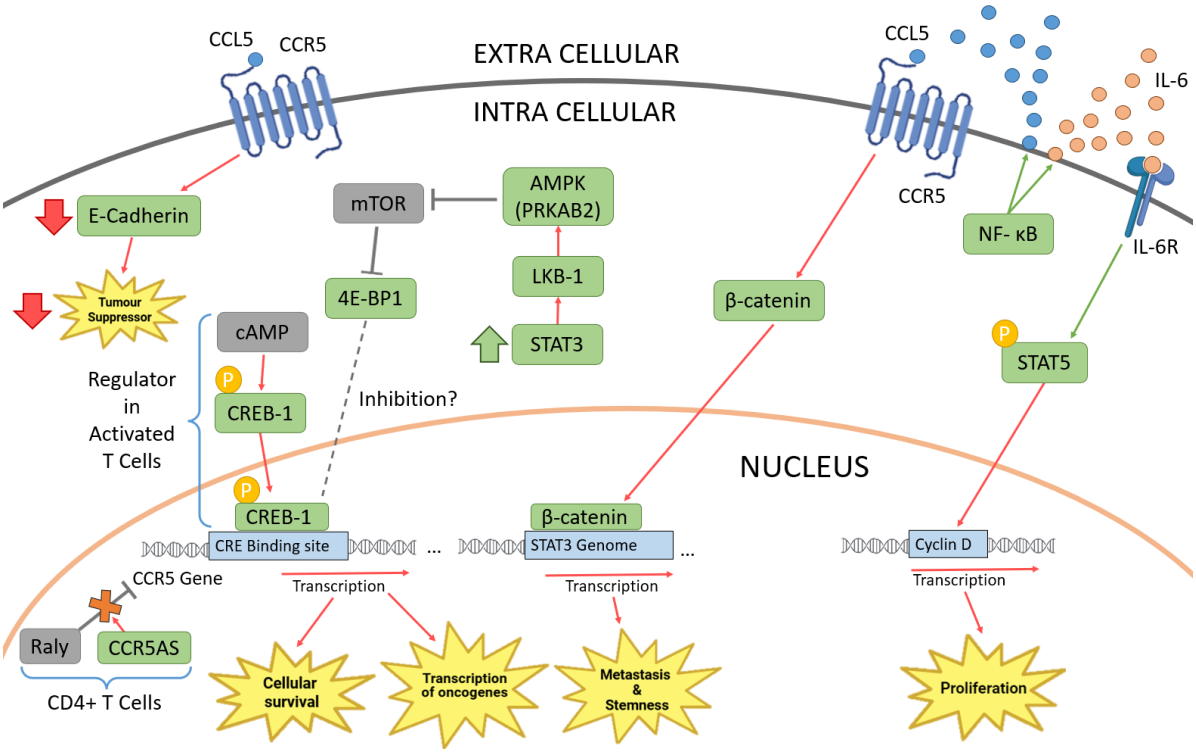

Figure 3: Schematic diagram summarising CCL5/CCR5 signalling pathways in human PCa cells and CD4+ T cells. Blue brace highlights the CCR5AS interaction found in CD4+ T cells. In green boxes are the signalling proteins to be measured at transcriptional level in the project. Red arrows indicate known activation between signalling pathways. In yellow shapes are the proposed cellular effects. The dashed lines highlight contradicting effects between signalling pathways (i.e. Garcia *et al.* 2006 and Pencik *et al.* 2023). PRKAB2 and 4E-BP1 is a subunit of AMPK and mTOR respectively.

1.5. Potential long-term effects of CCR5 stimulation in PCa

A milieu of cytokines and chemokines secreted by tumour cells, including CCL5, is involved in the subversion of immune cells from acting as cancer suppressors to supporting cancer progression, and for tissue cells to maintain a favourable TME (Aldinucci, Borghese and Casagrande, 2020). Constant presence of this milieu of cytokines in the TME may have a long-term effect on CCR5 regulation in cancer cells.

Amongst these cytokines in the TME is IL-6, which has been found to be linked to the CCL5/CCR5 axis (Colombatti *et al*., 2009). This enables a link to the STAT3 pathway as mentioned previously (Huang *et al*., 2020), where a synergetic feedback loop is proposed between CCL5/CCR5/NF-κB/IL-6/JAK2/STAT3 (**Figure 4**). IL-6 induces growth via STAT3 signalling pathway in most PCa cell lines, except for LNCaP (an androgen-dependent PCa cell line) where IL-6 causes growth arrest (Lou *et al*., 2000). Lou *et al*. postulated that IL-6 undergoes a functional transition from a paracrine growth inhibitor to an autocrine growth stimulator, inducing an androgen resistant phenotype, reminiscent of PC3, which is an androgen-independent PCa cell line. Thus, IL-6 could act as an alternative pathway for growth and proliferation of androgen-independent PCa cells, making it an excellent target for androgen resistant CRPC. A summary of the proposed positive feedback loop is outlined in **Figure 4**.

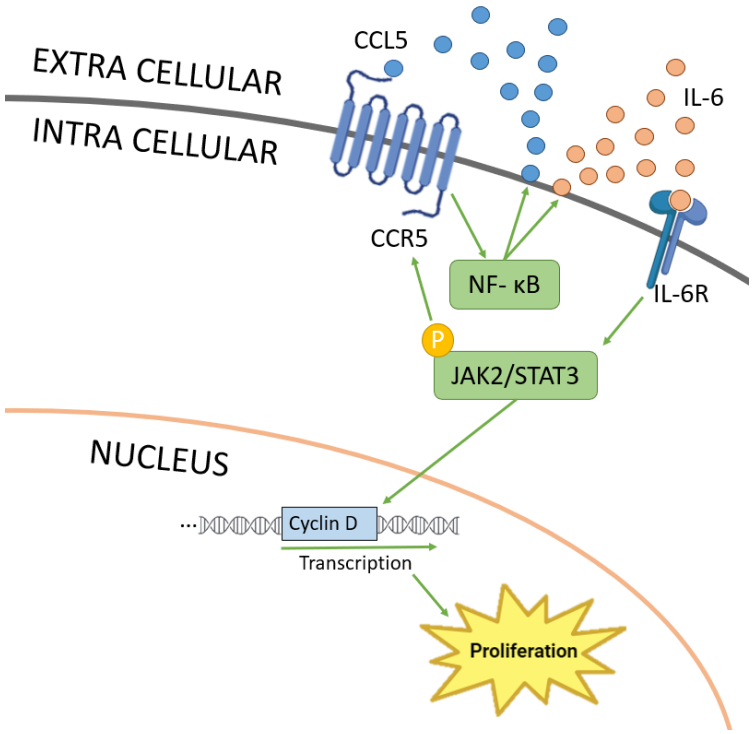

Figure 4: Schematic diagram summarising proposed positive feedback loop. Green arrows indicate known activation between signalling pathways. In yellow shape is the proposed cellular effect.

1.6. IL-6: An overview

IL-6 is a pleiotropic cytokine, which plays a role in immune responses, specifically modulating the differentiation of immune cells but is also implicated in diseases linked to inflammation and cancer (Culig *et al*., 2005).

1.6.1. IL-6 in cancer

IL-6 secretion and signalling are associated with many cancer cell lines, including breast (Jin, Pandey and Popel, 2018), prostate (Chen, Wang and Farrar, 2000) and melanoma (Weber *et al*., 2020) cell lines. In PCa, IL-6 has been found to stimulate PCa cell proliferation, inhibition of apoptosis (Lee *et al*., 2003), metastasis and angiogenesis (Adekoya and Richardson, 2020). In patients with aggressive PCa, increased levels of IL-6 serum and plasma levels in patients have been found, making IL-6 a potential biomarker for aggressive PCa (Shariat *et al*., 2001).

1.6.2. Expressing cells and molecular mechanism

IL-6 is expressed by a variety of cell types from macrophages, neutrophils, B and T cells to structural cells such as fibroblasts, endothelial and mesothelial cells. IL-6 binds its receptors IL-6R (gp80) and gp130, forming a dimerisation complex between IL-6/IL-6R/gp130, which initiates intracellular signalling pathways, such as JAK/STAT, MAPK and PI3-K/AKT. (Azevedo *et al*., 2011)

The gp80 subunit exists as a membrane-bound (IL-6R) and a soluble (sIL-6R) form, activating the classical and trans-signalling IL-6 pathways, respectively. sIL-6R is found within bodily fluid due to cleavage of IL-6R by MMPs or mRNA splicing. The gp130 subunit of the IL-6 activation complex is expressed by all cells and universally binds to all IL-6 family cytokines. (Rose-John *et al*., 2006)

In the classical signalling pathway, the IL-6 first binds to the IL-6R, then two gp130 subunits are recruited to form the complex, inducing signal transduction activating JAK-STAT, MAPK and PI3-K/AKT pathways leading to cell survival, proliferation and mitosis. In the trans-signalling pathway, IL-6 binds to sIL-6R, which binds to membrane bound gp130, where signal transduction activates JAK-STAT pathway,

but not MAPK and PI3-K/AKT pathways, leading again to cell survival, proliferation and mitosis (Rose-John *et al*., 2023). **Figure 5** summarises these two modes of IL-6 activation.

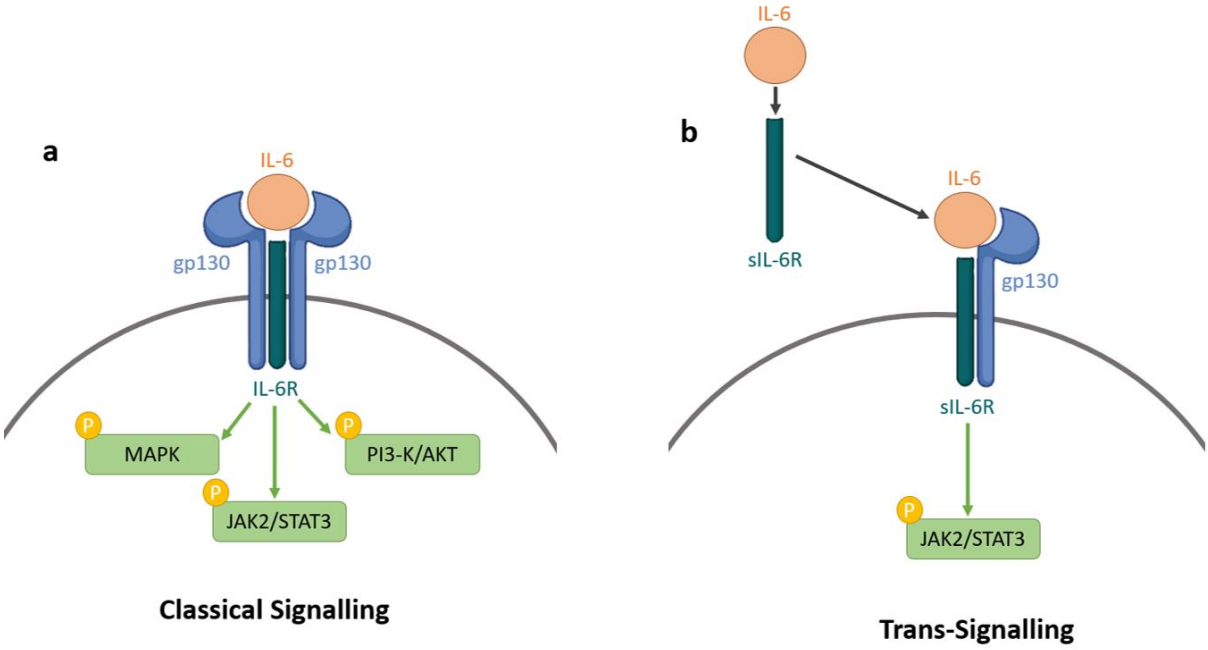

Figure 5: Schematic diagram illustrating IL-6 signalling. Classical (a) and trans (b) signalling in **IL-6 activation.** Green arrows show the activated signalling pathways.

1.7. Project overview

The general hypothesis of the project is to elucidate the consequences of CCL5/CCR5 axis activation in mPCa cell models LNCaP and PC3, i.e. changes in the expression of CCR5/CCR5AS mRNA transcripts, CCR5 cell surface expression, and the activity of downstream tumourigenic signalling pathways. I focus on changes occurring at the transcriptional rather than at the protein level, supplementing these observed changes with some protein studies. Consequently, I aim to find which CCR5 transcripts are involved in the expression of CCR5 in mPCa models. I will also investigate whether the CCL5/CCR5 axis synergises with the known tumourigenic IL-6/IL-6R axis in a positive feedback loop, by treating mPCa cell models with CCL5 with or without IL-6 co-stimulation. Finally, to mimic cancer cells in TME, I explored the effect of long-term (24 to 48h) cytokine stimulation.

2. Materials and Methods

2.1 - Reagents

Reagents used are detailed in **Table 2-3.**

Table 2: Buffers

Buffer name	Composition	Use
50X TAE buffer	2M Tris Base, 1M Acetic Acid, 50mM EDTA made up in ddH_2O	Preparing agarose gels and medium for DNA gel electrophoresis
FACS buffer	1% FCS (Foetal Calf Serum), 0.05% Sodium Azide made up with PBS	Washing and resuspending cells for Flow Cytometry
Lysis buffer	20mM Tris pH 8, 150mM NaCl, 2mM EDTA, 1% IGEPAL	Lysing cells for Western Blot prep
Sample buffer (reducing)	62.5 µM Tris-HCl pH 6.8, 35 % glycerol, 2 % SDS, 0.16 %, bromophenol blue, 5 % β-Mercaptoethanol	Reduce samples further, allow samples to sink and add colour to see the samples sink into wells for SDS PAGE
Running buffer	1x Tris/Glycine/SDS (Geneflow, cat. no. B9-0032)	Medium for SDS-PAGE
Transfer buffer	1x Trans-Blot Turbo Transfer Buffer (cat. no. 10026938), 20% methanol	Semi-dry transfer for Western Blot

Table 3: Antibodies

Antibody name	Specificity	Use	Working concentration	Catalogue no. and Source
HEK/1/85a	CCR5	1° ab (FC)	5 µg/ml	313720, Biolegend
T21/8	CCR5 N-terminus	1° ab (FC)	5 µg/ml	14-1957-82, Invitrogen
Histone (H3)	Mouse	1° ab (WB)	1 µg/ml	68345-1-Ig, ProteinTech
α-Tubulin	Mouse	1° ab (WB)	0.3 µg/ml	A21371, Invitrogen
β-actin	Rabbit	1° ab (WB)	0.15 µg/ml	20536-1-AP, Proteintech
STAT3	Mouse	1° ab (WB)	0.057 µg/ml	9139S, Cell Signalling Technology
Phospho-STAT3 (Tyr705)	Rabbit	1° ab (WB)	0.05 µg/ml	9145S, Cell Signalling Technology
Goat Anti-Mouse Streptavidin 647	Mouse	2° ab (FC)	4 µg/ml	A21245, Invitrogen
Goat Anti-Rat Streptavidin 647	Rat	2° ab (FC)	4 µg/ml	A21247, Invitrogen
Goat Anti-Mouse HRP	Mouse	2°ab (WB)	0.2 µg/ml	12-349, Sigma-Aldrich
Goat Anti-Rabbit HRP	Rabbit	2°ab (WB)	0.2 µg/ml	Sigma-Aldrich, 12-348
IgG Isotype 1	Mouse	Isotype control (FC)	5 µg/ml	400101, Biolegend
IgG2a Negative Control	Rat	Isotype control (FC)	5 µg/ml	MAB003, R&D Systems
Human IgG	N/A	Blocking ab (FC)	20 µg/ml	I8640, Sigma-Aldrich

1° - Primary, 2° - Secondary, ab – antibody, FC - flow cytometry, WB - Western Blot

2.2 - Cell lines

The prostatic carcinoma cell lines, LNCaP (lymph node metastasis, androgen sensitive) and PC3 (bone metastasis, androgen insensitive) were sourced from the American Type Culture Collection (ATCC) and were grown in TC treated plates, in RPMI 1640 containing 2 mM glutamine, pen/strep (100 units/ml penicillin, 0.1mg/ml streptomycin), 10 mM HEPES and 10% FCS or in Ham's F12 medium with glutamine, pen/strep and 7% FCS, respectively. PBMCs (peripheral blood mononuclear cells), MDMs (monocyte derived macrophages) and T cells were isolated from human blood using single donor blood cones sourced from the NHS blood transplant (NHSBT) by Dr Dave Boucher (Ethics number: DB202111, approved by the Biology Ethics Committee). PBMCs were isolated using Ficoll density gradient with LeucoSep Tubes (Greiner), and T Cells were isolated using EasySep Direct Human T Cells Isolation Kit (Cat no. 19661, Stem Cell Technology). Macrophages were derived from monocytes (MDMs) by culture in RPMI 1640 containing glutamine, pen/strep, 10% FCS in presence of macrophage colony stimulating factor 1 (MCSF1, 50 ng) for 7 days. CHO CCR5, a stable cell line over-expressing CCR5 (Mack *et al*. 1998) were grown in MEM-alpha containing glutamine, pen/strep and 5% FCS. Non-expressing CCR5 cell lines CHO K1 and HEK-293 were also from ATCC and grown in DMEM-F12 or DMEM containing glutamine, pen/strep and 10 % FCS, respectively.

2.3 - Cytokine Stimulation

For cytokine stimulation experiments, LNCaP and PC3 cells were plated at 2 x 10^5 cells per well in 6 well plates. 48 hours after seeding, cells were stimulated with 10nM of CCL5 (made in house, IH-CCL5; Tufail *et al*. 2024) and/or with 2nM (1500IU) of recombinant human IL-6 (Proteintech). Cells were harvested at 24 or 48 hours after stimulation. As the half-life of IL-6 is 15.5 hours (Kuribayashi, 2018), more IL-6 was added at 24h for cells receiving 48h of stimulation. Additionally, unstimulated cells were cultured alongside stimulated cells and collected at time points 0, 24 and 48 hours. For the cell harvest, cells were lifted using 1x trypsin/EDTA and counted using a haemocytometer to measure total cell count. 2 x 10^6 cells were pelleted by centrifugation and pellets were kept at -80°C until RNA extraction for end-point PCRs and/or qPCRs.

2.4 - RNA Extraction and cDNA synthesis

RNA extraction was performed using RNeasy Mini Prep Kit (QIAGEN) according to manufacturer's protocol. RNAse-free DNase set (QIAGEN) was used to digest excess DNA. Nanodrop (ThermoScientific) was used to quantify the RNA concentration of each sample.

For the cDNA synthesis step, to prevent RNA degradation, samples were treated with RiboLock RNase Inhibitor (Thermofisher Scientific). cDNA synthesis was performed in a Techne thermocycler (Model: FTGENE2D) using a Superscript RT II kit (Thermofisher Scientific) according to manufacturer's protocol. For end-point RT-PCR or RT-qPCR samples, 1 or 5 µg of RNA extracted from each sample (with an upper volume limit of 10.5µl) were added for cDNA synthesis reactions, respectively.

2.5 – End-Point RT-PCR

Two-step Reverse Transcriptase – Polymerase Chain Reaction (RT-PCR) was performed; the first step being the cDNA synthesis via RT as outlined in **Section 2.4**, and the second step being PCR.

For the PCR step, a set of primers named P1, P2 and P3 annealing within or flanking the ORF region of the CCR5 gene (**Table 6**), as well as a pair of primers for the housekeeping reference gene GAPDH (**Table 10**), were specifically designed for detection via End Point PCR. PCR reactions were performed using GoTaq Hot Start Polymerase kit from Promega following manufacturer's protocol. 1µl of cDNA was added to each 25µl PCR reaction using Techne (Model: FTGENE2D) or AppliedBiosystems (VertiPro) thermocyclers using settings for each primer pair as reported in **Table 4.**

Table 4: PCR run method.

Initial Denaturing Stage			Final Extension stage
94°C for 5 mins	35x for P1 or 40x for all other pairs	**Denaturing stage:** 95°C for 1 min	72°C for 10 mins
		Annealing stage: 68°C for P1 66°C for P2 or P2/P1 54°C for P3 60°C for GAPDH and all other signalling proteins For 30 secs	
		Extension stage: 72°C for 1 min 30 secs or 72°C for 3 mins for P3 only	

2.6 - DNA Gel electrophoresis

2% agarose gel made up of 1x TAE buffer, stained with SYBR Safe (Thermo Fisher Scientific) was prepared. Gels were run at 50V in 1x TAE buffer. 11µl of samples, 6µl of 100 bp molecular weight ladder (Promega, cat. no. G210A) or 1000 bp molecular weight ladder (BioLabs, cat. no. N3232S) were loaded for each gel. Images were taken by using a gel imager (Invitrogen, iBright1500 or SynGene) and ImageJ was used to process and adjust brightness and contrast of images. Relative density was measured by plotting peaks of the bands for each gene of interest and dividing the value with that of GAPDH.

2.7 - Designing of RT-qPCR Primers

Another set of CCR5 specific primers including primers for CCR5 Exon 1 and Exon 3 containing transcripts, signalling proteins of interest and the housekeeping reference gene GAPDH (see **Table 8 - 12**) were either selected from the literature, or designed using BLAST for mRNA quantification by RT-qPCR. SnapGene was used to visualise genes and primer locations.

Primers were additionally screened, which involved the following criteria:

- Between 18-30 bases (ThermoFisher, 2022a)
- Yielding an amplicon between 70-150 bp (Prediger, 2024)
- Having a GC content of 40-60% (ThermoFisher, 2022a)
- Be specific to one gene of interest, as tested using BLAST nucleotide to nucleotide (Altschul *et al*., 1990).

2.8 – RT-qPCR

As with end point RT-PCR, RT-qPCR was performed in two steps: cDNA synthesis via RT and qPCR reaction. The cDNA synthesis step is outlined in **Section 2.4**.

qPCR was performed using Fast SYBR Green Master Mix 2x (Applied Biosystems), according to manufacturer's protocol using mostly 96 well plates. Where indicated, 384 well plates were used. Each pair of primers were validated, and primer-specific parameters optimised as per the methods outlined below. Results from these qPCR primers validations and subsequent positive control validations are presented in the **Appendix (Section 5.1 and 5.2)**. All experimental qPCR reactions were run in triplicate to eliminate outliers. Most assays were run using a qPCR machine compatible with 96 well plate (Step One Plus, Applied Biosystems). The rest of the assays were run on a qPCR machine compatible with a 384 well plate (Quantstudio 7, ThermoFisher). The final conditions used for qPCR assays were reported as in **Table 5**.

Table 5: qPCR run method

<table>
<tr><th>Initial Denaturing Stage</th><th colspan="2"></th><th>Melt Curve Stage</th></tr>
<tr><td rowspan="4">95°C for 5 mins</td><td rowspan="4">40x</td><td rowspan="2">Denaturing stage:
95°C for 1 sec</td><td>Denaturing stage:
95°C for 1 sec</td></tr>
<tr><td>Annealing & Extension stage:
60°C for 20 secs
(Incremental temperature increase)</td></tr>
<tr><td rowspan="2">Annealing & Extension stage:
58°C for CCR5AS
60°C for rest of qPCR primers
For 35 secs</td><td rowspan="2">Denaturing stage:
95°C for 1 sec</td></tr>
<tr><td></td></tr>
</table>

2.9 - qPCR Data Analysis

For the Step One Plus and Quantstudio 7, StepOne Software v2.3 and ThermoFisher Connect were used to analyse qPCR data respectively. Baseline and threshold were set according to manufacturer's protocol (Applied Biosystems, 2002). mRNA expression was quantified using comparative ΔCT method, (Livak and Schmittgen, 2001) where GAPDH was used as a housekeeping gene.

2.10- PCR Primers

Details and relevant information regarding all PCR primers used for this study are provided in **Tables 6 - 12** below.

Table 6: Primers targeting CCR5 transcripts for End-Point PCR and their sequences, Tm according to New England Labs' Tm calculator (NEB, No date) and their GC content. GC content should ideally be between 40-60%. (Prediger, 2024)

Primer name	Sequence (5' to 3')	Length (bp)	Tm (°C) (NEB)	GC Content (%)
P1 CCR5 forward	GAGGCACAGGGCTGTGAGGC	20	68	70
P1 CCR5 reverse	TGCTCGCTCGGGAGCCTCTT	20	68	65
P2 CCR5 forward	GGGTGGAACAAGATGGATTATCAAGTG	27	60	44
P2 CCR5 reverse	ACCCCCAGCCCAGGCTGTGTAT	22	69	64
P3 CCR5 forward	CCTTCAGACCAGAGATCTATTCTC	24	56	46
P3 CCR5 reverse	AATAACTTGATGCATGTGAAG	21	52	38

Table 7: Primer combinations for primers targeting CCR5 transcripts and their expected PCR product lengths as per reported on primer BLAST (Ye *et al*., 2012) under the CCR5 gene/mRNA sequence database (NCBI, 2009).

RT-PCR Product	RT-PCR product length (bp)	Transcripts primers detect	Sequence location on CCR5 gene
P1 Forward and Reverse	319	ORF containing	6185 to 6503
P2 Forward and Reverse	1149	ORF and non-coding region of Exon 3	5487 to 6635
P3 Forward and Reverse	1559*	CCR5A	3363 to 6821*
P2 Forward and P1 Reverse	1017	ORF containing	5487 to 6503
P3 Forward and P1 Reverse	1238*	CCR5A	3363 to 6503*
P4 Forward and Reverse	111	ORF containing	6258 to 6368
P5a Forward and Reverse	88	Exon-1 containing	2683 to 2770
P5b Forward and Reverse	91	Exon-1 containing	2688 to 2888
CCR5A Forward and Reverse	71	CCR5A*	2784 to 3355*
CCR5B Forward and Reverse	71	CCR5B*	2784 to 5493*

*****Due to splicing, regions in the genomic sequence do not get included in the matured CCR5A/B transcript, hence why the RT-PCR product length is shorter than the length between the sequence locations of the primers on the CCR5 gene.

Table 8: Primers targeting CCR5 transcripts for qPCR.

Primer	Sequence (5' to 3')	Length (bp)	Tm (°C) (NEB)	GC Content (%)	Reference
P4 CCR5 forward	GTCCTTCTCCTGAACACCTTCCA	23	61	52	(Gao *et al*., 2022)
P4 CCR5 reverse	GCAGTGCGTCATCCCAAGAG	20	62	60	
P5a CCR5 forward	CATAAAGAACCTGAACTTGACCATATACTT	30	58	33	(Mummidi *et al*., 2007)
P5a CCR5 reverse	GGATTCTTCACTCCAGATATAATCTATCTG	30	59	37	
P5b CCR5 forward	AGAACCTGAACTTGACCATATACT	24	55	38	N/A
P5b CCR5 reverse	AGGTGGCAGGATTCTTCACTC	21	60	52	
CCR5A forward	TCTGGCATAGTATTCTGTGTAGTGG	25	56	44	N/A
CCR5A reverse	ACGGGCTTTTCTCACTGGAT	20	63	50	
CCR5B forward	TCTGGCATAGTCTCATCTGG	20	56	50	N/A
CCR5B reverse	TCCACCCGGGGAGAGTTTC	19	56	63	

Table 9: Primers targeting CCR5AS transcripts for qPCR.

Primer name	Seq. (5' to 3')	Product length (bp)	Tm (°C) (NEB)	GC Content (%)	Reference
CCR5AS forward	TCCTGGTCCCCGTATTGAAT	111	58	50	(Kulkarni *et al*., 2019)
CCR5AS reverse	AGGAAGGTATGTGGTGACCA		58	50	

Table 10: Primers targeting GAPDH transcripts for End Point PCR and qPCR, designed to cover a conserved sequence shared between human and hamster transcriptome.

Primer name	Seq. (5' to 3')	Product length (bp)	Tm (°C) (NEB)	GC Content (%)
GAPDH forward	AAGGTGAAGGTCGGAGTCAA	108	60	50
GAPDH reverse	AATGAAGGGGTCATTGATGG		59	42

Table 11: Primers targeting signalling protein transcripts for qPCR.

Primer name	Seq. (5' to 3')	Product length (bp)	Tm (°C) (NEB)	GC Content (%)	Reference
CREB-1 forward	GCTGCCTCTGGAGACGTACAA	50	62	57	(Wang *et al*., 2015)
CREB-1 reverse	GCTAGTGGGTGCTGTGCGA		64	63	
β-catenin forward	GCTTTCAGTTGAGCTGACCA	77	58	50	(Huang *et al*., 2020)
β-catenin reverse	CAAGTCCAAGATCAGCAGTCTC		58	50	
STAT3 forward	CTCTGCCGGAGAAACAGG	92	59	61	(Huang *et al*., 2020)
STAT3 reverse	CTGTCACTGTAGAGCTGATGGAG		60	52	
LKB1 forward	GCCGGGACTGACGTGTAGA	63	63	63	(Alkaf *et al*., 2017)
LKB1 reverse	CCCAAAAGGAAGGGAAAAACC		57	48	
PRKAB2 forward	GCCAAAGCTCACTGTTGTTGGTTA	139	60	46	(Dong and Du, 2019)
PRKAB2 reverse	GACAGACACAGAGCTGCACTCATTC		62	52	
EIF4EBP1 forward	ACCAGCCCTTCCAGTGATG	107	61	55	(Akbarian *et al*., 2020)
EIF4EBP1 reverse	TCCATCTCAAACTGTGACTCTTC		57	43	

Primer name	Seq. (5' to 3')	Product length (bp)	Tm (°C) (NEB)	GC Content (%)	Reference
Inhibitor Nfκ-B (IκB-α) For	GCTGAAGAAGGAGCGGCTACT	72	63	57	(Bottero *et al*., 2003)
Inhibitor Nfκ-B (IκB-α) Rev	TCGTACTCCTCGTCTTTCATGGA		60	48	
E-cadherin forward	ACAGCCCCGCCTTATGATT	56	60	53	(Lau and Leung, 2012)
E-cadherin reverse	TCGGAACCGCTTCCTTCA		60	56	

Table 12: Primers targeting positive control CCL4 for qPCR. Catalogue number (Cat. no.) is listed as primers were bought pre-validated from a company.

Primer name	Seq. (5' to 3')	Product length (bp)	Tm (°C) (NEB)	GC Content (%)	Cat. no. and Source
CCL4 forward	GCTTCCTCGCAACTTTGTGGTAG	140	59	52	HP206589, Origene
CCL4 reverse	GGTCATACACGTACTCCTGGAC		58	55	

2.11 - Flow Cytometry

LNCaP and PC3 cells were cultured and stimulated with cytokine as described in **section 2.2** and **2.3**. At the end of the incubation period, cells were lifted using 10nM EDTA in PBS instead of 1x trypsin/EDTA. Cells were resuspended in media and plated on U-bottomed 96 well plates in triplicate. Cells were kept at 4°C and spun down at 405g for 3-5 mins, vortexed and washed in FACS buffer three times. To prevent possible binding of mouse monoclonal antibodies to Fc receptors present on PCa cells (Larsson *et al*., 2022), cells were treated with 20 µg/ml of human IgGs in FACS buffer for 20 minutes at 4°C. To detect the presence of CCR5 receptors at their surface, cells were labelled with monoclonal antibodies that recognise different extracellular epitopes of CCR5 (Fox *et al*., 2015), namely HEK/1/85a (Rat) or T21/18 (Mouse) at 5 µg/ml in FACS buffer, Anti rat IgG2a and anti-mouse IgG1 were used

as negative controls, respectively. Primary antibody incubation was performed for 1 hour at 4°C under shaking condition. Cells were then spun down, vortexed and washed in FACS buffer 3 times in between antibody staining as described. Cell-bound anti-CCR5 antibodies were detected by staining cells with a species-specific secondary antibody, either Goat Anti-Rat Alexa 647 for HEK/1/85a, or Goat Anti-Mouse Alexa 647 for T21/8, for 50-55 minutes at 4°C. A secondary antibody only control was also used. After 3 FACS buffer washes, cells were fixed in 1% formaldehyde in FACS buffer overnight. After washing 3 times and resuspending in FACS buffer, samples were run and data acquired using a CytoFLEX S (Beckman Coulter) flow cytometer. Flow cytometry data was analysed using CytExpert and Mean Fluorescence Intensity (MFI) values were exported into Microsoft Excel for further analysis.

2.12 - Cell lysates preparation for Western Blot

LNCaP and PC3 cells were cultured and stimulated with cytokine as described in **section 2.2 and 2.3** before being detached in 1x trypsin/EDTA and spun down to collect cell pellets. Cells were lysed in lysis buffer containing protease inhibitor (Roche, cat. no. 11697498001) and phosphatase inhibitor (Roche, cat. no. 04906837001) at a concentration of 1 x 10^6 cells per 100µl of lysis buffer. Cell lysates were spun at 11,180 xg for 10 mins to separate the nuclear and cytosolic fractions. For the nuclear fractions, lysis buffer was then supplemented with sodium chloride (NaCl) to reach a final concentration of 400mM NaCl (Baldwin, 1996). To both the nuclear and cytosolic fractions, reducing sample buffer was added to make 1x. Samples were boiled at 95°C for 10 minutes and kept at -20°C until run on Western Blot.

2.13- SDS-PAGE and Western Blot

Samples were run by sodium dodecyl sulphate-polyacrylamide gel electrophoresis (SDS-PAGE) loaded on a 10% acrylamide gel under denaturing conditions, to separate proteins according to their size. A protein ladder (cat. no: 26616, Thermo Scientific) was loaded alongside samples. A semi-dry transfer (Transblot Turbo Transfer System, Bio-Rad) onto a nitrocellulose membrane (Bio-Rad, cat. no.

1704271) was performed, followed by ponceau staining of membrane to check transfer uniformity. The membrane was blocked with 5% milk (prepared from skim milk powder, Sigma Aldrich) in 0.1% PBS-Tween for 1 hour at room temperature. For the primary antibody, STAT3 or phosho-STAT3 were prepared diluted at 1:1000 dilution containing either 5% milk in 0.1% PBS-Tween or 5% BSA in 0.1% TBS-Tween. The membrane was then incubated in primary antibody overnight at 4°C. Between antibody incubations, the membrane was washed once in PBS Tween 0.1% and then twice in PBS Tween 0.5% at room temperature. For the secondary antibody, anti-mouse HRP was used and diluted in 5% milk in 0.1% PBS-Tween to 1:500 dilution. The membrane was incubated in secondary antibody for 1 hour in room temperature. After PBS-Tween washes as described, Immobilon Forte or Crescendo Western HRP substrate (Millipore, cat. no. WBLUR0020 and WBLUF0500) was added to the membrane for detection of the protein of interest. These membranes were re-probed for loading controls of nuclear or cytosolic cell fractions. Briefly, they were washed in PBS-Tween and incubated in 5% milk at room temperature for an hour before being incubated with an anti-Histone 3 (nuclear) or anti-Tubulin or β-catenin (both cytosolic) antibody in 5% milk at 4°C overnight and probed with a secondary antibody anti-mouse HRP as described, above.

All membrane were imaged using a gel imager (Invitrogen, iBright1500) and ImageJ was used to measure relative density by plotting peaks of the blots for each protein of interest and dividing the value with that of the loading control; protocol was obtained from Davarinejad, no date.

2.14 - Statistical Analysis

qPCR and Flow Cytometry statistical analysis and graphs were generated using GraphPad Prism 9. For baseline expression comparing between timepoints, Two-stage linear step-up procedure of Benjamini, Krieger and Yekutieli was used to prevent false positive discoveries. For comparisons between more than two categorical variables (e.g. Stimulation and time), two-way ANOVA was used. Tukey's multiple comparisons test was conducted due to low biological replicates. Statistical analysis notation was as follows: ns = not significant, * = $p<0.05$, ** = $p<0.01$, *** = $p<0.001$, **** = $p<0.0001$.

3. Results

3.1 – Baseline transcriptional presentation of PCa cell-lines compared to reference cell types.

Ideal conditions were set to detect total CCR5 transcripts on different cell lines by end point RT-PCR. Different combinations of primers were used that specifically annealed within or flanked the CCR5 coding region, thus would detect all CCR5 transcripts, including those leading to protein expression. P1 and P4 anneal within the ORF. P2 primers flank the ORF. P2 forward contains - starting from 5' to 3' - 1 base in the intron region, 8 bases within the exon and 18 bases in the coding region. P2 reverse is entirely in the non-coding region of Exon 3. P4 was specifically designed for qPCR. **Table 7** in the Materials and Methods section details the location on the CCR5 gene/mRNA which is amplified for each primer combination used. Additionally, a diagram of the rough location of the primers used on the CCR5 coding region – which is within exon 3 - is shown in **Figure 6a**.

3.1.1 - Expression of total CCR5 transcripts

To identify the varying transcriptional lengths of Exon 3 in CCR5 transcripts present in each cell type, the P1 pair, P2 forward/ P1 reverse, and finally P2 pair were tested. Gel electrophoresis results are presented in **Figure 6b.** MDMs were used as positive control for expression of all CCR5 transcripts, as they are known to strongly express CCR5 endogenously (Kim *et al*., 2022; Fox *et al*., 2015). CHO CCR5 cells were stably transfected with a plasmid containing only the CCR5 coding sequence (cDNA) amplified from genomic DNA of human PBMCs (Mack *et al*. 1998) and show a very strong band with the P1 pair within the CCR5 ORF, however have a very faint band for P2 forward / P1 reverse and no band for P2 pair. This suggests that they lack the boundary sequences of Exon 3, outside the ORF. HEK-293 shows a faint band for all primer combinations, showing that they express CCR5 at a transcriptional level. It was previously reported by Qi *et al*. that HEK-293 is heterozygous for a CCR5 Δ32 mutation, which could not be confirmed with the set of primers I used, as the sequence for the Δ32 mutation lies outside their range. The same group confirmed detectable transcript but found no CCR5 protein expression (Qi *et al*., 2016). Negative control CHO K1 is not known to express CCR5, thus shows no bands for each primer.

In terms of PCa cell lines, LNCaP had a fainter band than MDMs, while PC3 had the faintest band out of all the positive cell types. The strength of the bands differed between primer pairs, for example, the band for PC3 was barely visible with the P2 pair but was better defined, however still faint, in P1 forward / P2 reverse pair. This suggests a very low transcription level for CCR5 in PCa cell lines.

To ensure that the differences in CCR5 amplification between cell lines was due to transcription, end point RT-PCR was repeated to amplify CCR5 transcript using the P1 pair and for the housekeeping gene GAPDH as an internal control for each sample. Results are presented in **Figure 6c** and confirmed the relative differences in CCR5 Exon 3 containing transcripts, with MDM and CHO CCR5 > THP-1 > PC3 and LNCaP. As end point RT-PCR is not quantitative, we could not confirm which PCa cell line produces more total CCR5 transcripts than the other. For this reason, RT-qPCRs using P4 were run.

To quantify relative baseline expression of CCR5 transcripts, RT-qPCR was performed and results are presented in **Figure 6d.** THP-1 was chosen as the cell line for normalisation, as THP-1 have previously been used to define the existence of different CCR5 transcripts (Mummidi *et al*., 1997) and are known to express CCR5 at a stable but very low level (Park *et al*., 2007). This is unlike MDMs where expression levels can be very high but vary widely between individuals (Fox *et al*., 2015; Tuttle *et al*., 1998). CCR5 transcriptional level in THP-1 was mostly similar to T cells and confirmed large variability between cell types. Relative to THP-1, MDMs, CHO-CCR5 and PBMCs (which represent a mixture of CCR5 expressing cells, including T cells and monocytes) showed the highest expression of Exon 3 containing transcripts, while PC3 and LNCaP had the lowest expression levels, and this may explain the large spread between biological replicates for LNCaP and PC3 for all CCR5 transcripts due to high Ct values. Thus, RT-qPCR confirmed the trends in CCR5 mRNA expression seen by end point RT-PCR.

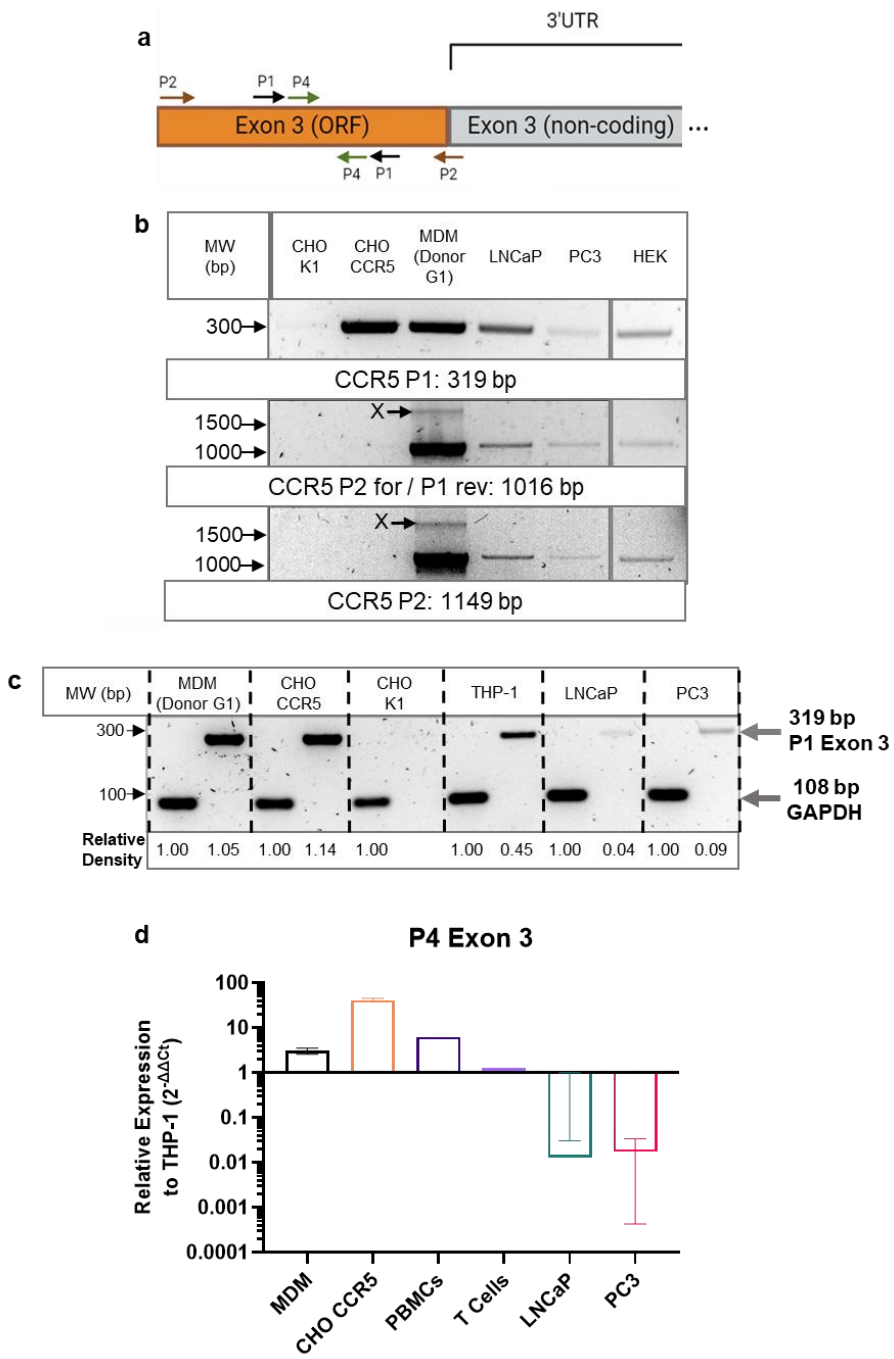

Figure 6: Total CCR5 transcriptional expression varies between different cell types. (**a**) Diagram showing location of primer pairs specifically detecting CCR5 transcripts within the ORF (P1 and P4) or flanking the ORF (P2), all of which encompass total CCR5 transcripts. (**b**) Gel electrophoresis showing the end-point RT-PCR products when using different combinations of primers targeting different regions of the CCR5 mRNA as detailed in (**a**), in CCR5 positive and negative cell types and PCa cell lines. n=3 (**c**) Gel electrophoresis showing the end point PCR products using P1 which detects all CCR5 transcripts, and GAPDH in CCR5 positive and negative cell types, as well as PCa cell lines. n=5 (**d**) qPCR data presenting relative expression of all transcripts of CCR5 to THP-1, normalised to GAPDH, on positively expressing CCR5 cell types (n=2 for MDM and CHO CCR5, n=1 for PBMC and T cells) and PCa cell lines (n=6). X: Unexpected band. Statistical analysis was not performed.

3.1.2 – Expression of previously published Exon-1 containing transcripts

To cover CCR5 full-length transcripts reported in the literature, primers targeting Exon 3 were used, namely P1 pair and P4 pair from Gao *et al*. 2022, described in **section 3.1.1**. To cover CCR5 transcripts leading to protein expression, primers targeting Exon 1 were used, namely P5a pair from Mummidi *et al* 2007 (see **Figure 7a**). However, after sequence alignment verification, I found that the published P5a pair targets a region in the 5'UTR upstream of Exon 1, which theoretically should not be part of the CCR5 mRNA. Additionally, the P5a reverse primer did not exactly match with the CCR5 mRNA sequence (NCBI, 2009). However, as the P5a pair had been published, it was decided to test them but to circumvent the mismatch in P5a reverse primer, by designing new primers (P5b) overlapping with the sequence of P5a (**Figure 7a**) using primer BLAST (as described in **Section 2.7**).

To focus on CCR5 transcripts leading to protein expression (CCR5A and B), another primer pair was selected based on CCR5 genomic sequence analysis, with an amplicon extending from Exon 2A to Exon 3 (P3; 1559 bp). P3 should detect CCR5A and not CCR5B transcript, which lacks the 2A part of Exon 2 (**Figure 7b and c**)**.** So far, none of the primers can differentially amplify CCR5B. Hence, using primer BLAST, new primers were designed, where the forward primers annealed to the exon-junctions between Exon 1 and 2 either specific for CCR5A containing exon 2A, or CCR5B containing exon 2B. Reverse primers for CCR5A and B annealed within Exon 2A or 2B, respectively. (**Figure 7b and c**, respectively).

Characterisation of the different CCR5 transcripts was carried out as shown in **Figure 8a**. The two primers amplifying Exon-3 containing transcripts (P1 and P4) confirmed CCR5 mRNA expression in all cell types tested, albeit a very low signal was detected for the PCa cell lines. However, P5a and P5b primer pairs, specific for the proposed transcripts leading to protein expression (Mummidi *et al*. 1997), only led to PCR product amplification for MDMs, T cells and the THP-1 cell line. The newly designed CCR5A and B specific primers showed faint bands but only for MDMs, and not for T cells or THP-1. As expected, CHO CCR5 only showed a band with primers annealing within the CCR5 ORF (see **Section 3.1.1**). Amplification of

the internal loading control GAPDH as a readout for baseline transcription, suggested low abundance of Exon 1-containing transcripts compared to ORF covering transcripts (**Figure 8a**).

For additional validation, the PCR reactions were repeated using P3 primers on MDMs, PCa cell lines and HEK-293 cells as negative control for CCR5 expression but reported to have CCR5 transcripts (Qi *et al*., 2016; Venkatesan *et al*., 2002). The P3 primers were mixed in different combinations to amplify CCR5A transcripts covering from Exon 2A in the 5'UTR (P3 forward) to the 3' end of Exon 3 (either P3 reverse or P1 reverse, see **Figure 7b**). In these experiments, only MDMs showed a band of the expected size as shown in **Figure 8b.** Only a lower non-specific band was visible with the P3 pair combination for PCa cells and HEK-293 cells. This band was absent for the P3 forward/ P1 reverse end-point RT-PCR, confirming that the CCR5A transcript was only present in MDMs.

Since the CCR5 protein expressing transcripts encompassing Exon 1 were barely detectable in PCa cell lines using end point RT-PCR, we decided to move to RT-qPCR as a more sensitive technique, to better quantify the expression of these transcripts.

For RT-qPCR analysis, only CCR5A and CCR5B primer pairs were used, as both P5a and P5b pairs failed the required initial qPCR primer validation (see **Appendix 1: qPCR Primer Validation**). **Figure 9: Baseline levels of proposed CCR5 protein encoding transcripts.** qPCR data presenting expression of the CCR5A (**a**) and CCR5B (**b**) transcripts relative to THP-1 cells after normalisation to GAPDH, for primary blood cells from Donor G1 (MDM, PBMC and T cells, n=2) and PCa cells (n=6). CCR5A (**c**) and CCR5B (**d**) qPCR data presented as relative expression of total CCR5 transcripts measured in these same samples normalised to GAPDH. Statistical testing was not performed.**a** and **b** present the baseline relative expression determined by RT-qPCR for CCR5A and CCR5B, respectively. There was a large variability of CCR5 transcriptional expression between cell types. Relative to THP-1, PBMCs showed higher and PCa cell lines lower expression for both transcripts, while MDMs seemed to express more CCR5B transcript only. T

cells remained comparable to THP-1. However, the general variability in CCR5 transcriptional activity seen between cell lines (**Figure 8**) may explain these differences. Therefore, I re-analysed the RT-qPCR results reporting the relative expression of CCR5A or CCR5B transcript as a percentage of total CCR5 transcriptional expression for each cell line **Figure 9: Baseline levels of proposed CCR5 protein encoding transcripts.** qPCR data presenting expression of the CCR5A (**a**) and CCR5B (**b**) transcripts relative to THP-1 cells after normalisation to GAPDH, for primary blood cells from Donor G1 (MDM, PBMC and T cells, n=2) and PCa cells (n=6). CCR5A (**c**) and CCR5B (**d**) qPCR data presented as relative expression of total CCR5 transcripts measured in these same samples normalised to GAPDH. Statistical testing was not performed.**c** and **d**.

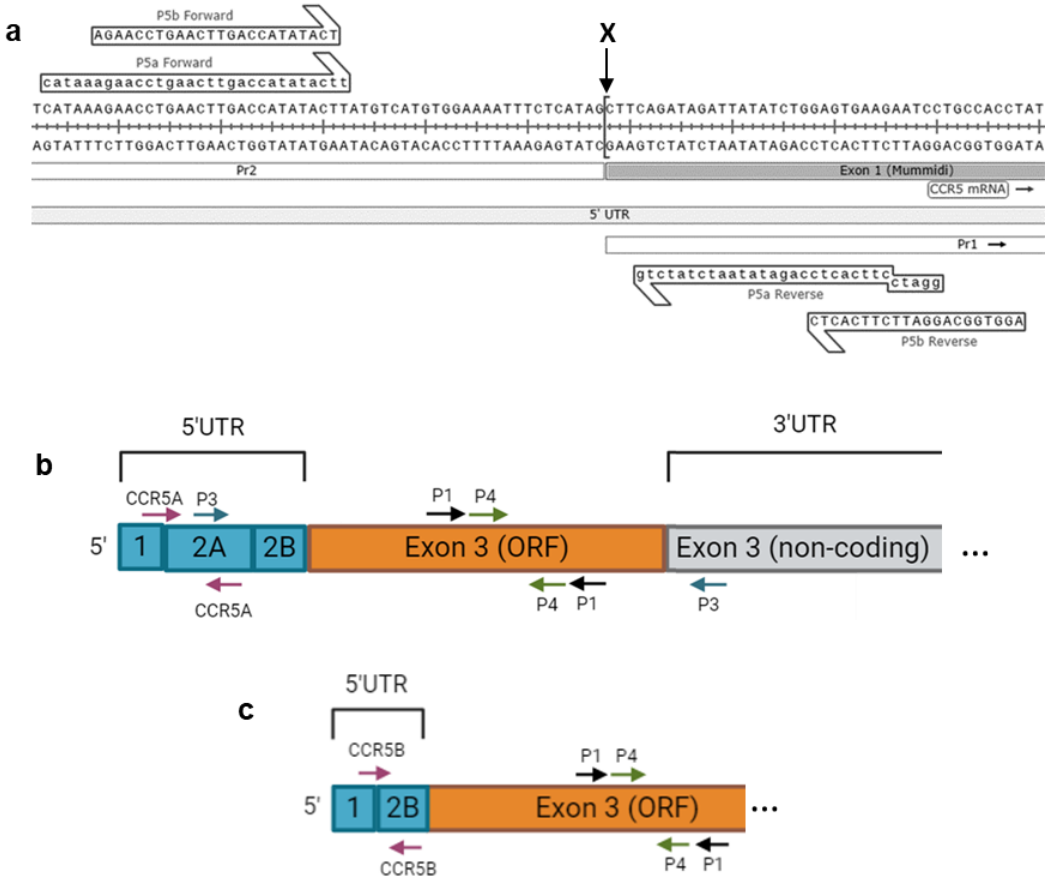

Figure 7: Locations of primers detecting Exon-1 containing transcripts. (**a**) Screenshot of the CCR5 DNA sequence on Snap Gene, showing the position of primers P5a and P5b, which detect exon 1 containing transcripts. P5a and P5b forward both anneal to the Pr2 (P_u) region upstream of where the CCR5 mRNA begins, which is marked at Point X. P5b primers mostly overlap P5a primers and correct for the mismatch found in P5a reverse primer. (**b and c**) Diagram showing location of primers specifically detecting each variant: CCR5A (**b**) and CCR5B (**c**).

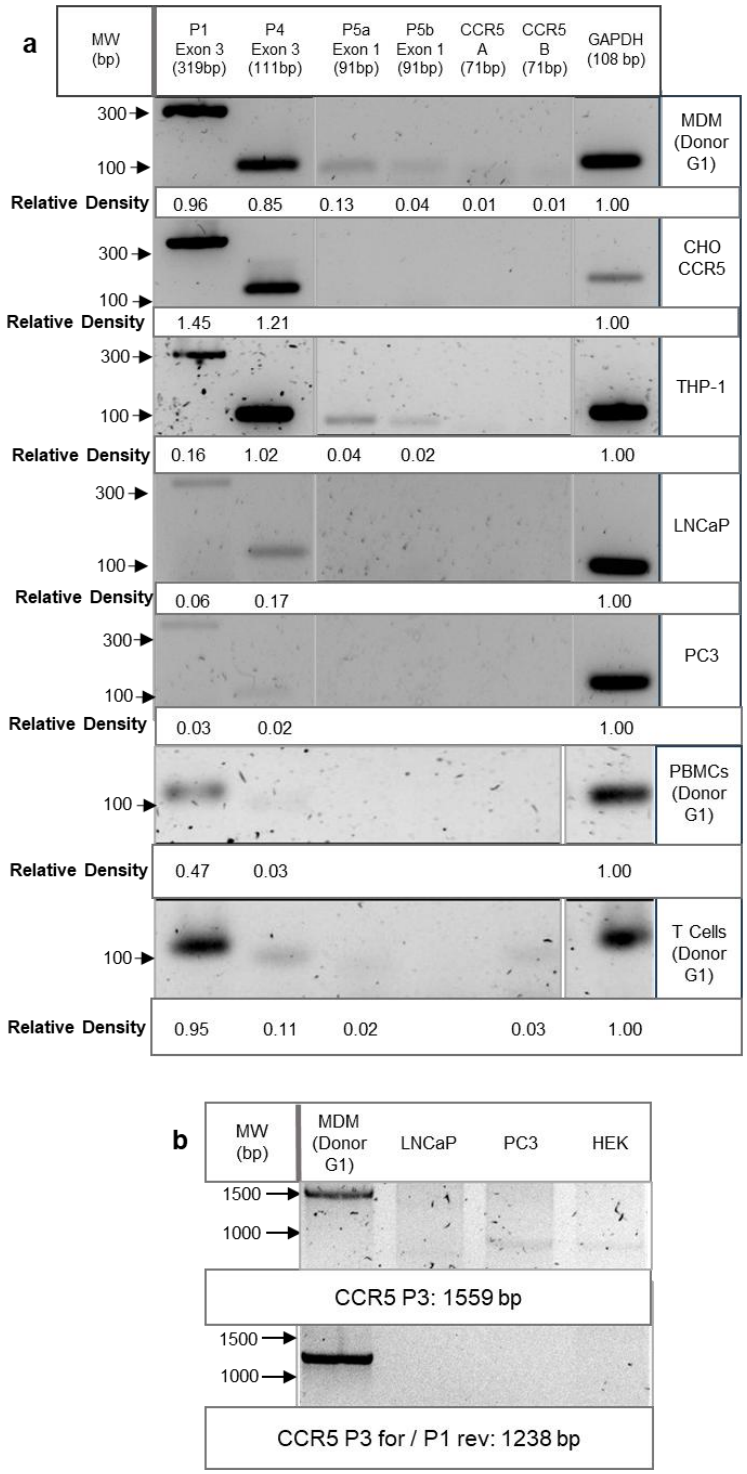

Figure 8: Proposed protein expressing transcripts are low in immune and PCa cells. (**a**) Gel electrophoresis showing end point RT-PCR products using P1, P4, P5a, P5b, CCR5A, CCR5B and GAPDH detecting mRNA on endogenously expressing CCR5 cells MDMs, THP-1, PBMCs and T cells, transfected cell line CHO CCR5 and PCa cell lines. N=3. (**b**) Gel electrophoresis showing the end point RT-PCR products using primer pair P3, which is specific to CCR5A transcript, and P3 forward / P1 reverse on PCa cell lines, CCR5 protein expressing MDMs from donor G1 and HEK-293 cells as negative control. Representative images from n=3 experimental repeats.

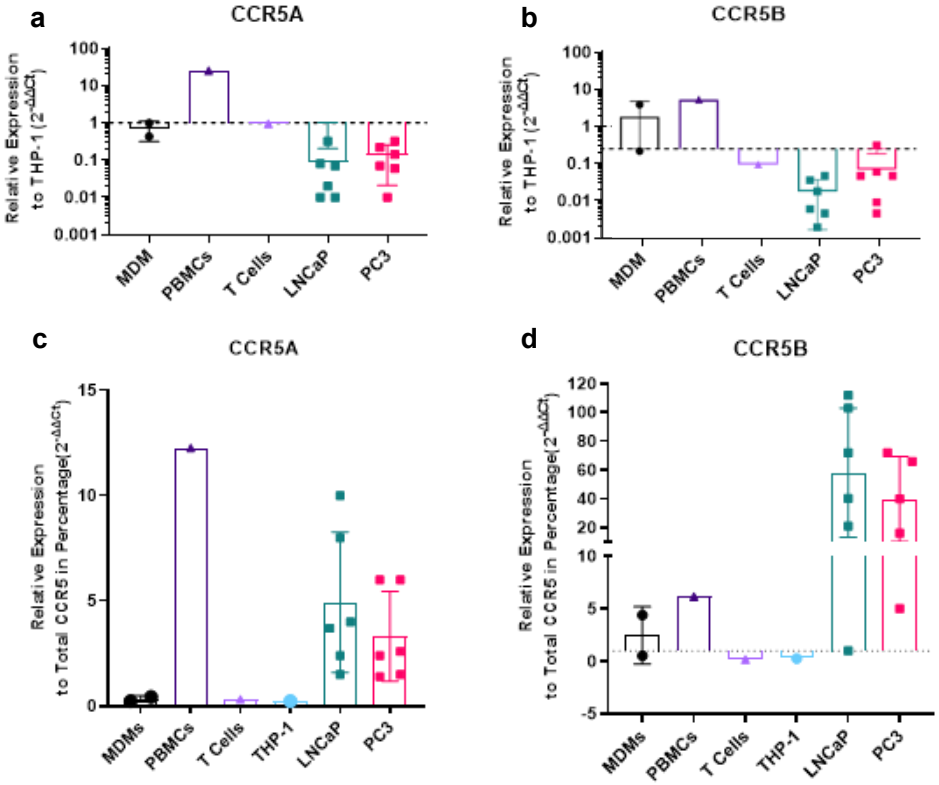

Figure 9: Baseline levels of proposed CCR5 protein encoding transcripts. qPCR data presenting expression of the CCR5A (**a**) and CCR5B (**b**) transcripts relative to THP-1 cells after normalisation to GAPDH, for primary blood cells from Donor G1 (MDM, PBMC and T cells, n=2) and PCa cells (n=6). CCR5A (**c**) and CCR5B (**d**) qPCR data presented as relative expression of total CCR5 transcripts measured in these same samples normalised to GAPDH. Statistical testing was not performed.

For THP-1 and T cells, CCR5A and B transcripts represent a very small pool of total transcripts, while for PBMCs CCR5A transcripts were slightly more dominant. Interestingly, PCa cell lines on the other hand, showed a wide spread of values between replicates but seemed to indicate that the dominant transcript detected in the cells may relate to CCR5B expression.

However, since the general level of CCR5 transcripts detected by either end-point RT-PCR or RT-qPCR in PCa cell lines is very low (**Figure 6** and **8**), and that the CCR5A or B transcript amplification fail to show bands for PCa cell lines by end-point PCR, we need to be cautious regarding the meaning of such differences.

3.1.3 – Expression of CCR5 antisense (CCR5AS) RNA.

A recent publication has described the presence of a CCR5 antisense RNA, which is a long noncoding RNA that is supposed to regulate the expression of the CCR5 gene in primary T cells. **Figure 10** outlines the position of CCR5AS on human chromosome 3 in relation to CCR5. Using primers from Kulkarni *et al*., 2019, amplification of part of CCR5AS was tested by end-point RT-PCR (**Figure 11**) and validated for qPCR (see **Appendix: Section 5.1 and 5.2**) for relative quantification and comparison between the different cell lines (**Figure 12**).

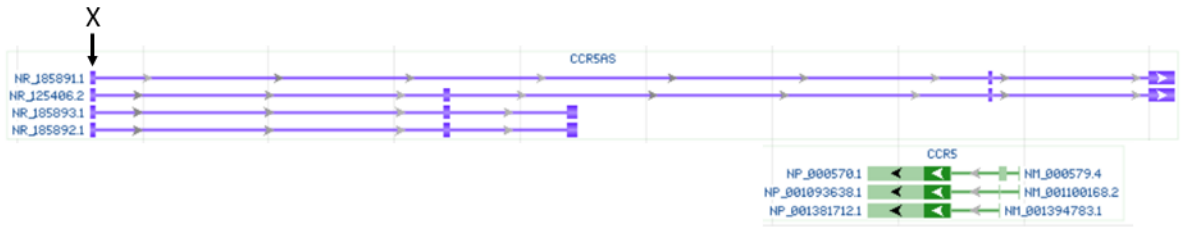

Figure 10: Graphic of known CCR5AS transcripts 1-4 in relation to known CCR5 transcripts CCR5A-C, sourced from NCBI, Seq. NC_000003.12. CCR5AS primers anneal within the region denoted by X, which covers all known CCR5AS transcripts (NCBI, No date).

Interestingly, PC3 cells appeared to express the highest level of CCR5AS by end-point RT-PCR (**Figure 11**). However, when repeating amplification by qPCR with normalisation relative to THP-1 cells used as reference, the results for PC3 and LNCaP cells were highly variable (**Figure 12a**). Nevertheless, it seems that like MDMs, PBMCs and T cells, PC3 express more CCR5AS than THP-1 while LNCaP express very low levels. This is intriguing as the expression of CC5AS is thought to be correlated with the level of cell surface CCR5 receptors, but we know that PC3 and LNCaP cells have little amount of surface CCR5 compared to the other cell types.

3.1.4 - Expression of signalling protein transcripts

We were interested in investigating if activation of the CCL5/CCR5 axis in PCa cell lines would impact the transcriptional expression of downstream signalling pathways as reported in the literature (Huang *et al*., 2021). I therefore initially assess the basal

transcript levels for the signalling proteins of interest within each cell line, and whether this correlated with what has been reported in the literature.

End point RT-PCR was performed initially to test primers specificity and get a general feel for how baseline expression of these transcripts compares between cell types (**Figure 11**). PBMCs, T cells and THP-1 showed a band for all signalling proteins selected. MDMs did express all but one transcript for E-cadherin. All primers were specific to the human transcriptome but the fact that CHO CCR5 cells had a band for several signalling proteins including CREB-1, β-catenin and EIF4EBP1 suggest that the mRNAs are conserved in rodents. For PCa cell lines, LNCaP showed a band for all signalling proteins, while PC3 showed a band for all signalling proteins except STAT3 as expected from the literature. (Bellezza *et al*., 2006)

qPCR was then used to quantitatively compare the basal transcriptional levels of the signalling proteins relative to THP-1, as shown in **Figure 12a** for CCR5AS and **Figure 12b** for signalling proteins. Although end point PCR is not quantitative, several of the transcripts' relative expression matched their relative densities in end point RT-PCR: High CCR5AS expression for PC3, Inhibitor NF-kB was higher for PBMCs and T cells, E-cadherin was higher for LNCaP and PC3 relative to the rest of the cell lines and finally, EIF4EBP1 was at comparable levels for all cell lines. Thus, qPCR confirms their transcriptional level of expression. However, some results for end point PCR do not match with qPCR, such as LKB1 and STAT3, which were not detected in PBMCs for end point RT-PCR, however both proteins were detected in qPCR.

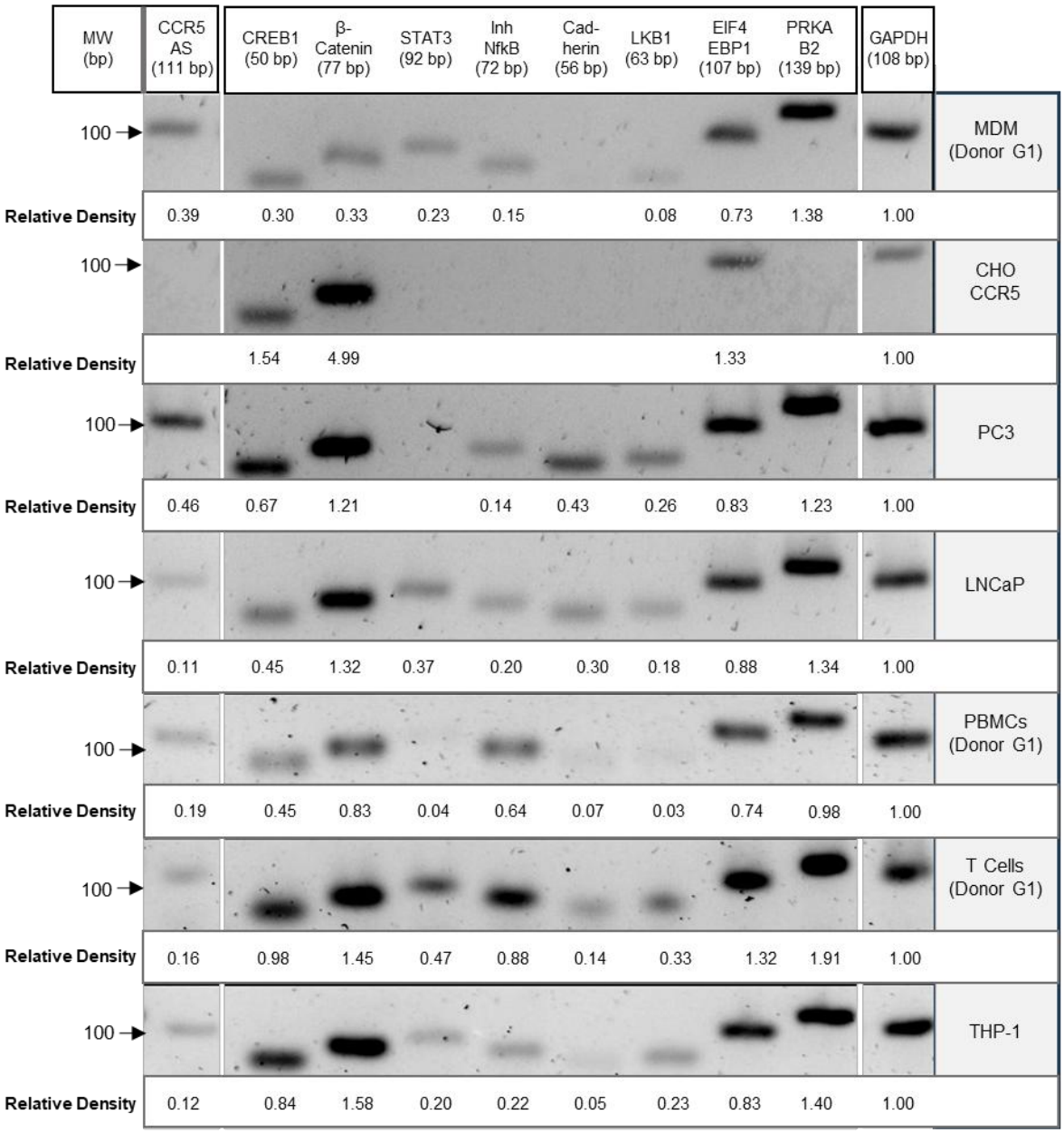

Figure 11: Baseline expression of signalling proteins in different cell types: End point RT-PCR. Gel electrophoresis showing end point RT-PCR products using primers targeting selected signalling proteins, CCR5AS and housekeeping gene GAPDH. CCR5 positive cell types were tested, as well as PCa cell lines. N=3.

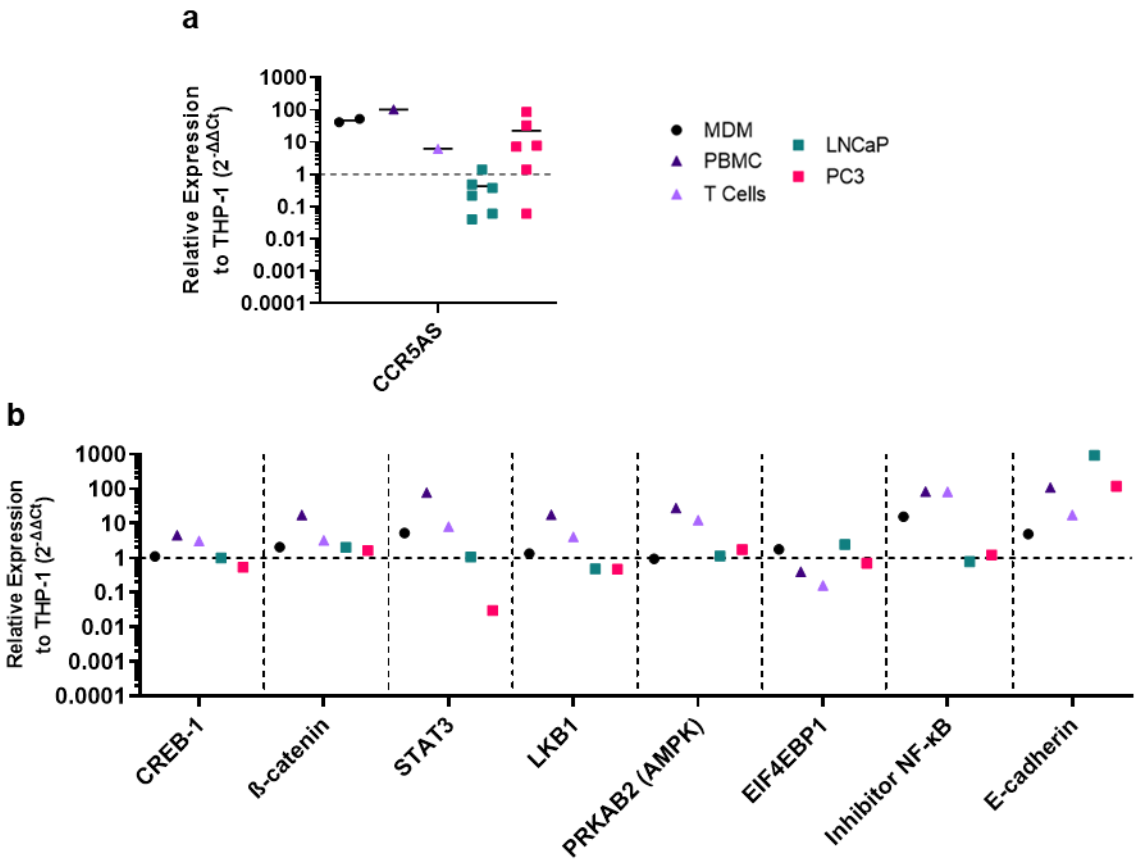

Figure 12: Baseline expression of signalling protein mRNAs in different cell types: qPCR. (**a**) qPCR data presenting relative expression of CCR5AS to THP-1, normalised to GAPDH, on positively expressing CCR5 cell types (MDM, n=2; PBMCs and T cells, n=1) and PCa cells lines (n=3). (**b**) qPCR data presenting relative expression of all signalling proteins' transcriptional expression to THP-1, normalised to GAPDH for the same samples in (**a**). Only the mean is shown for each point. Statistical testing was not performed.

The selected signalling proteins were all expressed in resting PCa cells and immune cells at varying levels, demonstrating that the signalling pathways mentioned in the literature were present and in the cell types we were working with.

3.1.5 – Assessing changes of transcriptional expression due to cell culture and growth.

As reported in the literature, CCR5, as well as many of the signalling proteins selected are involved in cell proliferative and metabolic pathways (Huang *et al*., 2021). We were interested in seeing whether the expression of all our transcripts would change with PCa cell lines growth and increased confluency. Thus, we

investigated the transcriptional expression over 48 hours of culture after cell seeding, which would reproduce the conditions of later experiments investigating the impact of cytokine/chemokine stimulation (see **section 3.2**).

RT-qPCR data were generated for LNCaP and PC3 cells upon seeding (Time 0h) or after 24 or 48 hours of culture were normalised to GAPDH as above. Results for all transcripts are presented relative to their expression at Time 0 (**Figure 13**).
With CCR5 related transcripts, despite experimental variability, no significant differences were found for LNCaP and PC3 respectively (**Figure 13a** and **d**), probably due to generally low transcriptional levels. Note that for CCR5AS transcriptional expression, even though there were no significant changes, there was a trend for increase after 48h in PC3 cells (p=0.11, **Figure 13e**).

For the signalling proteins' transcripts (**Figure 13c** and **f**) the transcriptional expression tended to increase from 24h to 48h for PC3 as cell confluency increased but not for LNCaP cells were the relative levels remained close to 1 (meaning no fold change). Despite this, statistical analysis indicated a significant increase in STAT3 between 24h and 48h (q=0.0155) for LNCaP cells, as well as for EIF4EBP1 (q=0.0006) and LKB1 (q=0.0160) in PC3 cells. This suggests that as cell grow and confluency increases, some transcripts can specifically fluctuate and it is therefore, time point matches untreated cell samples will be required in our cytokine/chemokines stimulation experiments to control for such fluctuations.

3.2 – Changes in transcriptional levels upon CCL5 Stimulation

To elucidate whether CCL5 stimulation could drive a feedback loop on CCL5/CCR5 expression as reported in the literature at 50nM, and/or induce transcriptional changes for downstream signalling proteins associated with the CCL5/CCR5 activation pathway (Huang *et al*., 2020), we were interested in looking at long term CCL5 stimulation.

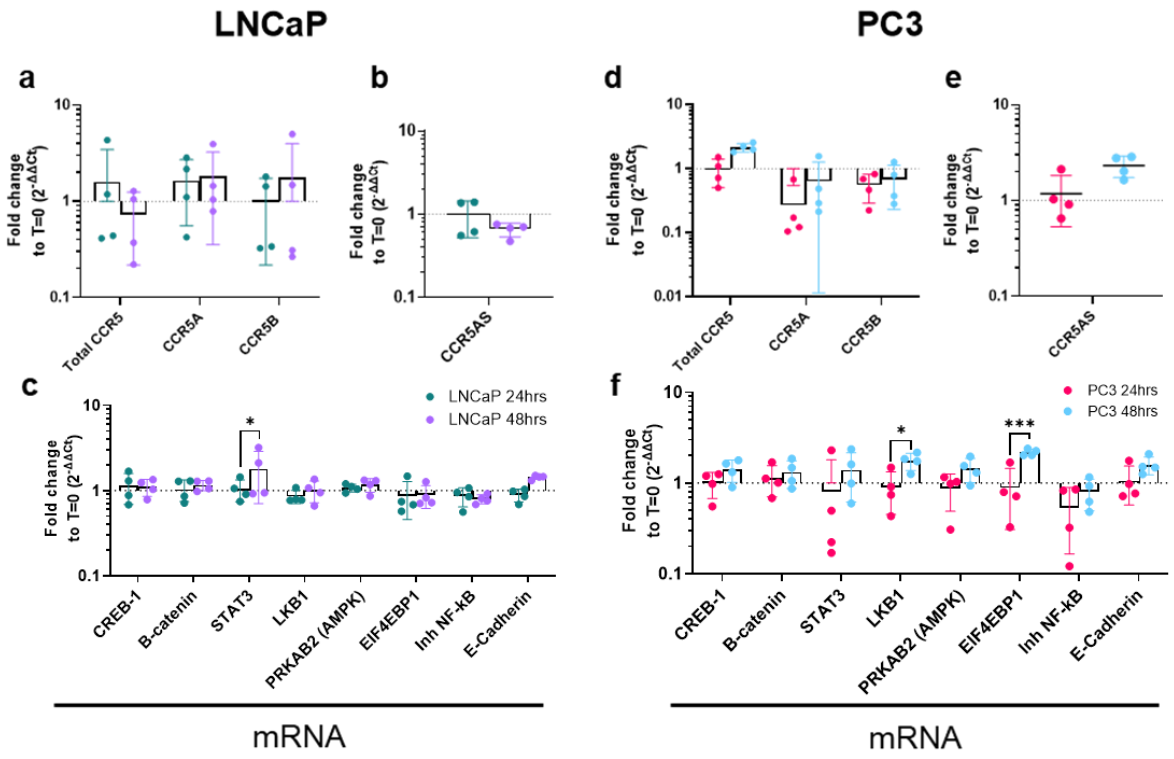

Figure 13: Changes in mRNA expression over time in PCa cells. qPCR data presenting fold change of CCR5 related transcripts, CCR5AS and various signalling proteins' mRNA expression to resting cells at 0h, normalized to GAPDH in resting PCa cells; LNCaP (**a**, **b**, **c** respectively) and PC3 (**d**, **e**, **f** respectively) (n=4, where 2 experiments run with technical duplicates). 384 well plates were used for all genes except for CCR5AS. Two-stage linear step-up procedure of Benjamini, Krieger and Yekutieli used, therefore q value instead of p value plotted, which matches the notation as described in **Section 2.14.**

As the lab has worked mostly on mechanistic actions of CCR5 upon short-term chemokine stimulation from 15 minutes to 6h, focusing mostly on immediate mechanistic actions such as phosphorylation of the receptor and calcium efflux, my project aims to explore long-term cytokine stimulation, onwards from 24h. Long-term regulation of chemokine receptors encompasses how changes in gene, mRNA and protein expression leads to a change of receptor molecules, and thus the activation of certain signalling proteins, allowing them to accumulate and generate an overall cellular effect (Bennett, Fox and Signoret, 2011). We chose time points 24h and 48h to replicate a previous study (Huang *et al*., 2020).

Experiments were performed on PCa cells with time matched unstimulated samples to control for transcription fluctuations due with cell growth. In this context, RT-qPCR was performed for CCR5 and signalling proteins described in **Section 3.2 and Section 3.3**.

3.2.1 - CCR5:

Results for CCR5 transcripts including fold change of total CCR5 transcripts compared to unstimulated sample at time point 0h plus the relative expression of CCR5A and B specific transcript over total CCR5, are presented in **Figure 13.** With LNCaP, total CCR5 transcript expression remained stable over the period of the experiment with no effect of CCL5 treatment, while PC3 cells showed an increase in CCR5 transcription between 24 and 48h related to cell growth rather than exposure to CCR5 ligand (24 vs 48h for untreated cells, p=0.0085) (**Figure 14a**).

For protein encoding transcripts CCR5A and CCR5B, the fold changes values varied widely for both PCa cell lines, with no significant differences between CCL5-treated and untreated samples (**Figure 14b**). However, for LNCaP, there seems to be a trend for an increased representation of CCR5A and CCR5B transcripts over time, yielding up to 100% of CCR5B within total CCR5 transcripts in these cells.
The level of CCR5-specific antisense RNA, CCR5AS, in LNCaP and PC3 cells also remained constant and was not affected by CCL5 stimulation (**Figure 15**).
Overall, if these experiments indicate a potential effect of cell growth on CCR5 transcription, they do not support the idea that CCL5 activation of CCR5 directly impact on CCR5 gene expression.

3.2.2. Downstream signalling proteins:

Results from RT-qPCR experiments carried out investigate changes in CREB-1, β-Catenin, STAT3, LKB1, AMPK, EIF4EBP1, Inhibitor NF-κB (Inh NF-κB) and E-Cadherin gene expression are presented in **Figure 16.** No significant changes were seen with LNCaP cells for most of the signalling proteins tested. PRKAB2, EIF4EBP1 and Inh NF-kB may indicate a transient upregulation of expression at 24h, which settles to baseline at 48h. For PC3 cells, most of the transcripts tested

remained level after 24h but increased after 48h of treatment, compared to untreated samples from matching timepoints (fold changes generally ≤1 or ≥1, respectively).

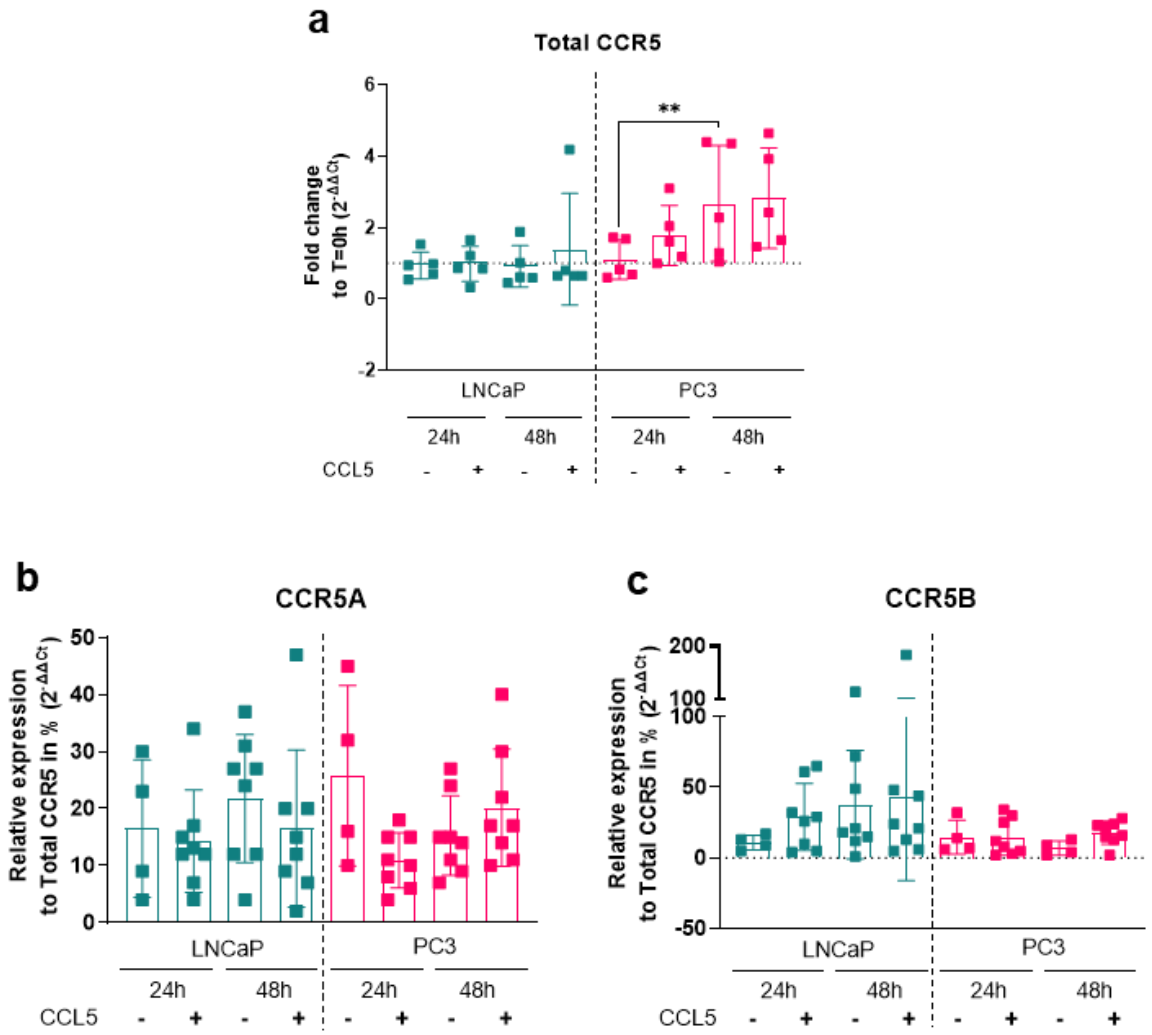

Figure 14: Expression of CCR5 transcripts upon CCL5 stimulation in PCa cells. (**a**) qPCR data presenting fold change of total CCR5 transcriptional expression, normalised to GAPDH, relative to resting sample at time point 0h (n=5, where 3 experiments were run; 2 with technical duplicates, 1 without duplicates). qPCR data presenting relative expression of CCR5A (**b**) and CCR5B (**c**) to each sample's own total CCR5 expression, normalised to GAPDH, expressed in percentage (For 24h unstimulated samples, n=4, where 2 experiments were run with technical duplicates; for rest of samples, n=8, where 4 experiments were run with technical duplicates). Two-way ANOVA was performed.

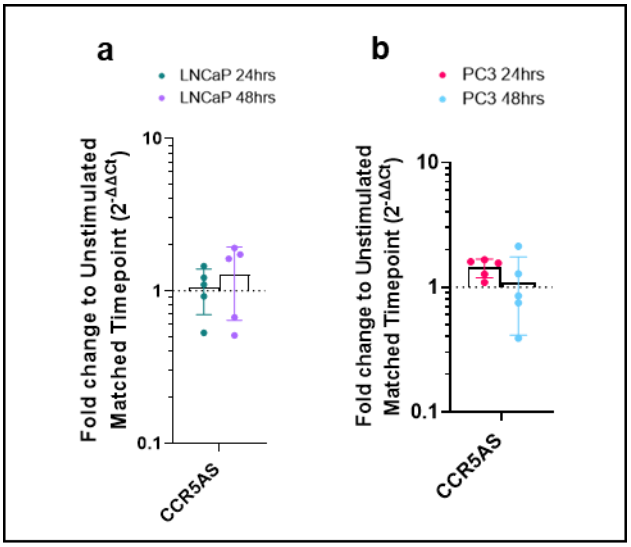

Figure 15: CCR5AS transcriptional presentation upon CCL5 stimulation in PCa cells. qPCR data presenting fold change of CCR5AS (n=6, where 3 experiments were run with technical duplicates) relative to resting sample at matched time point, normalised to GAPDH, in LNCaP and PC3 (**a, b** respectively). Statistical analysis found no significant differences.

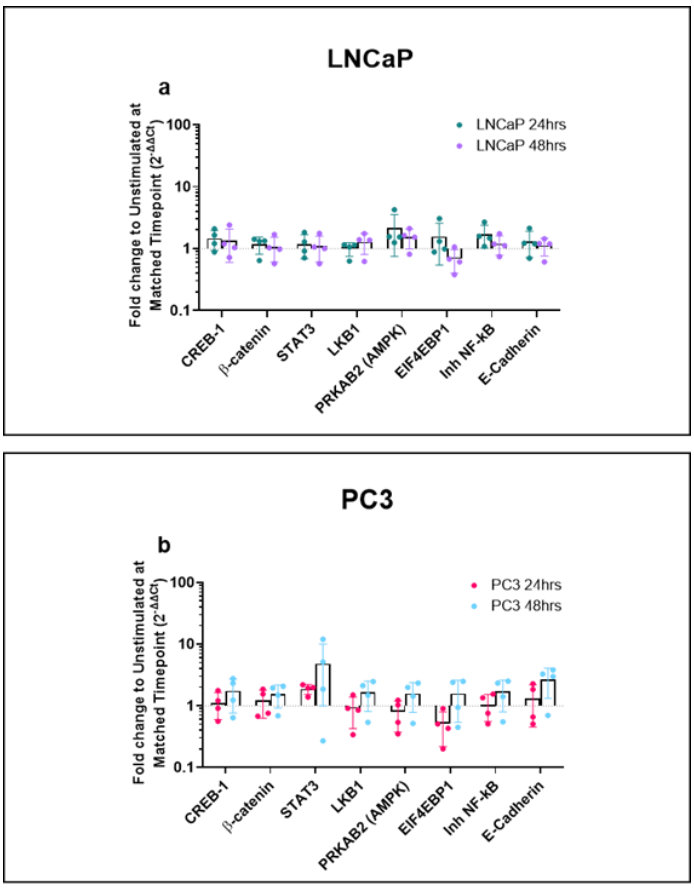

Figure 16: Signalling proteins' transcriptional presentation upon CCL5 stimulation in PCa cells. qPCR data presenting fold change of selected signalling proteins (n=4, where 2 experiments were run with technical duplicates), relative to resting sample at matched time point, normalised to GAPDH, in LNCaP and PC3 (**a, b** respectively). Statistical analysis found no significant differences.

In summary, contrary to evidence of a possible CCL5/CCR5 feedback loop, long term CCL5 stimulation of PCa cell lines does not change the transcriptional expression of CCR5 and its associated downstream signalling proteins as hypothesised based on previous studies mostly looking into protein levels, on the same PCa cell lines.

3.3 – Changes in transcriptional levels upon IL-6 Stimulation with or without CCL5

As we did not observe any transcriptional changes upon CCL5 stimulation alone, we wondered whether CCL5 plays a synergistic effect alongside other cytokines to propagate the downstream signalling pathways as reported in Colombatti *et al*., 2009. One such cytokine is IL-6, which has been suggested to regulate CCR5 expression in cancer (Weber, R. *et al*., 2020). Thus, we stimulated PCa cells with IL-6 only as well as IL-6 in combination with CCL5 and performed RT-qPCR for CCR5 and two of the signalling proteins previously tested, which appeared most relevant to our experiment, namely STAT3 known to be activated by IL-6 (Chen, Wang and Farrar, 2000), NF-κB part of the IL-6 autocrine activation pathway in prostatic tumour cells (Colombatti *et al*., 2009), EIF4EBP1 and E-Cadherin proteins related to IL-6 and STAT3 pathways of activation in cancer (Shen, X. *et al*. 2021).

3.3.1 – Expression of total CCR5 transcripts and CCR5AS

In these experiments, LNCaP cells did not show any changes for CCR5 related transcripts for any of the treatment conditions (**Figure 17a and c**). For PC3, there was an increase in CCR5 mRNAs over time but independently of treatment (**Figure 17b**) and probably due to the cell growth effect reported earlier (see **Figure 13**). For the antisense CCR5AS in PC3 cells, there was an IL-6 driven increase that appeared at 24h, remained by 48h and was not affected by additional CCL5 treatment (**Figure 17d**). However, due to low technical replicates and a large spread of values, no significant differences were found for both PCa cell lines.

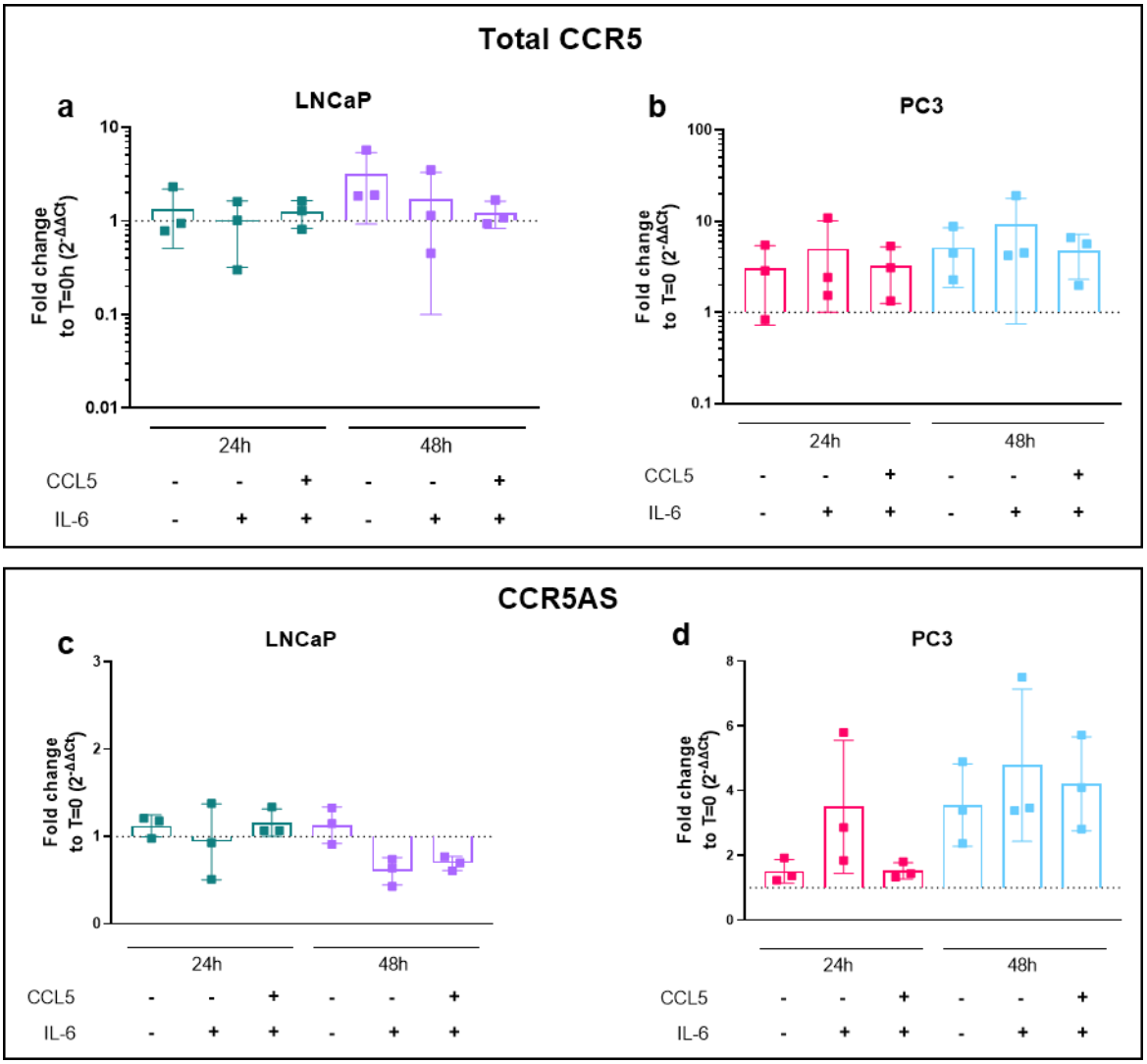

Figure 17: Transcriptional presentation of total CCR5 and CCR5AS upon cytokine stimulation in PCa cells. PCa cells were treated with cytokines IL-6 with or without CCL5. qPCR data presenting fold change of total CCR5 and CCR5AS relative to resting sample at 0h normalised to GAPDH, for LNCaP (**a, b** respectively) and PC3 (**c, d** respectively) (n=3, where 2 experiments were run, with 1 containing technical duplicates). Statistical analysis found no significant differences.

3.3.2 – Expression of STAT3, Inh NFκB, EIF4EBP1 and E-Cadherin transcripts.

With regards to STAT3 and the inhibitor of NFκB, IL-6 stimulation led to a sustained and statistically significant increase in expression for STAT3 (****=p<0.0001) but not in Inh NFκB with LNCaP cells (**Figure 18a and c).** The 2-3-fold change in STAT3 mRNA was sustained throughout the period of stimulation and was independent of the presence or absence of CCL5 in the culture (**Figure 18a**). However, this was not

the case with PC3 cells, which failed to show any indication of a transcriptional response to either IL-6 or IL-6 plus CCL5 in these same experiments (**Figure 18b and d**).

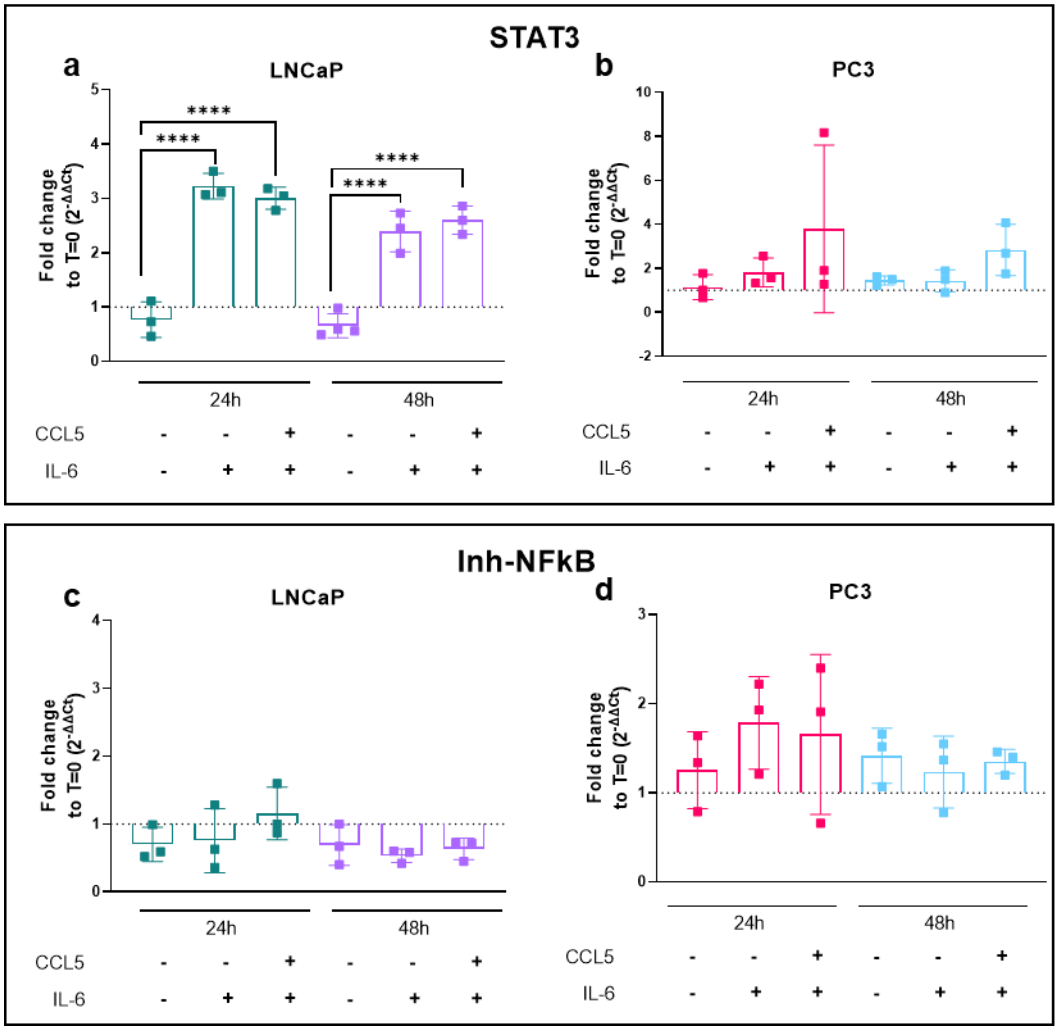

Figure 18: STAT3 and Inhibitor NF-kB (Inh NF-kB) transcriptional presentation upon cytokine stimulation in PCa cells. Cytokines treated included IL-6 with or without CCL5. qPCR data presenting fold change of STAT3 and Inh NF-kB, relative to resting sample at 0h, normalised to GAPDH, in LNCaP (**a, c** respectively) and PC3 (**b, d** respectively). Two-way ANOVA was performed.

It has been shown that in cancer, EIF4EBP1 can be transcriptionally upregulated (Voeltzke *et al*., 2022), while STAT-3 activation is associated with downregulation of E-cadherin (Xiong *et al*., 2012). With LNCaP cells, no statistical changes in transcript levels were detected for EIF4EBP1 or E-Cadherin upon IL-6 stimulation either in presence or absence of CCL5 (**Figure 19a and c**). There was a trend of

downmodulation rather than increase for E-cadherin, but this seems to be related to the duration of the experiment rather than the treatment conditions (**Figure 19c**). Interestingly with PC3 cells, there was a significant increase in EIF4EBP1 signal for samples with only dual stimulation of IL-6 and CCL5 for 48h compared to untreated samples at the same time point (**Figure 19b**). An upregulation was not seen after 24h or in the presence of IL-6 alone, suggesting a slow accumulative effect of dual CCL5 and IL-6 stimulation in PC3 cells. E-cadherin transcription levels for PC3 appeared unaffected by any of the treatments, but results from replicates were very variable for this transcript specifically (**Figure 19d**).

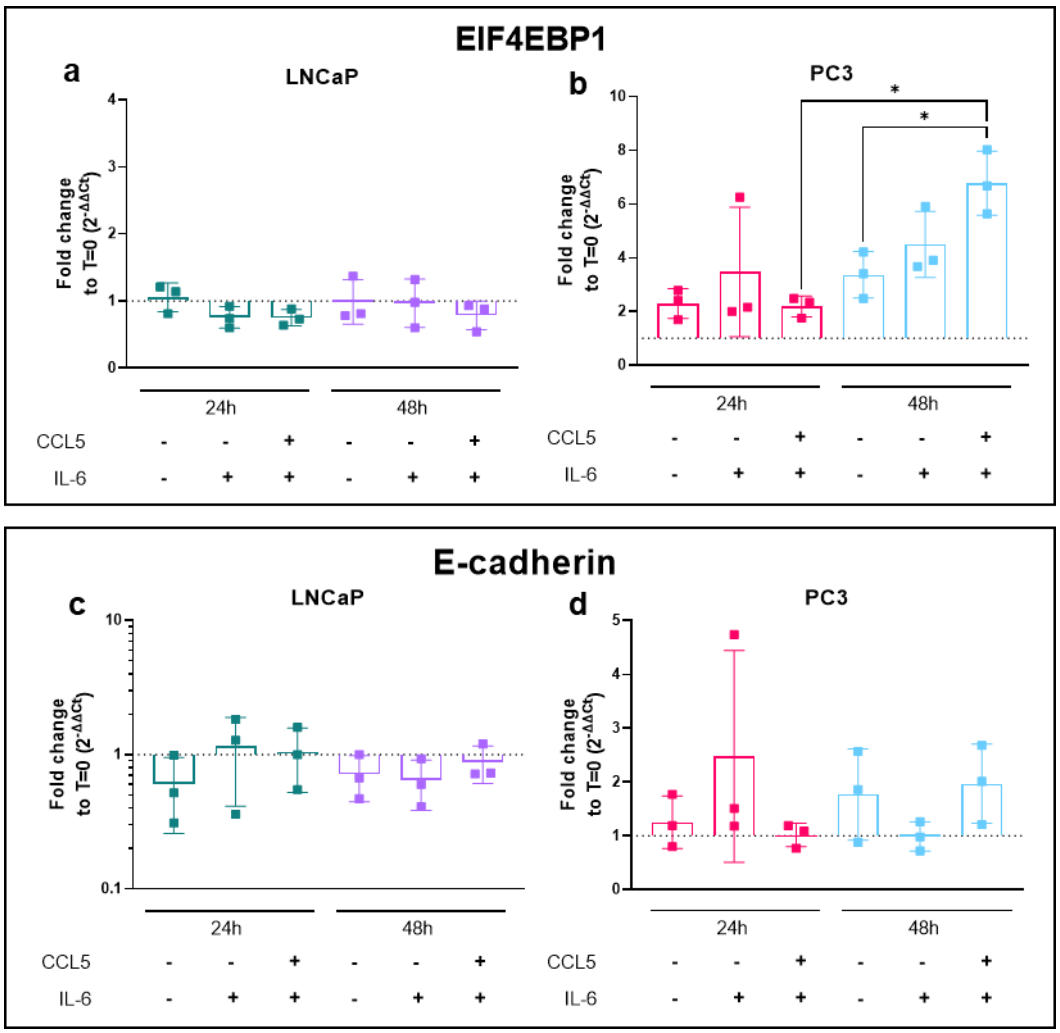

Figure 19: EIF4EBP1 and E-cadherin transcriptional presentation upon cytokine stimulation in PCa cells. Cytokines treated included CCL5 and IL-6. qPCR data presenting fold change of EI4EBP1 and E-cadherin, relative to resting sample at 0h, normalised to GAPDH, in LNCaP (**a, c** respectively) and PC3 (**b, d** respectively). Two-way ANOVA was performed.

Overall, IL-6 stimulation led to upregulation of STAT3 in LNCaP from 24h to 48h, with no differences when combined with CCL5, while the dual cytokine stimulation resulted in a delayed increase in expression of EIF4EBP1 in PC3 between 24h and 48h.

3.4 – CCR5 stimulation in LNCaP cells induces transcription of its ligand CCL4.

Unpublished observations from the Signoret lab (Afzaal Tufail PhD) indicated that CCL5 stimulation led to the secretion of chemokines (CCL2, CCL4 and CCL20) in the supernatant of LNCaP cells that were detected only after treatment. What remains uncertain is whether this is due to new transcription or simple release of pre-existing chemokines stored within the cells via the Golgi apparatus (Kuo, I.-Y. *et al.*, 2022). Cell-induced secretion should occur within minutes not hours, while transcription would take longer to feed into the extracellular release of mature chemokines. To address this issue of secretion versus transcription, we decided to measure CCL4 transcriptional levels for LNCaP and PC3 cells left untreated or treated with CCL5 for 24h, keeping the same conditions to all previous qPCR experiments. Here, we used a commercially available and validated pair of primers for CCL4 (see **Material and Methods: Table 12**). **Figure 20a** shows the fold change for both PCa cell lines, comparing CCL5 stimulated cells with unstimulated cells at matched time point, which suggest that there is an increase in CCL4 transcription upon CCL5 stimulation in LNCaP and PC3 cells. LNCaP was found on average, to have a higher fold change in CCL4 transcriptional levels compared to PC3 (LNCaP average = 9.53, PC3 average = 3.20). To confirm the upregulation of CCL4 transcripts, we performed RT-qPCR on LNCaP cells and used MDMs known to constitutively express CCL4 as amplification reference. The graph of **Figure 20b** presents paired relative expression levels of CCL4 for unstimulated and 24h CCL5-treated LNCaP cells when normalised to MDMs. This experiment confirmed that CCL5 treatment had a significant effect on CCL4 transcription in LNCaP cells.

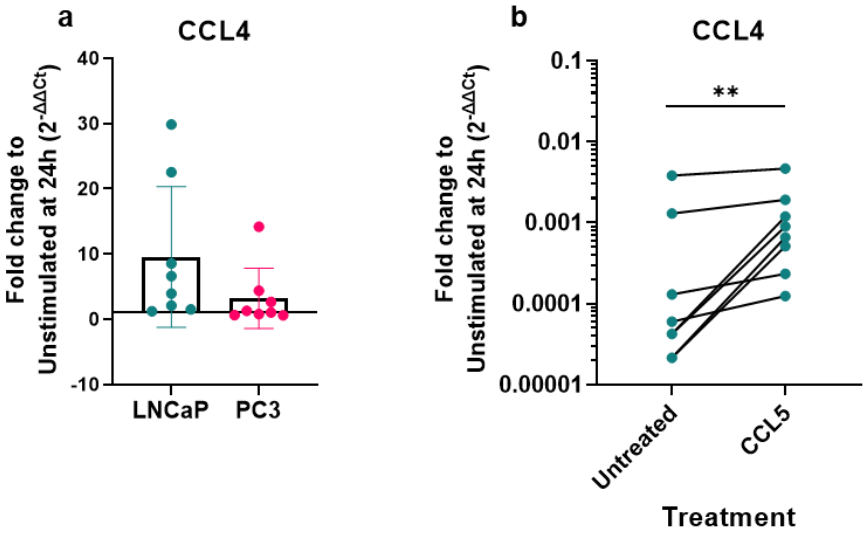

Figure 20: CCL4 transcriptional expression upon stimulation with CCL5 for 24h in PCa cells. (**a**) qPCR data presenting fold change of CCL4 relative to resting sample at 24h, normalised to GAPDH, for LNCaP and PC3 (n=8). (**b**) qPCR data presenting relative expression of CCL4 to MDM Donor G1, normalised to GAPDH, for untreated and CCL5 treated LNCaP (n=8). Paired t-test was performed.

Overall, the CCL4 findings support the hypothesis that CCL5 stimulation does induce intracellular signals driving transcriptional expression in PCa cells, leading to protein translation and ultimately secretion of CCL4.

3.5 – Changes in protein expression linked to the stimulations

After looking into the changes of transcriptional expression of CCR5 and its associated downstream signalling proteins upon IL-6 and CCL5 stimulation, we were interested in seeing whether these stimulations had an impact at the protein level. We looked at CCR5 cell surface expression itself and total STAT3 protein expression in LNCaP, as STAT3 transcripts observed a significant increase upon cytokine stimulation.

3.5.1 – CCR5 cell surface presentation

CCR5 has been reported to be present on the surface and within PCa cell lines (Vaday *et al*., 2006). Using flow cytometry, we detected CCR5 on intact cells using two different antibodies HEK/1/85a and T21/8 that recognise two distinct cell surface epitopes on the receptor (Scurci *et al*., 2021).

LNCaP are difficult cells to handle for flow cytometry staining and one critical point for my experiments was to ensure that only intact cells were accounted for in this assay. **Figure 21** shows the gating strategy that was chosen for both primary antibodies.

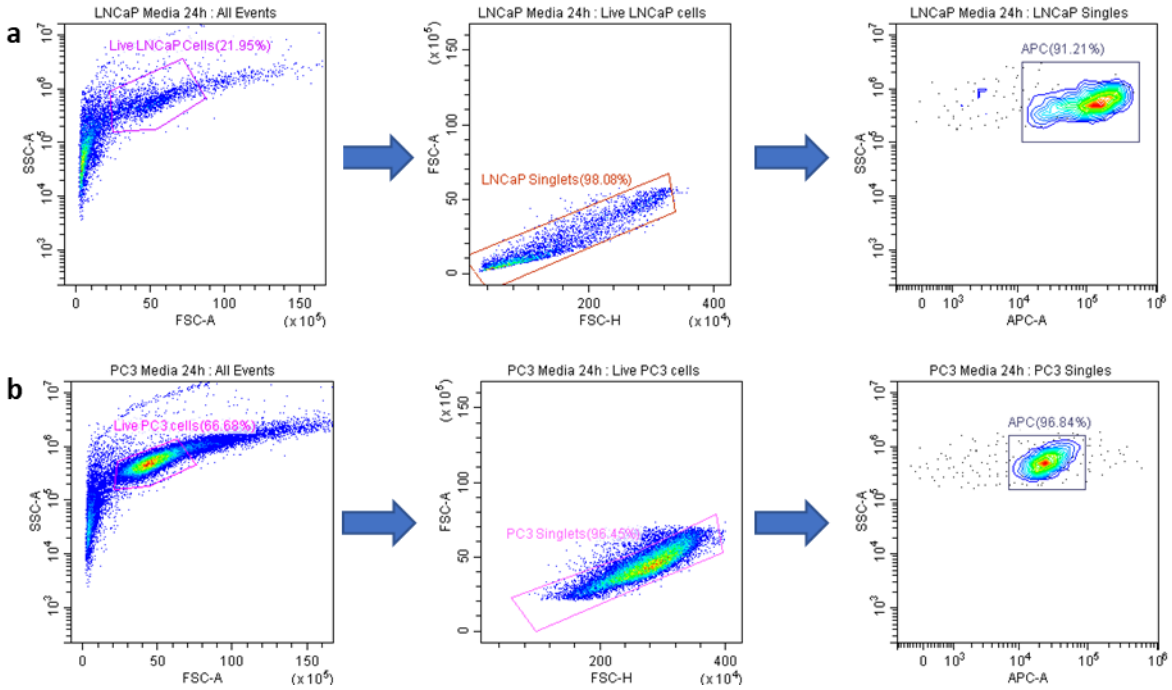

Figure 21: Example flow gating strategy to isolate live, APC expressing singlets for PCa cell lines. Gating strategy for LNCaP (**a**) and (**b**) PC3.

As shown in **Table 13,** for all samples stained with both primary antibodies, the raw MFI of experimental samples was higher compared to secondary antibody control, demonstrating some presence of the CCR5 receptor on the cell surface of both PCa cell lines. However, **Table 13** highlights the striking difference between specific MFI (difference between mean values with primary or secondary antibody only) for HEK/1/85a and T21/8, suggesting that not all CCR5 epitopes are as well recognised on PCa cells. This observation has already been reported by the lab for immune cells (Fox *et al*., 2015).

Table 13: Raw MFI (APC-A) from flow cytometry experiment showing Mean and Standard Deviation (SD) using antibody HEK/1/85a and T21/8 on PCa cell lines. 2° ab shown in bold to highlight and compare mean value with experimental samples. (n=3, technical triplicate from one experiment, n=1 for 2° ab)

Cell line	1° ab	Time point (h)	Sample	Mean	SD
LNCaP	HEK/1/85a	24	Media	8452.20	368.75
			IL-6	8834.20	324.84
			CCL5	8376.57	33.84
			IL-6 CCL5	9180.23	430.91
			2° ab	**3677.90**	N/A
		48	Media	7793.53	263.93
			IL-6	10991.93	152.32
			CCL5	8819.50	100.04
			IL-6 CCL5	11550.40	530.78
			2° ab	**3643.90**	N/A
	T21/8	24	Media	6344.37	186.58
			IL-6	6594.30	227.46
			CCL5	6921.93	236.65
			IL-6 CCL5	7118.50	194.34
			2° ab	**4022.80**	N/A
		48	Media	6391.63	145.23
			IL-6	7510.17	623.94
			CCL5	6048.40	50.92
			IL-6 CCL5	8153.67	285.33
			2° ab	**4290.1**	N/A
PC3	HEK/1/85a	24	Media	5734.50	203.22
			IL-6	5289.27	269.40
			CCL5	5121.50	331.37
			IL-6 CCL5	4836.33	254.06
			2° ab	**2019.70**	N/A
		48	Media	4776.90	237.62
			IL-6	5022.60	46.05
			CCL5	4581.70	89.01
			IL-6 CCL5	4562.40	28.28
			2° ab	**2053.20**	N/A
	T21/8	24	Media	2642.37	24.40
			IL-6	2685.13	71.47
			CCL5	2819.97	55.98
			IL-6 CCL5	2716.60	19.49
			2° ab	**2149.80**	N/A
		48	Media	2776.87	42.99
			IL-6	2712.83	57.28

PC3	T21/8	48	CCL5	2585.30	16.54
			IL-6 CCL5	2658.43	37.31
			2° ab	**2209.9**	N/A

1° ab = Primary antibody, 2° ab = Secondary antibody

CCR5 cell surface presentation increased significantly with time on IL-6 stimulated cells for HEK/1/85a in LNCaP (**Figure 22**). At 24h, all experimental samples had comparable ratio MFI, however all IL-6 stimulated cells at 48h increased dramatically compared to both media and their counterparts at 24h. The same trend was found in T21/8 for LNCaP, although without significant differences. Contrary to HEK/1/85a, for T21/8 there was a drop of expression between 24h and 48h for CCL5 only stimulated LNCaP.

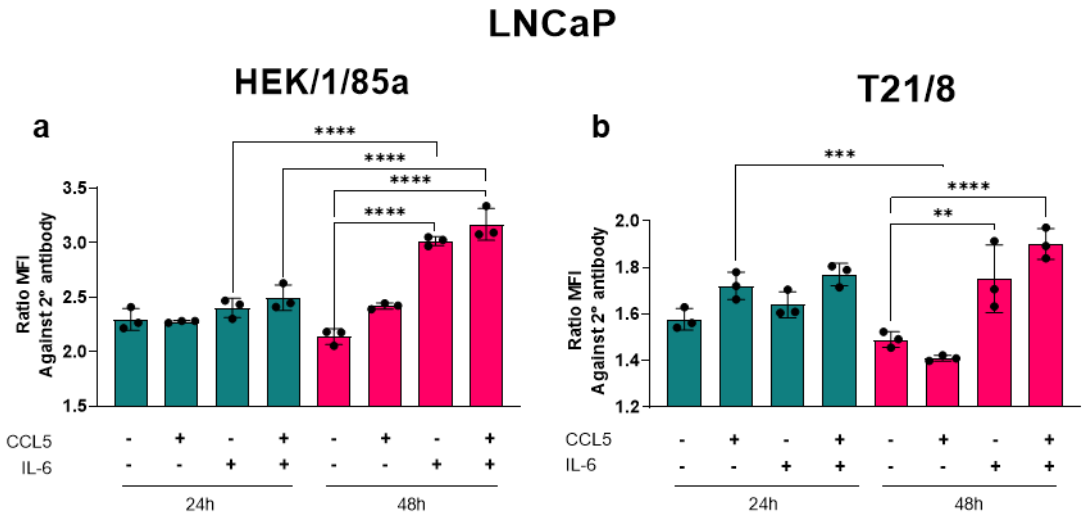

Figure 22: CCR5 cell surface presentation of LNCaP upon cytokine stimulation using HEK/1/85a and T21/8 antibodies. Flow data presenting ratio MFI (Raw MFI of experimental sample divided by Raw MFI of secondary antibody only) using primary antibody HEK/1/85a and T21/8 (**a** and **b** respectively). Two-way ANOVA was performed.

On PC3 cells, CCR5 cell surface detection by HEK/1/85a decreased over the period of the experiment, even in medium alone but the decrease was more pronounced with CCL5 treatment at 24h and 48h (**Figure 23**), suggesting an additive effect of chemokine stimulation. As for T21/8, a transient increase upon CCL5 treatment was observed at 24h compared to media at the same time point with a return to baseline by 48h.

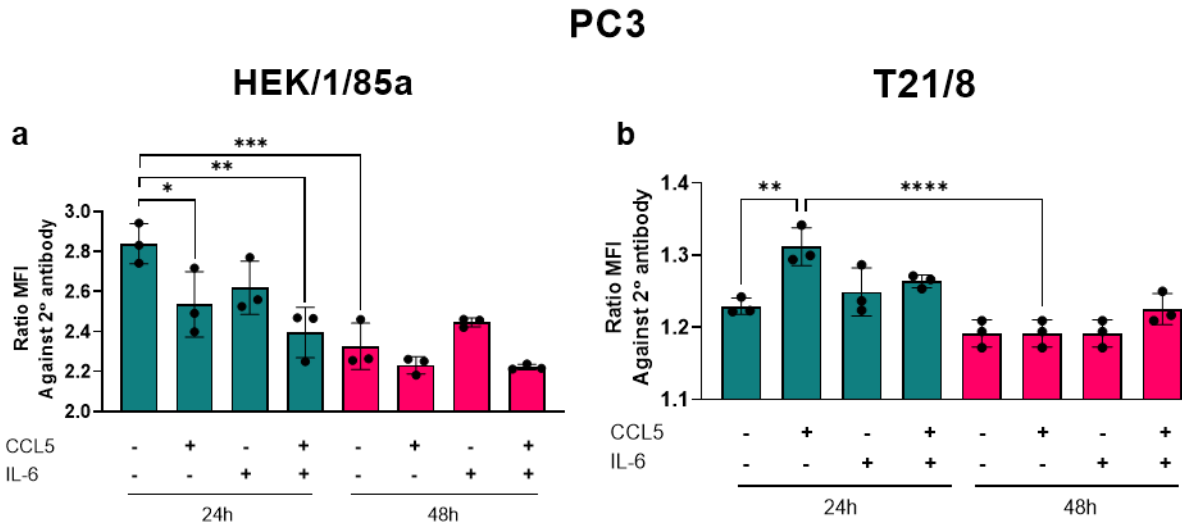

Figure 23: CCR5 cell surface presentation of PC3 upon cytokine stimulation using HEK/1/85a and T21/8 antibodies. Flow data presenting ratio MFI (Raw MFI of experimental sample divided by Raw MFI of secondary antibody only) using primary antibody HEK/1/85a and T21/8 (**a** and **b** respectively). Two-way ANOVA was performed.

Interestingly, this drop in T21/8 detected change in surface CCR5 between 24h and 48h of CCL5 treatment was also noted with LNCaP cells (**Figure 22**). However, the low level of T21/8 specific fluorescent signal for LNCaP (Mean of experimental sample divided by mean of secondary only, see **Table 13**), and even lower signal for PC3 makes it difficult to ascertain whether this reflects a true modulation of CCR5.

In summary, using both antibodies to stain for CCR5 at the cell surface, LNCaP showed an increase with time amplified by IL-6 stimulation while PC3 showed a decrease with time. With both cell lines, the T21/8 antibody indicated a transient CCL5 mediated positive change compared to cells kept in medium at 24h with a

return to baseline by 48h. These represent cell-line specific and very subtle changes that would require extensive experimental repeats for validation.

3.5.2 – Total STAT3 presentation

As indicated in the RT-qPCR results, long term IL-6 stimulation with and without CCL5 induces a significant upregulation of STAT3 transcription in LNCaP. We wanted to investigate whether this increase in STAT3 transcriptional level consequently led into an increase in STAT3 protein level. We were also interested in whether, upon long-term stimulation of IL-6, which could potentially induce an IL-6 autocrine loop, STAT3 would phosphorylate at Tyr705 and subsequently be translocated into the nucleus as indicated in the literature (Lee *et al*., 2012). Hence, Western Blot was performed on lysates of PCa cell lines after long-term stimulation of IL-6 with or without CCL5, which were separated into cytosolic and nuclear fractions and tested for total and phospho-STAT3 (Tyr705) separately. Cytosolic fractions are presented only, as the loading control of the nuclear fractions failed.

Presence of total and phospho-STAT3 (Tyr705) for the cytosolic fraction of LNCaP is shown in **Figure 24.** IL-6 stimulation increased STAT3 protein levels in the cytosol compared to untreated, an effect that was sustained regardless of CCL5 treatment. Mirroring transcriptional levels, IL-6 stimulation transiently increases STAT3 at 24h and tapers at 48h, for both total and phospho-STAT3. Interestingly, for both proteins at 24h, dual cytokine stimulation has a slightly higher relative density than IL-6 stimulation only, suggesting a possible synergistic action. Dual and IL-6 only stimulation tapers at 48h to a similar relative density for both total and phospho-STAT3, implying that multiple isoforms of STAT3 other than phospho-STAT3 at Tyr705 could be responding at a similar rate. CCL5 stimulation only does not change STAT3 levels. It is important to note that the bands for phospho-STAT3 at Tyr705 appears smeared, suggesting multiple isoforms, known as STAT3α and STAT3β, at different sizes of STAT3 are at play (Hevehan, Miller and Papoutsakis, 2002).

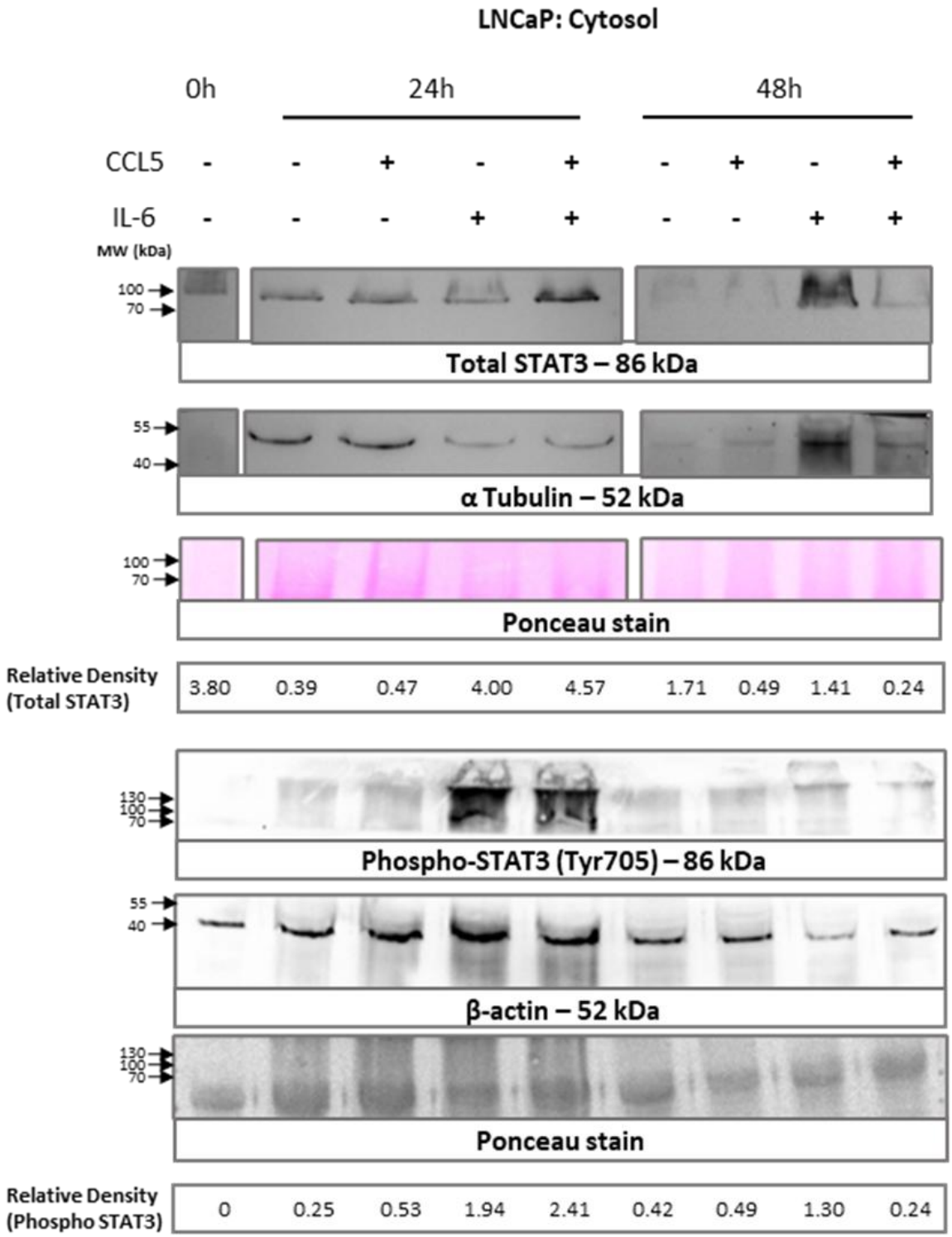

Figure 24: Detection of Total and Phospho-STAT3 (Tyr705) in the cytosolic fraction of LNCaP upon long term cytokine stimulation. Western blots present cytosolic fractions stained with antibodies against Total and Phospho-STAT3. For the loading control, cytosolic fractions were stained with antibodies against α-Tubulin and β-actin respectively. N=1 for Total STAT3. N=2 for Phospho-STAT3.

STAT3, both total and phosphorylated at Tyr705, in LNCaP increase with IL-6 treatment. The small increment seen with CCL5 co-stimulation would fit with existence of a synergy between CCL5 and IL-6 acting to potentiate STAT3 expression, but further validation would be required to ascertain the reproducibility of these changes.

Finally, **Figure 25** evidences the lack of STAT3 protein expression in PC3 regardless of timepoint and treatment. Since PC3 do express CCR5 even if at a very small level, this would suggest that any synergy may be context specific.

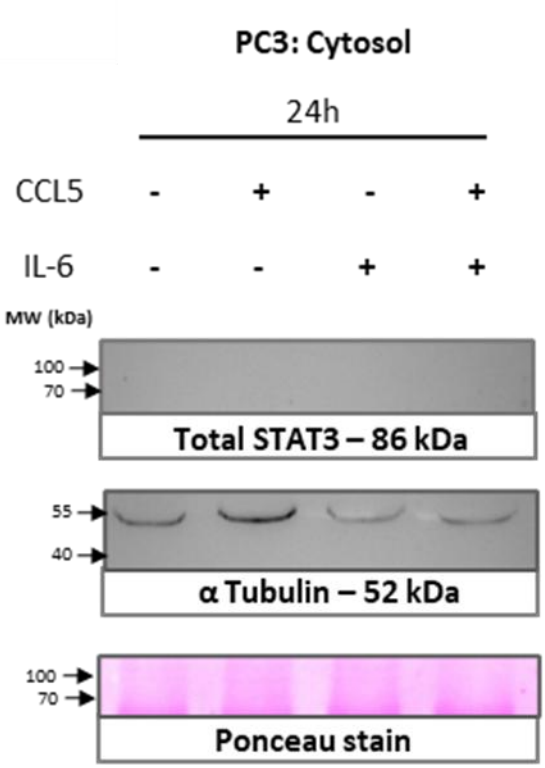

Figure 25: Detection of Total STAT3 in PC3 upon long term cytokine stimulation. Western blots present cytosolic fractions stained with antibodies against Total STAT3. For the loading control, cytosolic fractions were stained with antibodies against α-tubulin. N=1.

4. Discussion

My project aimed to investigate whether cytokine stimulation – in the form of CCL5 with or without IL-6 stimulation – on PCa cell lines would impact the transcriptional modulation of CCR5 and its associated downstream signalling pathways in tumourigenesis. The results I have gathered indicate that, although both PCa cell lines model for metastatic PCa (Sampson *et al*., 2013), LNCaP and PC3 are very different in their baseline mRNA levels, as well as cell surface CCR5 expression levels, and signal transduction responses to cytokines. IL-6 induced intracellular changes in STAT3 for LNCaP for both transcripts and protein, as well as EIF4EBP1 transcript in PC3.

Regarding both transcriptional and cell surface levels of CCR5, we cannot confirm the presence of a CCL5/CCR5 autocrine loop due to inconsistent, non-significant findings and low experimental repeats. Furthermore, overall transcriptional expression of CCR5 was low in resting PCa cells compared to primary blood cells (MDMs, PBMC and T cells) and even THP-1. The THP-1 cell line is a human monocytic cell line derived from a blood leukemic origin and are less developed macrophages, which is a commonly used model for studying monocytes and macrophages (Chanput, Mes and Wichers, 2014). Therefore, THP-1 are akin to other primary immune cells and are likely to express CCR5. Vaday *et al* found that PC3 and LNCaP cells expressed CCR5 on the cell surface using flow cytometry (Vaday *et al*. 2006), and I confirmed such expression using two different CCR5 monoclonal antibodies albeit at very modest levels (**Table 12, Figure 22** and **23**).

I aimed to define which of the specific CCR5 transcripts may be associated with receptor expression, which were either CCR5A, B or any other truncated mRNAs as defined by Mummidi *et al*. 1997. However, we found some inconsistency by end-point RT-PCR as well as RT-qPCR particularly using the P1 and P4 primer pairs (**Figure 8a**). Theoretically, these pairs should amplify the same number of PCR product, however these primers bind within the ORF region, and wildtype transcripts of CCR5 should not differ in this region. A similar phenomenon was observed in MDMs, where there was strong amplification of P3 pair, which detects CCR5A

specifically, however very weak amplification in the BLAST designed CCR5A primers (**Figure 8**)**.** Regarding P1 and P4 pairs, their primers' efficacy could have varied due to Tm differences which affect annealing efficiency of primers, as listed in **Table 6** and **8**. As for P3, due to the primers annealing within Exon 2A and Exon 3, and not between exon-junctions like the BLAST designed CCR5A primers, P3 may have lacked specificity to CCR5A. P3 may have detected a truncated transcript, or several transcripts, which do not contain Exon 1, but are involved in the regulation of CCR5 (**Figure 2b** and **c**).

Primary blood cells and THP-1 additionally expressed exon 1-containing transcripts in both end point and RT-qPCR, which is expected as these cells are known to strongly express CCR5 transcripts (Tuttle *et al*., 1998) and exon-1 containing transcripts were defined in these cell types (Mummidi *et al*., 1997). This is unlike LNCaP and PC3 cells, which only showed weak amplification of these transcripts in the form of very high Ct values by RT-qPCR.

Primers for the specific detection of either CCR5A or B transcripts were very inefficient even in primary cells, suggesting that these represent only a marginal pool of CCR5 transcripts. Perhaps the number of CCR5A or B transcripts does not reflect the abundant cell-surface CCR5 seen on immune cells. Recently, the theory where single ORFs code for single proteins has been challenged and instead a single mRNA may code for multiple proteins. Proteomics and ribosome profiling have detected productive translation of alternative open reading frames leading to non-annotated alternative proteins, which in some cases can interact with the main known protein with functional consequences (Mouilleron, Delcourt and Roucou, 2015). Such a situation may account for the uncoupling of CCR5 mRNA and protein expression that we observed and that was recently raised as a limitation to our understanding of this receptor (Bauss *et al*. 2021). Note that although CHO CCR5 showed strong CCR5 expression, it was impossible to study CCR5 transcriptional regulation in these cell lines as they were transfected with CCR5 cDNA generated from the ORF sequence and therefore only contain exon 3 (Mack *et al*., 1998). Our experiments showed a better signal with primers annealing within the ORF, which seem to dominate the transcriptional activity in primary blood cells as well as cell

lines. This mirrors what is reported on Ensembl and NCBI, as all known CCR5 transcripts contain the ORF (Ensembl, no date – b; NCBI, 2009). Furthermore, as the primers would detect all CCR5 transcripts (i.e. protein coding and regulation) and this result may also reflect CCR5 protein expression, as described in the literature (Oppermann, 2004) and the findings in our lab (A. Tufail ongoing PhD).

Comparing LNCaP and PC3, I found that PC3 had more CCR5 transcripts containing Exon 3 than LNCaP for end point PCR, however, I could not confirm this with qPCR. A Gene Expression Omnibus (GEO) analysis compared the two PCa cell lines without treatment using studies that conducted microarrays: GSE56352 and GSE84970 (Wyce *et al*., 2013; Zhao *et al*., 2017). It was found that PC3 had a slightly higher CCR5 transcriptional expression, thus aligning with my end point PCR findings. I found by flow cytometry that the specific CCR5 protein signal was higher in LNCaP than in PC3 cells, and this is in agreement with previous findings from Vaday *et al*. showing that LNCaP expressed more CCR5 on their cell surface than PC3 (Vaday *et al*., 2006). Interestingly from these results, transcriptional expression may not equate to CCR5 cell surface expression and may be due to a large proportion of CCR5 transcripts being involved in regulation rather than protein expression (Dhamija and Menon, 2018).

CCR5A and CCR5B were not detected by end-point PCR in PCa cells but were detected at very low levels in qPCR, yielding high Ct values. The difficulty with weak amplifications is the high variability in determining values for relative expression and fold changes especially between biological replicates. For some of the CCR5 transcripts, amplification was close to the lower limit of quantification, which is generally accepted to be above 100 copies, under 30 Ct. (Taylor *et al*., 2019). Besides very low number of transcripts, variability can come from redundancy, however all primers had been screened for specificity prior to testing using BLAST. This is also why it is highly unlikely that the protein transcripts (CCR5A and B) encompass a high proportion of total CCR5 transcripts, as total CCR5 transcripts for some samples were measured close to the lower limit of detection as well, inflating their proportions. Taking the results from end point PCR and qPCR together, CCR5A and B occupy a very low number of transcripts for all cell types tested. Comparing

the abundance in detection of non-protein coding transcripts using P3 primers in MDMs, this emphasises the magnitude of regulating transcripts occupying the transcriptome.

The basal expression of signalling proteins fluctuated with cell growth, an indication that these signalling pathways are involved in general cell activities, like attachment spreading, division, etc. Note that STAT3 was found to be expressed in LNCaP but not in PC3, a finding which matches what has been published by others (Mohanty *et al*., 2017; Pencik *et al*., 2023). Pencik *et al*. postulated that in STAT3 expressing cells, mTOR pathway is negatively regulated by the LKB1/pAMPK/STAT3 pathway, whereas in STAT3 deficient cells (i.e. PC3), mTOR and LKB1/pAMPK pathways become independent of STAT3. My results support this, as upon growth with time in PC3, LKB1 and EIF4EBP1 (a subunit of mTOR) increase in conjunction and are therefore not expressed in contrast to one another. This supports the theory that PC3 is a more aggressive PCa model than LNCaP, following a non-canonical pathway, whereas LNCaP appears to follow the canonical LKB1/pAMPK/mTOR pathway (Shaw, 2009).

Furthermore, upon IL-6 and CCL5 stimulation, mTOR activity is increased in PC3, which was further amplified from 24h to 48h, suggesting a self-sustaining loop. IL-6 acts to suppress mTOR in mice models of PCa, specifically in LNCaP (Chang *et al*., 2014). Interestingly, androgen deprivation was key to achieve this result. As PC3 is androgen insensitive, potentially PC3 adapted an alternative molecular mechanism to surpass this suppression, resulting in the opposite effect. Audet-Walsh *et al*. found that in androgen insensitive PCa models, mTOR can transcriptionally and phenotypically alter metabolism related pathways, suggesting that mTOR plays a crucial role in cell metabolism in the absence of AR signalling, upon long term exposure to mTOR antagonists (Audet-Walsh *et al*., 2017). This effect could be compounded with a tumourigenic milieu of cytokines like IL-6 and CCL5 derived from the TME by TAMs, leading to dysregulated metabolism; one of the hallmarks of cancer.

Aligning with my findings, it has been reported in the literature that LNCaP and PC3 were found to react differently in terms of the inflammatory signalling in response to

IL-6 (Bennett *et al*., 2023). This could be due to the expression of PSMA, STAT3, Suppressor of Cytokine Signalling 3 (SOCS3), and/or AR, all of which apply to LNCaP, and interestingly, not to PC3. SOCS3 acts to suppress STAT3 expression, so consequently LNCaP has low SOCS3 expression, while PC3 has high SOCS3 expression. IL-6 specifically activates STAT3 (Bellezza *et al*., 2006). Additionally, STAT3 status is associated with AR signalling, (Chen, Wang and Farrar, 2000), and LNCaP is AR dependent. Interestingly, Chung *et al*. reported that LNCaP does not secrete IL-6, while PC3 does, and both PCa cell lines were reported to express IL-6R and gp130 (Chung *et al*., 1999). All mentions of transcriptional expression findings from studies have been confirmed with the GEO analysis as mentioned previously. IL-6 secreted by tumour associated immune cells of the TME could be acting via the STAT3 pathway in LNCaP, promoting tumorigenesis, again following a canonical pathway. In PC3, representing a later stage of mPCa, IL-6 could be constitutively being produced, to promote tumourigenesis in other cells of the TME. IL-6 can promote androgen independent growth in LNCaP, but only in an androgen derived microenvironment, which models castrate resistant PCa TME, suggesting that IL-6 is a key growth factor in castrate resistant cancer (Lee *et al*., 2003).

The IL-6/JAK2/STAT3 pathway plays a role in cancer (Huang, Lang and Li, 2022), has been found to regulate CCR5 expression (Wang *et al*., 2024) and is strongly linked to IL-6 dependent cancer cell activation (Xu *et al*., 2021). Furthermore, Huang *et al*. found that CCL5 secreted by TAMs promotes PCa metastasis via the CCR5/β-catenin/STAT3 pathway (Huang *et al*., 2020). Vice versa, CCL5/CCR5 axis could lead to IL-6 production in PCa cells. Additionally in the same study, IL-6 and CCL5 work synergistically to promote cell proliferation in PCa cells via NF-kB (Colombatti *et al*., 2009). However, in my study, no change on NF-kB was observed, therefore the IL-6/JAK2/STAT3 pathway may have taken an alternative pathway. One such pathway could be via upregulation of SOCS3, as previously demonstrated in melanoma (Tang, Jiang and Liu, 2015), where blockade of CCR5 suppressed IL-6/STAT3 pathway, specifically in myeloid derived suppressor cells (MDSCs). MDSCs may be exploited to secrete immunosuppressive mediators such as IL-6 in favour of the maintenance of the TME.

Activation of the IL-6/STAT3 pathway was observed in LNCaP at both the transcriptional and protein level. This is a known response that has been studied extensively, confirming that the IL-6 used in my study is active (Huang, Lang and Li, 2022). Only phospho-STAT3 at Tyr705 was tested and not Ser727, which has been reported to be required for maximal transcriptional activation (Wen, Zhong and Darnell, 1995), however, may not have been required as it has been reported to be associated with short term response (Lee *et al*. 2012). Tyr705 has been found to be associated with protein synthesis, which aligns with our finding as phospho-STAT3 Tyr705 levels corresponds with the total STAT3 levels for all cytokine treatments, suggesting that this response represents protein synthesis. Regarding protein levels, IL-6 treatment leads to a sustained response at 48h, while dual cytokine treatment appears to return to baseline at 48h. However, regarding mRNA levels, STAT3 response is sustained for both IL-6 only and dual cytokine treatment. As the STAT3 primers cover all mRNA transcripts of STAT3, and the Western Blot antibodies cover distinct isoforms STAT3α and STAT3β, alternatively spliced from the same RNA (Schaefer, Sanders and Nathans, 1995), potentially the type of protein isoforms was altered from an isoform containing a phosphorylation group at Tyr705, to an isoform that does not, upon long-term cytokine stimulation, while keeping the total STAT3 mRNA content. The other isoforms of STAT3, which do not contain Tyr705, known as STAT3γ and STAT3δ, may have increased, with functions not as clear as STAT3α and STAT3β, however have been postulated to have negatively regulating functions, which could explain why protein levels decreased while mRNA levels remained stable (Hevehan, Miller and Papoutsakis, 2002; Aigner, Just and Stoiber, 2019).

In the literature, there has been discussion regarding the role of STAT3 as a tumour promoter, and whether it can be used as a target for therapy. Likely in my study, STAT3 was acting as a tumour promoter, as the IL-6/STAT3 pathway has been linked closely with cancer as mentioned (Huang, Lang and Li, 2022). STAT3 has been reported to be acting as a tumour suppressor under certain conditions, one being under PTEN deficiency, loss of which is common in PCa metastasis and consequently in the cell lines tested. However this is contrary to LNCaP, which expresses STAT3, but has loss of PTEN (Pencik *et al*., 2023; Iglesia *et al*., 2008;

Sharrard and Maitland, 2007). IL6/STAT3 axis has been studied as a potential target under scrutiny, as knockdown studies of IL-6, PTEN and STAT3 aggravate PCa (Pencik *et al*., 2015). Additionally, the two main isoforms, STAT3α and STAT3β, are associated with tumour promoting and suppressing respectively. These findings suggest a multifaceted role of STAT3 in cancer.

E-cadherin was also highly expressed in PCa cell lines relative to the rest of the cells tested. E-cadherin is a known tumour suppressor protein which is involved in cell adhesion – loss of which is involved in epithelial-mesenchymal transition. Both LNCaP and PC3 express E-cadherin at a basal level, which is contradictory to E-cadherin being a tumour suppressor protein. However, in one study on liver metastasis in PCa, it was found that E-cadherin expression is switched on during distant metastasis, to prevent cell death and aid with cell migration (Ma *et al*., 2016). As both LNCaP and PC3 are cell lines isolated from metastasis of PCa, this could explain why they express E-cadherin.

CCL5 does not appear to have any effect of the CCR5 transcription and its related downstream signalling pathways in PCa cell lines, contrary to the literature. This could be due to the different experimental conditions, such as starvation of PCa cells before chemokine stimulation done in many of the studies mentioned, which may not be replicable in real life conditions as cancer cells grow and evolve in a nutrient rich cellular environment (Buono and Longo, 2018). A simpler explanation could be that there is lack of CCR5 expressing on PCa cells, so insufficient CCR5 binding to CCL5 could not lead to an accumulative effect. However, the literature has been unable to show an upregulation of CCR5 in PCa tissues or primary cells from patients, specifically tumour infiltrating immune cells, which would be more biologically relevant, but CCL5 upregulation in patient samples has been reported (Huang *et al*., 2020; Gregg *et al*., 2010). Computational analysis of publicly available transcriptomic data from prostate clinical samples performed by a student in the lab, revealed that CCR5 gene expression was initially high relative to normal prostate in benign and localised PCa tissues, before decreasing at metastatic sites (Moxom, 2021). Low expressing CCR5 in mPCa aligns with what I have found. As the TME has a heterogeneous population consisting of fibroblasts, endothelial cells, epithelial

cells and immune cells to name a few (Bahmad *et al*., 2021), the CCR5/CCL5 axis may be mediating its effects as reported in the literature primarily in the immune cell portion of the TME.

CCL5 could induce remodelling in the TME, however this effect was exhibited with CCR1 rather than CCR5, evidencing that due to the promiscuous nature of both CCL5 and CCR5, these proteins are likely to function separately as a small part of an interconnected network (Kato *et al*., 2013). Thus, CCR5 not alone, but in synergy with other chemokine receptors may have an impact on tumourigenic effects as published. One study on coffee compounds having an anti-cancer effect on PCa, found that proliferation and migration of PCa were downregulated upon treatment as well as both CCR2, CCR5, STAT3, AR and some anti-apoptotic proteins.

The transcriptional upregulation in CCL4 induced by CCL5 stimulation shows that the CCL5 I used is active and supports another experiment where CCL4 was secreted by PCa cell lines upon CCL5 stimulation (A. Tufail ongoing PhD). Thus, CCL4 is being newly synthesised from mRNA to protein, and then secreted. The CCL5/CCR5 axis may have a role in the homing of cancer cells to develop metastasis (Sicoli *et al*., 2014), rather than proliferation. As a supplement, I tested whether CCL5 stimulation would increase cell count, finding non-significant differences (**Supplementary Figure 6**), thus substantiating that CCL5 has no effect on proliferation. Perhaps CCL5 induces secretion of other chemokines to induce homing of PCa cells in the TME, which is why CCL4 is secreted as a remnant of a migratory and metastatic phenotype. Interestingly, CCL4 mainly binds CCR5 (Onuffer and Horuk, 2002), has been reported to drive bone metastasis in breast cancer via CCR5 (Sasaki *et al*., 2016) and play an important role in chemotaxis of pathogenic T cells (Patterson *et al*., 2016). Fang *et al*. found that CCL4, via AR signalling and STAT3 activation, was key to macrophage-induced prostate tumourigenesis, which was tested by coculturing immortalised prostate epithelial cell lines and THP-1 (Fang *et al*., 2013). This finding aligns with what I have found in CCL5 stimulation, which led to CCL4 upregulation in LNCaP, as LNCaP are AR dependent and STAT3 positive. However, STAT3 was not upregulated upon CCL5 stimulation, suggesting that this effect is only observed in a mixed population of cells,

resembling the TME. As PC3 are not AR dependent and are STAT3 negative, this could be one reason why PC3 did not respond as strongly to CCL5.

Upon CCL5 stimulation, there is a disagreement between the two antibodies used in LNCaP, where HEK/1/85a shows an upregulation at 48h, and T21/8 shows a downregulation at 48h. Moreover, PC3 appears to decrease in number of CCR5 on the cell surface upon treatment, while LNCaP appears to do the opposite. This could be due to the nature of GPCRs that have a variety of conformational states depending on ligand binding and the membrane environment (Fox *et al*., 2015). As different cell lines I tested with possess vastly different characteristics, they are likely to react differently to CCL5 stimulation, and therefore the CCR5 on their cell surface will have different conformational states which bind differently to the antibodies tested. HEK/1/85a was found to bind outside of the CCR5 chemokine binding site (Mueller *et al*., 2002), therefore this antibody is not representative of how many available CCR5 binding sites there are. T21/8 recognises an epitope within the CCR5 N-terminus, which is required for ligand binding. Therefore, in both PCa cell lines, CCR5 may specifically take a conformation which is available for ligand binding, making it better recognisable by T21/8.

4.1. Future work

To accurately detect low expressing CCR5 transcripts CCR5A and CCR5B, it may be necessary in future studies to optimise a Taqman probe assay. The Taqman probe binds to the primers annealing to the sequence of interest. Upon binding, the probe emits fluorescence that is detected by the machine (ThermoFisher, No date). Therefore, it has higher precision to the sequence of interest, rather than binding non-specifically to any dsDNA as in SYBR Green.

I was interested in finding out whether increasing the seed number in PC3 would lead to higher RNA yield. Although I did not find a positive correlation between initial seed count and RNA yield, I found weak positive correlation between total cell count and RNA yield (**Supplementary Figure 7**). In future work, higher cell count may be required to achieve a better sensitivity to detect lower levels of transcripts such as CCR5A and CCR5B.

Taking a step further from qPCR, in the future, genome and transcriptome sequencing and mRNA microarrays could be performed on PCa cells with or without cytokine treatment. This way, many genes, transcripts and proteins can be tested at the same time with different treatments. It would also be in our interests in the future to further investigate STAT3 activation, and its associated proteins in a proteomic/transcriptomic manner, as the literature have cited STAT3 as a potential marker of advanced PCa. (Bishop, Thaper and Zoubeidi, 2014)

In this piece of work, I was not able to confirm receptor activation by testing with antagonists, i.e. Maraviroc for CCR5, Tocilizumab for IL-6R and siRNA for both receptors. In future work, it would be valuable to test receptor activation using antagonists to affirm the pathways discussed.

No studies have linked CCR5 mechanistic action with androgen receptor (AR) signalling but have speculated a link found between CCL5 and AR in bone metastasis via HIF2α pathway. CCL5 was found to inhibit the expression of AR related genes, altering AR signalling pathway (Luo *et al*., 2014). In this project, I have proposed a link between IL-6 and AR, however, was not able to find a link between CCR5 and AR, which could be an area for future work.

As LNCaP and PC3 cells model for metastatic PCa, however respond in vastly different mechanisms to cytokine stimulation, as well as differ in their cell surface receptors, it should be reconsidered whether these cell lines are good models for PCa. One study found that in androgen deprived conditions, LNCaP develops phenotypic characteristics like that of PC3 (Chang *et al*., 2014). Therefore, these cell lines may represent different stages of PCa (Tai *et al*., 2011). Additionally, there have been reports of many mutational changes affecting their signalling networks (Seim *et al*., 2017). This emphasises how diversified PCa is biochemically and is especially apparent in studies testing patient samples for prognostic markers. One such marker is PSMA, which was found to be expressed in primary and metastatic tumours with high variation, including few within the negative range (Mannweiler *et al*., 2009).

Due to the interconnected nature of the TME, explants derived from biopsies of patients at different stages of PCa should be studied in the future, as they better represent the TME. Further flow cytometry work could test not only the population of cells present, but what secretory proteins such as cytokines, cell surface markers and immune related receptors they express. Of particular interest would be testing the migratory effect of CCL5 on tumour infiltrating cells such as dendritic, MDSCs and T cells, as this cannot be done with non-migratory LNCaP and PC3. The transcriptome of multiple chemokine receptors could also be studied to elucidate a chemokine receptor milieu associated with this migratory effect commonly reported in studies.

An intricate network between cytokine-mediated activation of receptors and signalling proteins is at play - one type of PCa model may not show an effect that is found on another type of PCa model, due to differences in their transcriptional regulation.

4.2. Summary of findings

From this work, we are unable to confirm a mechanistic action of the CCL5/CCR5 axis present in PCa cell lines, however we show that long term CCL5 stimulation of LNCaP cells induced transcriptional expression of the CCR5-specific chemokine CCL4 compatible with the idea of a receptor-ligand feedback loop. The published literature focuses mostly on antagonising this axis in human PCa stem cells and tumour infiltrating immune cells, via CCL5 secretion by some immune cells and cancer associated fibroblasts derived from primary PCa tissue (Huang *et al*., 2021). Further work using cancer cells originating from the TME, and not from metastatic ‘descendants’ of lymph nodes and bone (Tai *et al*., 2011) would be required to enhance our current understanding of chemokine receptors in cancer biology.

5. Appendix

5.1. qPCR Primer Validation

To ensure that the primers were working as intended, primer validation assays were performed. One goal of primer validation assays was to assess primer efficiencies, which is a requirement when using the intended ΔΔCt method. (Livak and Schmittgen, 2001)

5.1.1. Method

cDNA used to validate primers was derived from 1µg of RNA from MDM (Donor G1). qPCR reactions were run in duplicate. Most primers were validated using PCR product obtained from a separate PCR reaction, where 1µg of monocyte-derived macrophages (MDM from Donor G1) RNA was added to the cDNA synthesis reaction. PCR products were diluted as follows - $1:1e^4$, $1:1e^5$, $1:1e^6$, $1:1e^7$ and $1:1e^8$. All primers were tested at a concentration of 0.3µM. Most primers passed on this concentration. To test the primers solely, qPCR analysis was set on auto threshold and auto baseline. The following conditions needed to be met to pass a primer:

- Primer efficiency should be between 90-110% (The primer efficiency formula used was $((10^{1/slope})-1) \times 100$) (Rogers-Broadway and Karteris, 2015)
- Melt curves for each primer at every serial dilution produced a single peak. (ThermoFisher, 2022b)
- Ct values between each serial dilution produces a linear regression slope over a range of dilutions, with a consistent difference between each serial dilution. (Elston and Deatherage, 2019)
- Linear standard curve, where $R2 > 0.980$ (Bio-Rad, No date)

5.1.2. Results

End point PCR and gel electrophoresis was performed before testing with qPCR to ensure that a single PCR product formed for each set of primers. Results are presented in **Figure 8** for CCR5 related primers and **Figure 11** for signalling proteins.

For the CCR5 transcripts, P4 (detects CCR5 containing Exon 3 transcripts) and CCR5A passed as described in the Methods section. Primer targeting Exon 1 (P5a and P5b) did not pass primer validation as they failed to produce consistent amplification plots. Primers for CCR5B passed using PCR product from MDMs (from Donor G1) where a higher volume of RNA (2µg) was added to the cDNA synthesis reaction. CCR5AS produced multiple melt curves, however upon halving the primer concentration for these primers, single peaks for each primer melt curve was observed. CCR5AS also required a lower annealing temperature (58°C) as it was observed during end-point PCR that CCR5AS primers would not work at annealing temperature 60°C.

Most of the primers detecting signalling proteins passed as described in the Methods section, with some exceptions. β-catenin passed primer validation on qPCR product with a serial dilution of stock, $1:1e^1$, $1:1e^2$, $1:1e^3$, and $1:1e^4$. Although primer efficiency was out of the range specified for β-catenin, at 115%, its melt curves produced a single peak and Ct value differences produced a linear regression slope, with a consistent spread of Ct values when plotted against dilution. EIF4EBP1, similarly to CCR5AS, produced multiple melt curves. Upon halving primer concentration, EIF4EBP1 produced single melt curves. Additionally, although EIF4EBP1 and PRKAB2 did not have the ideal linear standard curve, where $R^2 > 0.980$, both primers passed on the primer efficiency formula. EIF4EBP1 and PRKAB2 passed using cDNA from MDMs (Donor G1) and LNCaP cDNA respectively, rather than qPCR product. cDNA from cells has a lower concentration of the transcript of interest, leading to less efficient qPCR reactions compared to qPCR product. Melt curves, amplification plots and linear regression slopes are shown in **Supplementary Figure 1 - 3** respectively.

CCR5 Exon 3

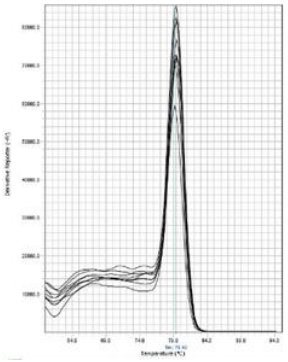

CCR5A

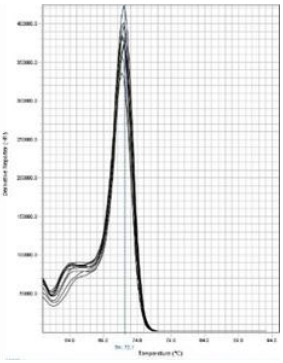

CCR5B

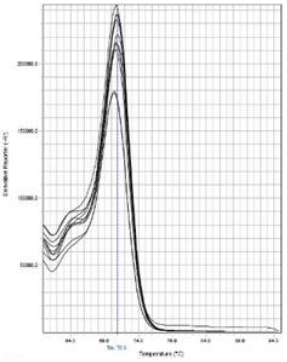

CCR5AS

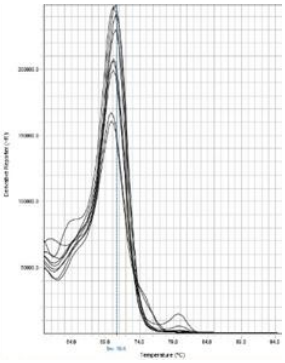

CREB-1

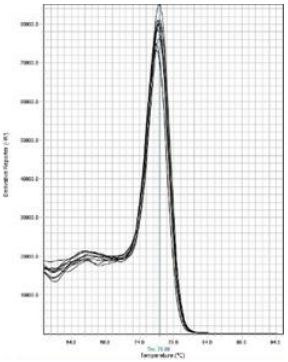

β-catenin

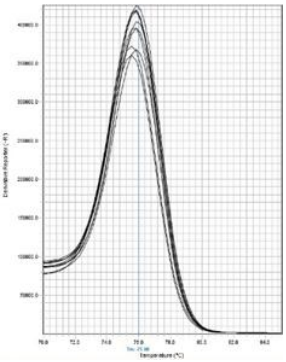

STAT3

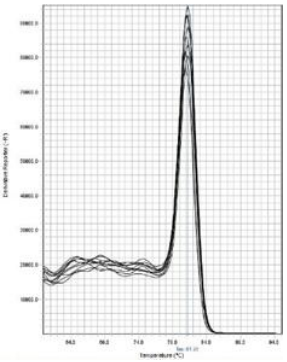

LKB1

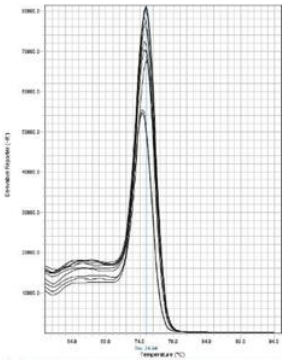

PRKAB2

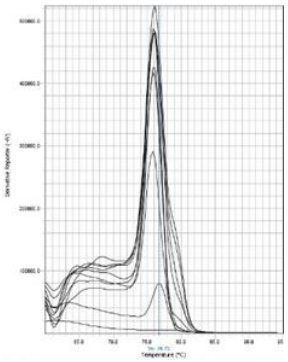

EIF4EBP1

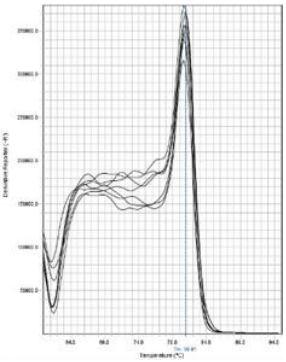

IκB-α (NF-κB)

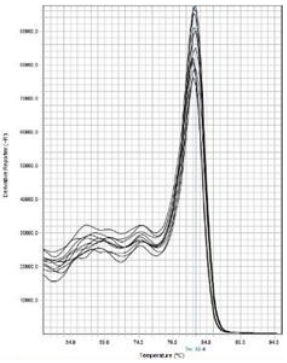

E-cadherin

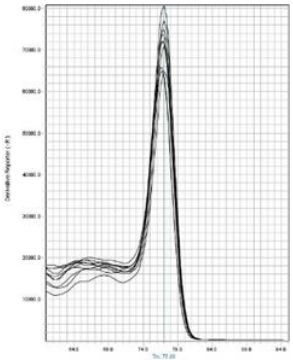

GAPDH

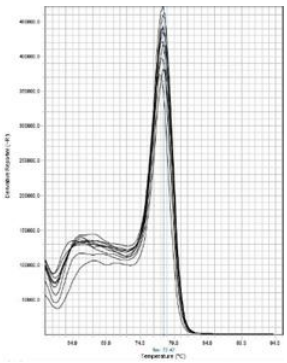

Supplementary Figure 1: Melt curves for each primer from passed primer validation assays. Each curve represents a single qPCR reaction. Peaks for each melt curve represent the temperature at which – during the melt curve step - a double stranded PCR product anneal and thus fluoresce due to intercalating SYBR green. As each primer pair produces a single specific PCR product, each primer shows a single peak. (ThermoFisher, 2022b) cDNA from a qPCR product which was produced from a previous assay using the same primers was run.

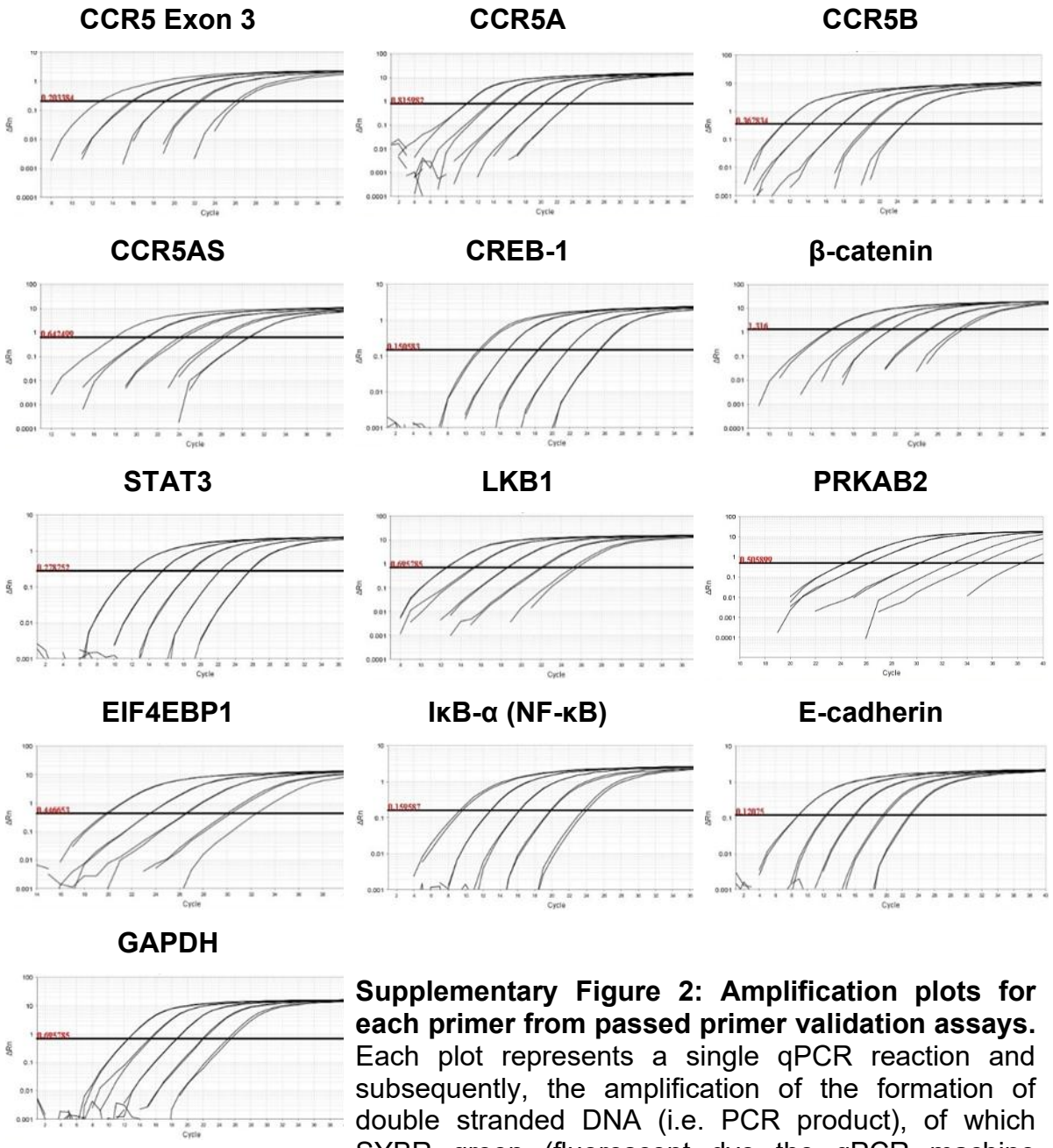

Supplementary Figure 2: Amplification plots for each primer from passed primer validation assays. Each plot represents a single qPCR reaction and subsequently, the amplification of the formation of double stranded DNA (i.e. PCR product), of which SYBR green (fluorescent dye the qPCR machine detects) intercalates with. When the number of newly formed PCR product exceeds the number of double stranded background cDNA, the reaction undergoes an exponential amplification phase. The number of cycles at which the amplification plot meets the set threshold is the Ct value. The more sequence of interest to begin with, the earlier the amplification is observed. (Sigma-Aldrich, No date) cDNA from qPCR product was run, except for β-catenin and EIF4EBP1, where MDMs (Donor G1) cDNA was used and LNCaP cDNA, for PRKAB2.

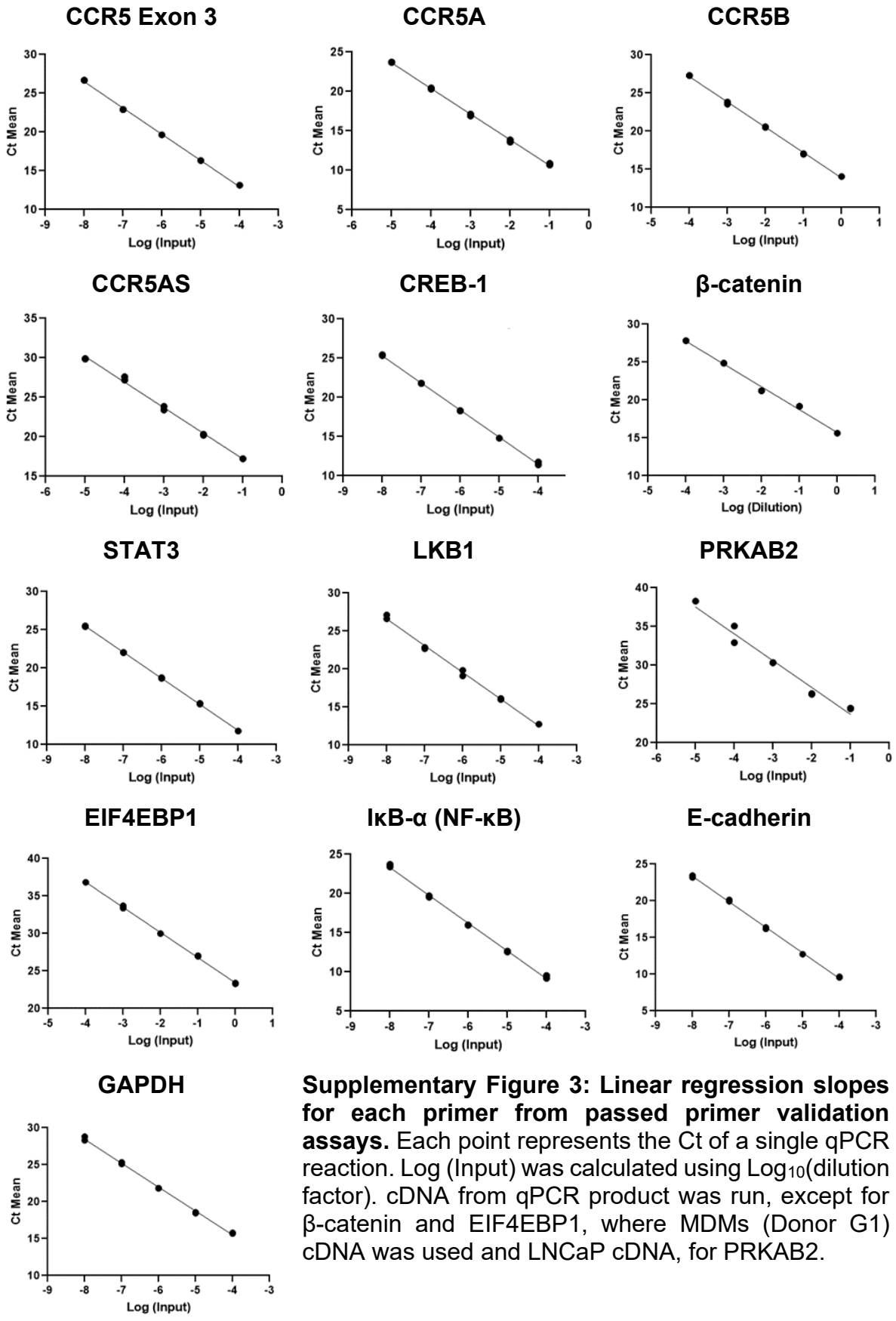

Supplementary Figure 3: Linear regression slopes for each primer from passed primer validation assays. Each point represents the Ct of a single qPCR reaction. Log (Input) was calculated using Log_{10}(dilution factor). cDNA from qPCR product was run, except for β-catenin and EIF4EBP1, where MDMs (Donor G1) cDNA was used and LNCaP cDNA, for PRKAB2.

5.2. Positive Control Validation Assays

After the primers were validated, it was crucial to assess how the primers would react with cDNA from cell lines, in particular how positive qPCR detection looks like. Therefore, positive control validation assays were performed. These were run to test positive controls with different primers to assess optimum dilutions of cDNA which both produced single melt curves and were within readable Ct values.

qPCR reactions were run in duplicate. The ideal dilution of cDNA was assessed for each primer, by running MDM (from donor G1) cDNA (1µg RNA added to cDNA reaction) in serial dilutions – stock, 1:2 and 1:4. MDM (from donor G1) was chosen as it was found to be positive for all primers as shown in end point PCR (See **Figure 8** and **11**). For a dilution to be deemed as ideal, its triplicate reactions must produce a melt curve with a single peak. From these results, a range of cDNA dilutions for each primer were found. The highest dilution was selected to conserve stock cDNA for other primers. For example, primers that produced a single peak at their melt curves for all dilutions were assigned to be tested at 1:4 dilution.

For CCR5 transcripts and CCR5AS, there was presence of multiple melt curves at cDNA samples given low RNA volumes. Therefore, for these primers, it was decided to synthesise cDNA with the highest dosage of RNA and to add stock cDNA, as the CCR5 transcripts and CCR5AS were only detectable at high MDM cDNA concentration. Stock cDNA was also used for STAT3 and CREB-1.

Additionally, threshold was set to approximately the middle of the amplification phase in logarithmic scale for all further assays. Baseline was set to two cycles less than when amplification begins for all further assays. Both threshold and baseline were set according to manufacturer's protocol (Applied Biosystems, 2002).

Melt curves and amplification plots showing thresholds set mid amplification phase for positive control validation assays are shown in **Supplementary Figure 4** and **Supplementary Figure 5.** The different parameters used for each primer are summarised in **Supplementary Table 1**.

CCR5 Exon 3

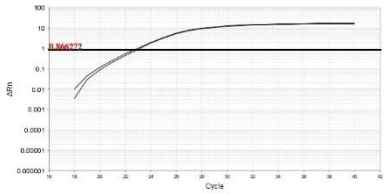

CCR5A

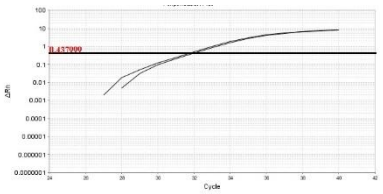

CCR5B

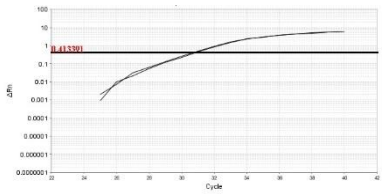

CCR5AS

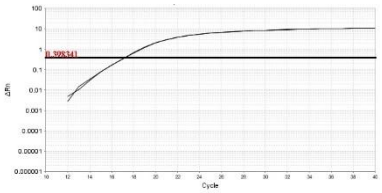

CREB-1

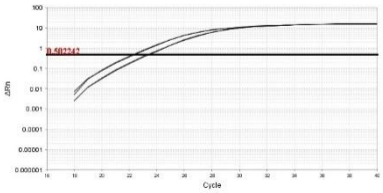

β-catenin

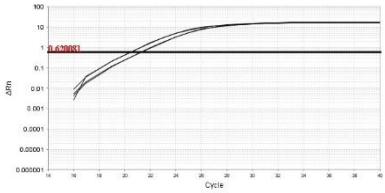

STAT3

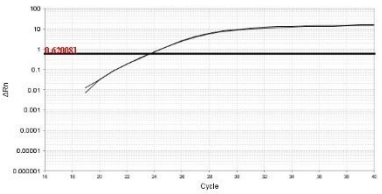

LKB1

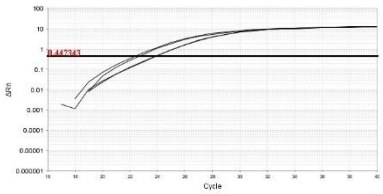

PRKAB2

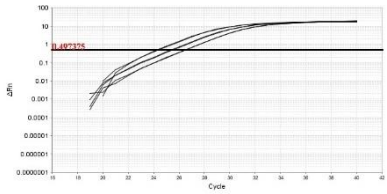

EIF4EBP1

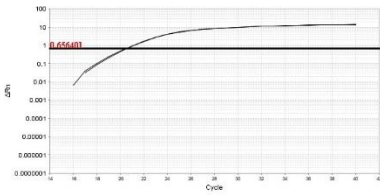

IκB-α (NF-κB)

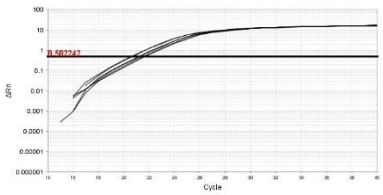

E-cadherin

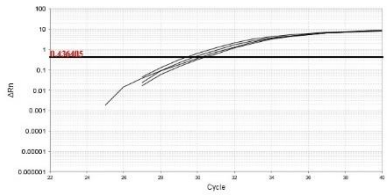

GAPDH

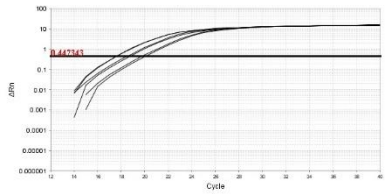

Supplementary Figure 4: Amplification plots for each primer showing dilutions that passed Positive Control Validation assays. cDNA from MDM (Donor G1) was run.

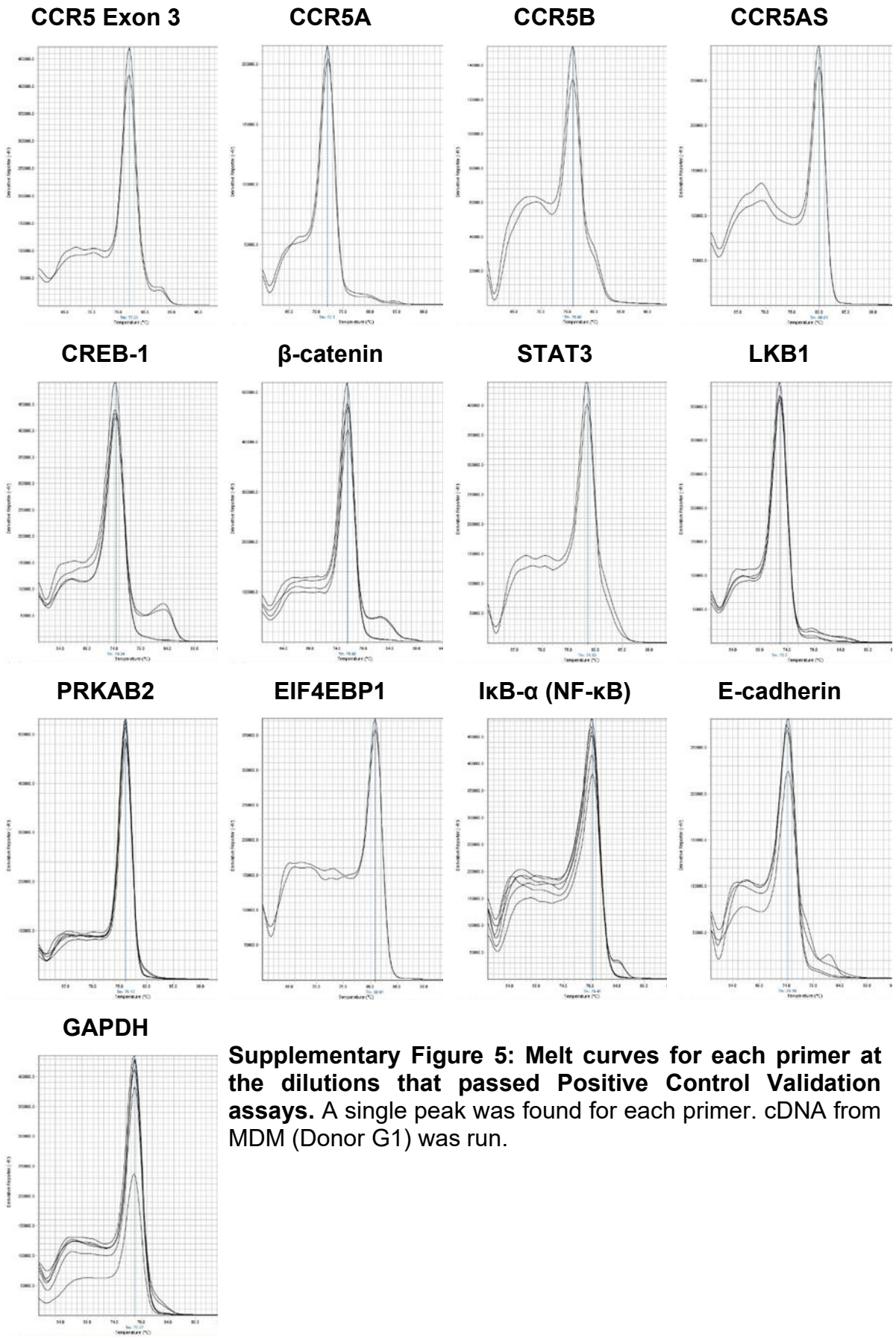

Supplementary Figure 5: Melt curves for each primer at the dilutions that passed Positive Control Validation assays. A single peak was found for each primer. cDNA from MDM (Donor G1) was run.

Supplementary Table 1: Validated primers and their corresponding parameters. Primers' efficiencies and slope were considered when validating. Annealing temperature and primer concentrations varied for some primers. Optimal cDNA dilution was assessed during Positive Control Validation (**Section 5.2**).

Primer	**Primer efficiency (%)**	**Slope (R^2)**	**Annealing temperature (°C)**	**Primer concentration (µM)**	**cDNA Dilution**
P4 (Exon 3 CCR5)	97.3	0.9989	60	0.3	Stock
CCR5A	103.1	0.9994	60	0.3	Stock
CCR5B	99.0	0.9992	60	0.3	Stock
CCR5AS	103.6	0.9968	58	0.15	Stock
CREB-1	94.7	0.9997	60	0.3	1:2
β-catenin	115.5	0.9946	60	0.3	1:2
STAT3	97.8	0.9999	60	0.3	Stock
LKB1	94.9	0.9975	60	0.3	1:2
PRKAB2 (AMPK)	91.7	0.9796	60	0.3	1:4
EIF4EBP1	103.4	0.9747	60	0.15	Stock
Inhibitor Nfκ-B (Iκα)	91.6	0.9984	60	0.3	1:4
Cadherin	93.9	0.999	60	0.3	1:2
GAPDH	103.8	0.9987	60	0.3	Varied

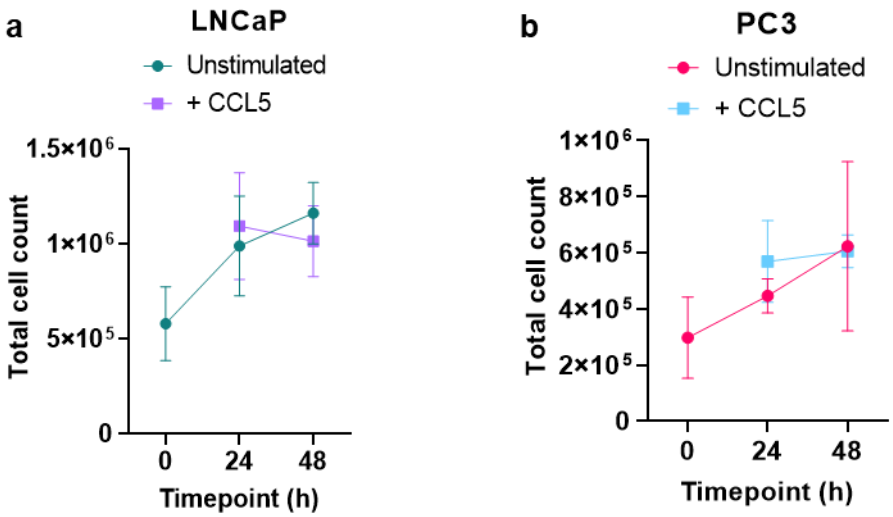

Supplementary Figure 6: Long term CCL5 stimulation does not increase total cell count compared to unstimulated cells. Total cell count of CCL5 stimulated and unstimulated cells at harvest time, determined using a haemocytometer in PCa cell lines: (**a**) LNCaP and (**b**) PC3. (n=3)

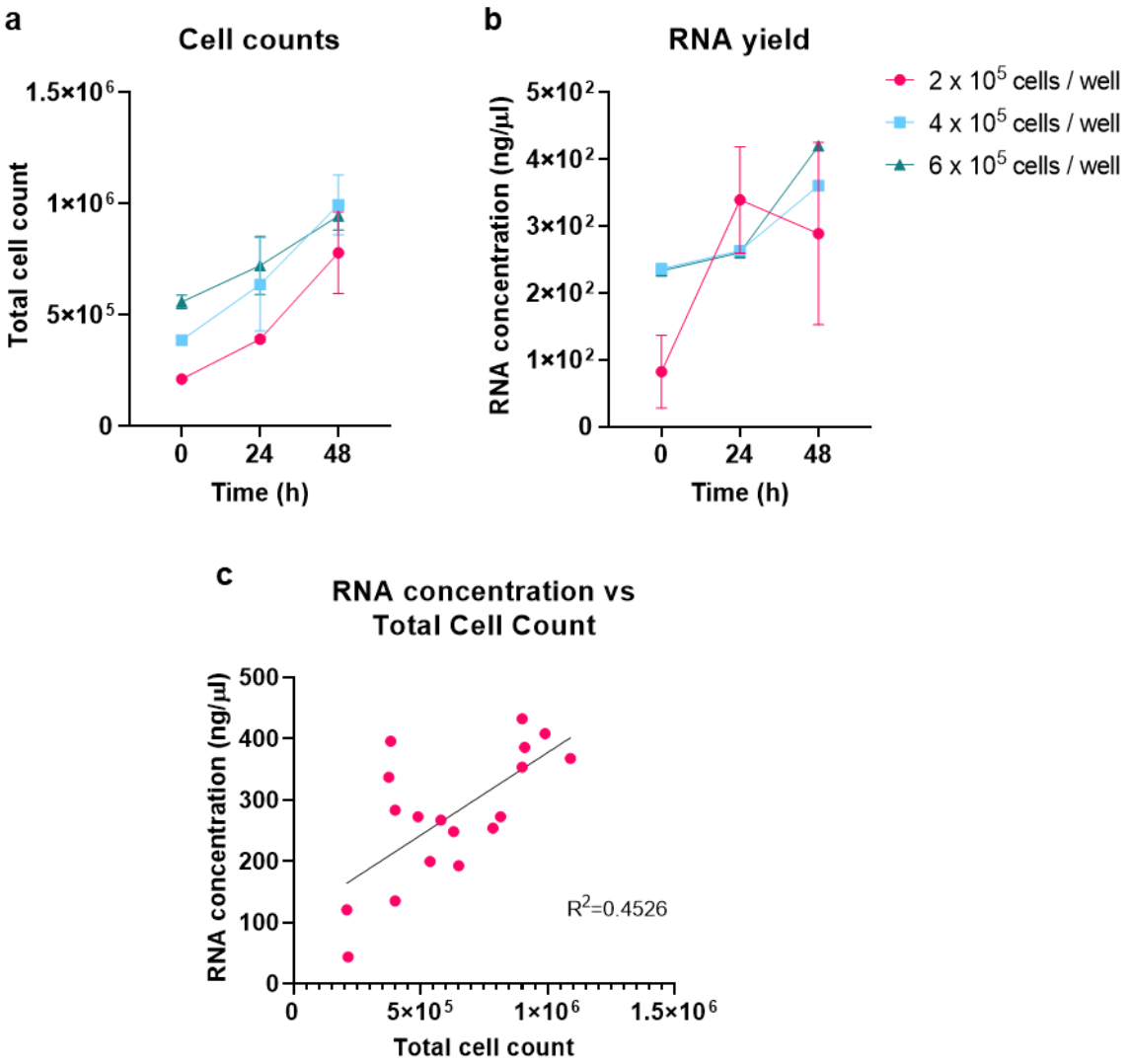

Supplementary Figure 7: Initial seeding density of PC3 cells does not affect cell counts and RNA concentration. Resting PC3 cells were seeded at increasing densities and harvested at time points replicating experimental conditions. Total cell counts (**a**) determined by haemocytometer and RNA yield (**b**) measured with nanodrop. (n=2) (**c**) Simple linear regression plotting total cell count and RNA concentration of observations in (**a**) and (**b**).

6. Abbreviations

Abbreviation	Definition
4EBP-1	See EI4EBP1
ab	Antibody
AC	Adenylyl Cyclase
AKT	Protein Kinase B
AMPK	Adenosine monophosphate activated protein kinase
ANOVA	Analysis of Variance
APC	Allophycocyanin
AR	Androgen receptor
BLAST	Basic Local Alignment Search Tool
bp	Base pair
BSA	Bovine serum albumin
cAMP	Cyclic adenosine monophosphate
CCL	C-C motif Chemokine Ligand
CCR	C-C Chemokine Receptor
CD	Cluster of Differentiation
cAMP	Cyclic adenosine monophosphate
cDNA	Complementary deoxyribonucleic acid
CHO	Chinese Hamster Ovary
CREB	cAMP response element-binding protein
CRPC	Castration resistant prostate cancer
ddH_2O	Double distilled water
DMEM	Dulbecco's Modified Eagle Medium
DNA	Deoxyribonucleic acid
EDTA	Ethylenediaminetetraacetic acid
EI4EBP1	Eukaryotic translation initiation factor 4E-binding protein 1
ELISA	Enzyme Linked Immunosorbent Assay
EMT	Epithelial-mesenchymal transition
ERK	Extracellular Signal-Regulated Kinase
FACS	Fluorescence activated cell sorting
FC	Flow Cytometry
FCS	Foetal calf serum
GAPDH	Glyceraldehyde 3-phosphate dehydrogenase

GEO	Gene Expression Omnibus
gp	Glycoprotein
GPCR	G-protein coupled receptor
GTP	Guanosine triphosphate
h	Hour/hours
H3	Histone 3
HEK	Human embryonic kidney
HEPES	4-(2-hydroxyethyl)-1-piperazineethanesulfonic acid
HIF	Hypoxia-inducible factor
HIV	Human immunodeficiency virus
HRP	Horseradish peroxidase
Ig	Immunoglobulin
IL	Interleukin
IU	International Units
IκB-α	Inhibitor of nuclear factor kappa B
JAK	Janus family tyrosine protein kinase
LKB	Liver Kinase B
LNCaP	Lymph Node Carcinoma of the Prostate
lncRNA	Long non-coding ribonucleic acid
MAPK	Mitogen-activated protein kinases
MCSF	Macrophage colony stimulating factor
MDM	Monocyte derived macrophages
MDSC	Myeloid-derived suppressor cells
MEM	Minimum Essential Medium
MFI	Median Fluorescence Intensity
miRNA	Micro ribonucleic acid
MMP	Matrix metalloproteinase
mPCa	Metastatic prostate cancer
mRNA	Messenger ribonucleic acid
mTOR	Mammalian target of rapamycin
NCBI	National Center for Biotechnology Information
ncRNA	Noncoding ribonucleic acid
NF-κB	Nuclear factor kapa-light-chain-enhancer of activated B cells
NHS	National Health Service
PBMC	Peripheral blood mononuclear cells
PBS	Phosphate buffered saline

PCa	Prostate cancer
PCR	Polymerase Chain Reaction
PI3-K	Phosphoinositide 3-kinase
PIN	Prostatic Intraepithelial Neoplasia
PSMA	Prostate specific membrane antigen
PTEN	Phosphatase and tensin homolog
qPCR	Quantitative polymerase Chain Reaction
RNA	Ribonucleic acid
RPMI	Roswell Park Memorial Institute
RT	Reverse Transcriptase
SD	Standard Deviation
SDS-PAGE	SDS-polyacrylamide gel electrophoresis
siRNA	Small interfering ribonucleic acid
snRNA	Small nuclear ribonucleic acid
snRNP	Small nuclear ribonucleoproteins
SOCS	Suppressor of cytokine signalling
STAT	Signal transducer and activator of transcription
TAE	Tris-acetate-EDTA
TAM	Tumour associated macrophage
TBS	Tris-buffered saline
TME	Tumour microenvironment

7. Bibliography

Adekoya, T. O. and Richardson, R. M. (2020). Cytokines and Chemokines as Mediators of Prostate Cancer Metastasis. International Journal of Molecular Sciences, 21 (12), p.4449. [Online]. Available at: doi:10.3390/ijms21124449.

Aigner, P., Just, V. and Stoiber, D. (2019). STAT3 isoforms: Alternative fates in cancer? Cytokine, 118, pp.27–34. [Online]. Available at: doi:10.1016/j.cyto.2018.07.014.

Akbarian, F. *et al*. (2020). Upregulation of MTOR, RPS6KB1, and EIF4EBP1 in the whole blood samples of Iranian patients with multiple sclerosis compared to healthy controls. Metabolic Brain Disease, 35 (8), pp.1309–1316. [Online]. Available at: doi:10.1007/s11011-020-00590-7.

Alberts, B. *et al*. (2022). The Molecular Biology of the Cell. 7th ed. W.W. Norton & Company.

Aldinucci, D., Borghese, C. and Casagrande, N. (2020). The CCL5/CCR5 Axis in Cancer Progression. Cancers, 12 (7), p.1765. [Online]. Available at: doi:10.3390/cancers12071765.

Alkaf, A. *et al*. (2017). Expression of STK11 gene and its promoter activity in MCF control and cancer cells. 3 Biotech, 7 (6), p.362. [Online]. Available at: doi:10.1007/s13205-017-1000-6.

Altschul, S. F. *et al*. (1990). Basic local alignment search tool. Journal of Molecular Biology, 215 (3), pp.403–410. [Online]. Available at: doi:10.1016/S0022-2836(05)80360-2.

Applied Biosystems. (2002). Data Analysis on the ABI PRISM 7700: Setting Baselines and Thresholds. [Online]. Available at: https://surf.ed.ac.uk/wp-content/uploads/2014/02/Setting-baselines-and-thresholds-.pdf

Audet-Walsh, É. *et al*. (2017). Nuclear mTOR acts as a transcriptional integrator of the androgen signaling pathway in prostate cancer. Genes & Development, 31 (12), p.1228. [Online]. Available at: doi:10.1101/gad.299958.117.

Azevedo, A. *et al*. (2011). IL-6/IL-6R as a potential key signaling pathway in prostate cancer development. World Journal of Clinical Oncology, 2 (12), p.384. [Online]. Available at: doi:10.5306/wjco.v2.i12.384.

Bahmad, H. F. *et al*. (2021). Tumor Microenvironment in Prostate Cancer: Toward Identification of Novel Molecular Biomarkers for Diagnosis, Prognosis, and Therapy Development. Frontiers in Genetics, 12. [Online]. Available at: doi:10.3389/fgene.2021.652747 [Accessed 8 November 2024].

Baldwin, A. S. (1996). The NF-kappa B and I kappa B proteins: new discoveries and insights. Annual Review of Immunology, 14, pp.649–683. [Online]. Available at: doi:10.1146/annurev.immunol.14.1.649.

Bauss, J. *et al*. (2021). CCR5 and Biological Complexity: The Need for Data Integration and Educational Materials to Address Genetic/Biological Reductionism at the Interface of Ethical, Legal, and Social Implications. Frontiers in Immunology, 12. [Online]. Available at: https://www.frontiersin.org/articles/10.3389/fimmu.2021.790041 [Accessed 23 October 2023].

Bellezza, I. *et al*. (2006). Suppressor of Cytokine Signaling-3 Antagonizes cAMP Effects on Proliferation and Apoptosis and Is Expressed in Human Prostate Cancer. The American Journal of Pathology, 169 (6), pp.2199–2208. [Online]. Available at: doi:10.2353/ajpath.2006.060171.

Bennett, J. L. *et al*. (2023). IL-6 evoked biochemical changes in prostate cancer cells. Cytokine, 161, p.156079. [Online]. Available at: doi:10.1016/j.cyto.2022.156079.

Bennett, L. D., Fox, J. M. and Signoret, N. (2011). Mechanisms regulating chemokine receptor activity. Immunology, 134 (3), pp.246–256. [Online]. Available at: doi:10.1111/j.1365-2567.2011.03485.x.

Bio-Rad. (No date). qPCR Amplification | Bio-Rad. [Online]. Available at: https://www.bio-rad.com/en-uk/applications-technologies/qpcr-amplification?ID=3edb4096-4520-87be-7382-9bd9c130e419 [Accessed 12 July 2024].

Bishop, J. L., Thaper, D. and Zoubeidi, A. (2014). The Multifaceted Roles of STAT3 Signaling in the Progression of Prostate Cancer. Cancers, 6 (2), pp.829–859. [Online]. Available at: doi:10.3390/cancers6020829.

Bottero, V. *et al*. (2003). Monitoring NF-κB Transactivation Potential Via Real-Time PCR Quantification of IκB-α Gene Expression. Molecular Diagnosis, 7 (3), pp.187–194. [Online]. Available at: doi:10.1007/BF03260037.

Buono, R. and Longo, V. D. (2018). Starvation, Stress Resistance, and Cancer. Trends in endocrinology and metabolism: TEM, 29 (4), p.271. [Online]. Available at: doi:10.1016/j.tem.2018.01.008.

Cancer Research UK (2023). Prostate cancer risk. https://www.cancerresearchuk.org/health-professional/cancer-statistics/statistics-by-cancer-type/prostate-cancer/risk-factors [Online]

Chang, P.-C. *et al*. (2014). Autophagy Pathway Is Required for IL-6 Induced Neuroendocrine Differentiation and Chemoresistance of Prostate Cancer LNCaP Cells. Migliaccio, A. (Ed). PLoS ONE, 9 (2), p.e88556. [Online]. Available at: doi:10.1371/journal.pone.0088556.

Chanput, W., Mes, J. J. and Wichers, H. J. (2014). THP-1 cell line: An in vitro cell model for immune modulation approach. International Immunopharmacology, 23 (1), pp.37–45. [Online]. Available at: doi:10.1016/j.intimp.2014.08.002.

Chen, T., Wang, L. H. and Farrar, W. L. (2000). Interleukin 6 Activates Androgen Receptor-mediated Gene Expression through a Signal Transducer and Activator of Transcription 3-dependent Pathway in LNCaP Prostate Cancer Cells1. Cancer Research, 60 (8), pp.2132–2135.

Colombatti, M. *et al*. (2009). The Prostate Specific Membrane Antigen Regulates the Expression of IL-6 and CCL5 in Prostate Tumour Cells by Activating the MAPK Pathways1. PLoS ONE, 4 (2), p.e4608. [Online]. Available at: doi:10.1371/journal.pone.0004608.

Culig, Z. *et al*. (2005). Interleukin-6 regulation of prostate cancer cell growth. Journal of Cellular Biochemistry, 95 (3), pp.497–505. [Online]. Available at: doi:10.1002/jcb.20477.

Davarinejad, H. (No date). Quantifications of Western Blots with ImageJ. [Online]. Available at: https://www.yorku.ca/yisheng/Internal/Protocols/ImageJ.pdf

Dhamija, S. and Menon, M. B. (2018). Non-coding transcript variants of protein-coding genes - what are they good for? RNA biology, 15 (8), pp.1025–1031. [Online]. Available at: doi:10.1080/15476286.2018.1511675.

Dong, H.-Q. and Du, Y.-X. (2019). The study of copy number variations in the regions of PRKAB2 and PPM1K among congenital heart defects patients. Revista da Associação Médica Brasileira, 65 (6), pp.786–790. [Online]. Available at: doi:10.1590/1806-9282.65.6.786.

Elston, K. and Deatherage, D. (2019). Barrick Lab :: PrimerEfficiencyqPCR. [Online]. Available at: https://barricklab.org/twiki/bin/view/Lab/PrimerEfficiencyqPCR [Accessed 27 November 2024].

Ensembl. (no date). Chromosome 3: 46,373,076-46,374,077 - Region in detail - Homo_sapiens - Ensembl genome browser 113. [Online]. Available at: https://www.ensembl.org/Homo_sapiens/Location/View?db=core;g=ENSG00000160791;r=3:46373076-46374077;t=ENST00000292303;v=COSV105113705;vdb=variation;vf=1196592904 [Accessed 26 October 2024a].

Ensembl. (no date - b). Gene: CCR5 (ENSG00000160791) - Summary - Homo_sapiens - GRCh37 Archive browser 113. [Online]. Available at: https://grch37.ensembl.org/Homo_sapiens/Gene/Summary?g=ENSG00000160791;r=3:46411633-46417697 [Accessed 6 November 2024b].

Fang, L.-Y. *et al*. (2013). Infiltrating Macrophages Promote Prostate Tumorigenesis via Modulating Androgen Receptor-Mediated CCL4–STAT3 Signaling. Cancer Research, 73 (18), pp.5633–5646. [Online]. Available at: doi:10.1158/0008-5472.CAN-12-3228.

Fox, J. M. *et al*. (2015). CCR5 susceptibility to ligand-mediated down-modulation differs between human T lymphocytes and myeloid cells. Journal of leukocyte biology, 98 (1), pp.59–71. [Online]. Available at: doi:10.1189/jlb.2A0414-193RR.

Gabela, N. C., Bhadree, S. and Mathibe, L. J. (2021). Costs of managing castrate-resistant metastatic prostate cancer patients at Inkosi Albert Luthuli Central Hospital. South African Journal of Surgery. Suid-Afrikaanse Tydskrif Vir Chirurgie, 59 (4), pp.176–178.

Gao, J., Arnold, J. T. and Isaacs, J. T. (2001). Conversion from a Paracrine to an Autocrine Mechanism of Androgen-stimulated Growth during Malignant Transformation of Prostatic Epithelial Cells1. Cancer Research, 61 (13), pp.5038–5044.

Gao, L.-F. *et al*. (2022). Tumor bud-derived CCL5 recruits fibroblasts and promotes colorectal cancer progression via CCR5-SLC25A24 signaling. Journal of Experimental & Clinical Cancer Research : CR, 41. [Online]. Available at: doi:10.1186/s13046-022-02300-w

Garcia, G. E. *et al*. (2006). Akt- and CREB-Mediated Prostate Cancer Cell Proliferation Inhibition by Nexrutine, a Phellodendron amurense Extract. Neoplasia (New York, N.Y.), 8 (6), p.523. [Online]. Available at: doi:10.1593/neo.05745.

Gregg, J. L. *et al*. (2010). Analysis of gene expression in prostate cancer epithelial and interstitial stromal cells using laser capture microdissection. BMC Cancer, 10, p.165. [Online]. Available at: doi:10.1186/1471-2407-10-165.

Hawila, E. *et al*. (2017). CCR5 Directs the Mobilization of CD11b+Gr1+Ly6Clow Polymorphonuclear Myeloid Cells from the Bone Marrow to the Blood to Support Tumor Development. Cell Reports, 21 (8), pp.2212–2222. [Online]. Available at: doi:10.1016/j.celrep.2017.10.104.

Helgstrand, J. T. *et al*. (2018). Trends in incidence and 5-year mortality in men with newly diagnosed, metastatic prostate cancer-A population-based analysis of 2 national cohorts. Cancer, 124 (14), pp.2931–2938. [Online]. Available at: doi:10.1002/cncr.31384.

Hevehan, D. L., Miller, W. M. and Papoutsakis, E. T. (2002). Differential expression and phosphorylation of distinct STAT3 proteins during granulocytic differentiation. Blood, 99 (5), pp.1627–1637. [Online]. Available at: doi:10.1182/blood.v99.5.1627.

Huang, B., Lang, X. and Li, X. (2022). The role of IL-6/JAK2/STAT3 signaling pathway in cancers. Frontiers in Oncology, 12. [Online]. Available at: doi:10.3389/fonc.2022.1023177 [Accessed 12 July 2024].

Huang, R. *et al*. (2020). CCL5 derived from tumor-associated macrophages promotes prostate cancer stem cells and metastasis via activating β-catenin/STAT3 signaling. Cell Death & Disease, 11 (4), pp.1–20. [Online]. Available at: doi:10.1038/s41419-020-2435-y.

Huang, R. *et al*. (2021). Research Trends and Regulation of CCL5 in Prostate Cancer. OncoTargets and therapy, 14, pp.1417–1427. [Online]. Available at: doi:10.2147/OTT.S279189.

Iglesia, N. de la *et al*. (2008). Identification of a PTEN-regulated STAT3 brain tumor suppressor pathway. Genes & Development, 22 (4), pp.449–462. [Online]. Available at: doi:10.1101/gad.1606508.

Jin, K., Pandey, N. B. and Popel, A. S. (2018). Simultaneous blockade of IL-6 and CCL5 signaling for synergistic inhibition of triple-negative breast cancer growth and metastasis. Breast cancer research: BCR, 20 (1), p.54. [Online]. Available at: doi:10.1186/s13058-018-0981-3.

Kant, R. *et al*. (2022). Deregulated transcription factors in cancer cell metabolisms and reprogramming. Seminars in Cancer Biology, 86, pp.1158–1174. [Online]. Available at: doi:10.1016/j.semcancer.2022.10.001.

Kato, T. *et al*. (2013). CCR1/CCL5 interaction promotes invasion of taxane-resistant PC3 prostate cancer cells by increasing secretion of MMPs 2/9 and by activating ERK and Rac signaling. Cytokine, 64 (1), pp.251–257. [Online]. Available at: doi:10.1016/j.cyto.2013.06.313.

Kim, J. Y. *et al*. (2022). CCR4 and CCR5 Involvement in Monocyte-Derived Macrophage Migration in Neuroinflammation. Frontiers in Immunology, 13. [Online]. Available at: doi:10.3389/fimmu.2022.876033 [Accessed 27 November 2024].

Kufareva, I. (2016). Chemokines and their receptors: insights from molecular modeling and crystallography. Current opinion in pharmacology, 30, pp.27–37. [Online]. Available at: doi:10.1016/j.coph.2016.07.006.

Kuipers, H. F. *et al*. (2008). CC chemokine receptor 5 gene promoter activation by the cyclic AMP response element binding transcription factor. Blood, 112 (5), pp.1610–1619. [Online]. Available at: doi:10.1182/blood-2008-01-135111.

Kulkarni, S. *et al*. (2019). CCR5AS lncRNA variation differentially regulates CCR5, influencing HIV disease outcome. Nature Immunology, 20 (7), pp.824–834. [Online]. Available at: doi:10.1038/s41590-019-0406-1.

Kuo, I.-Y. *et al*. (2022). Recent advances in conventional and unconventional vesicular secretion pathways in the tumor microenvironment. Journal of Biomedical Science, 29 (1), p.56. [Online]. Available at: doi:10.1186/s12929-022-00837-8.

Kuribayashi, T. (2018). Elimination half-lives of interleukin-6 and cytokine-induced neutrophil chemoattractant-1 synthesized in response to inflammatory stimulation in rats. Laboratory Animal Research, 34 (2), pp.80–83. [Online]. Available at: doi:10.5625/lar.2018.34.2.80.

Larsson, P. F. *et al*. (2022). FcγRIIIa receptor interacts with androgen receptor and PIP5K1α to promote growth and metastasis of prostate cancer. Molecular Oncology, 16 (13), pp.2496–2517. [Online]. Available at: doi:10.1002/1878-0261.13166.

Lau, M.-T. and Leung, P. C. K. (2012). The PI3K/Akt/mTOR signaling pathway mediates insulin-like growth factor 1-induced E-cadherin down-regulation and cell proliferation in ovarian cancer cells. Cancer Letters, 326 (2), pp.191–198. [Online]. Available at: doi:10.1016/j.canlet.2012.08.016.

Lee, M. M. K. *et al*. (2012). CCR1-Mediated STAT3 Tyrosine Phosphorylation and CXCL8 Expression in THP-1 Macrophage-like Cells Involve Pertussis Toxin-Insensitive Gα14/16 Signaling and IL-6 Release. The Journal of Immunology, 189 (11), pp.5266–5276. [Online]. Available at: doi:10.4049/jimmunol.1103359.

Lee, S. O. *et al*. (2003). Interleukin-6 promotes androgen-independent growth in LNCaP human prostate cancer cells. Clinical Cancer Research: An Official Journal of the American Association for Cancer Research, 9 (1), pp.370–376.

Liu, C. *et al*. (2020). Macrophage-derived CCL5 facilitates immune escape of colorectal cancer cells via the p65/STAT3-CSN5-PD-L1 pathway. Cell Death & Differentiation, 27 (6), pp.1765–1781. [Online]. Available at: doi:10.1038/s41418-019-0460-0.

Livak, K. J. and Schmittgen, T. D. (2001). Analysis of Relative Gene Expression Data Using Real-Time Quantitative PCR and the 2−ΔΔCT Method. Methods, 25 (4), pp.402–408. [Online]. Available at: doi:10.1006/meth.2001.1262.

Lou, W. *et al*. (2000). Interleukin-6 induces prostate cancer cell growth accompanied by activation of Stat3 signaling pathway. The Prostate, 42 (3), pp.239–242. [Online]. Available at: doi:10.1002/(SICI)1097-0045(20000215)42:3<239::AID-PROS10>3.0.CO;2-G.

Lu, Y. *et al*. (2007). CCR2 expression correlates with prostate cancer progression. Journal of Cellular Biochemistry, 101 (3), pp.676–685. [Online]. Available at: doi:10.1002/jcb.21220.

Ma, B. *et al*. (2016). Liver protects metastatic prostate cancer from induced death by activating E-cadherin signaling. Hepatology, 64 (5), p.1725. [Online]. Available at: doi:10.1002/hep.28755.

Mack, M. *et al*. (1998). Aminooxypentane-RANTES Induces CCR5 Internalization but Inhibits Recycling: A Novel Inhibitory Mechanism of HIV Infectivity. Journal of Experimental Medicine, 187 (8), pp.1215–1224. [Online]. Available at: doi:10.1084/jem.187.8.1215.

Mannweiler, S. *et al*. (2009). Heterogeneity of Prostate-Specific Membrane Antigen (PSMA) Expression in Prostate Carcinoma with Distant Metastasis. Pathology & Oncology Research, 15 (2), pp.167–172. [Online]. Available at: doi:10.1007/s12253-008-9104-2.

Massie, C. E. *et al*. (2011). The androgen receptor fuels prostate cancer by regulating central metabolism and biosynthesis. The EMBO journal, 30 (13), pp.2719–2733. [Online]. Available at: doi:10.1038/emboj.2011.158.

Mohanty, S. K. *et al*. (2017). STAT3 and STAT5A are potential therapeutic targets in castration-resistant prostate cancer. Oncotarget, 8 (49), pp.85997–86010. [Online]. Available at: doi:10.18632/oncotarget.20844.

Mouilleron, H., Delcourt, V. and Roucou, X. (2015). Death of a dogma: eukaryotic mRNAs can code for more than one protein. Nucleic Acids Research, 44 (1), p.14. [Online]. Available at: doi:10.1093/nar/gkv1218.

Moxom, A. (2021). Investigating Potential Drivers of Prostate Cancer Metastasis, Including the CCL5/CCR5 Axis. Project report, University of York.

Mueller, A. *et al*. (2002). Pharmacological characterization of the chemokine receptor, CCR5. British Journal of Pharmacology, 135 (4), p.1033. [Online]. Available at: doi:10.1038/sj.bjp.0704540.

Mummidi, S. *et al*. (1997). The Human CC Chemokine Receptor 5 (CCR5) Gene: MULTIPLE TRANSCRIPTS WITH 5′-END HETEROGENEITY, DUAL PROMOTER USAGE, AND EVIDENCE FOR POLYMORPHISMS WITHIN THE REGULATORY REGIONS AND NONCODING EXONS*.

Journal of Biological Chemistry, 272 (49), pp.30662–30671. [Online]. Available at: doi:10.1074/jbc.272.49.30662.

Mummidi, S. *et al*. (2007). Production of Specific mRNA Transcripts, Usage of an Alternate Promoter, and Octamer-Binding Transcription Factors Influence the Surface Expression Levels of the HIV Coreceptor CCR5 on Primary T Cells12. The Journal of Immunology, 178 (9), pp.5668–5681. [Online]. Available at: doi:10.4049/jimmunol.178.9.5668.

Murooka, T. T., Rahbar, R. and Fish, E. N. (2009). CCL5 promotes proliferation of MCF-7 cells through mTOR-dependent mRNA translation. Biochemical and Biophysical Research Communications, 387 (2), pp.381–386. [Online]. Available at: doi:10.1016/j.bbrc.2009.07.035.

Na, T.-Y. *et al*. (2020). The functional activity of E-cadherin controls tumor cell metastasis at multiple steps. Proceedings of the National Academy of Sciences, 117 (11), pp.5931–5937. [Online]. Available at: doi:10.1073/pnas.1918167117.

NCBI. (2009). Homo sapiens C-C chemokine receptor type 5 (CCR5) gene, complete cds. NCBI Nucleotide Database [Online]. Available at: http://www.ncbi.nlm.nih.gov/nuccore/GQ917109.1 [Accessed 25 November 2024].

NCBI. (No date). CCR5 C-C motif chemokine receptor 5 [Homo sapiens (human)] - Gene - NCBI. [Online]. Available at: https://www.ncbi.nlm.nih.gov/gene/1234 [Accessed 25 November 2024].

NEB. (No date). NEB Tm Calculator. [Online]. Available at: https://tmcalculator.neb.com/#!/main [Accessed 12 July 2024].

Ochoa-Callejero, L. *et al*. (2013). Maraviroc, a CCR5 Antagonist, Prevents Development of Hepatocellular Carcinoma in a Mouse Model. PLOS ONE, 8 (1), p.e53992. [Online]. Available at: doi:10.1371/journal.pone.0053992.

Onuffer, J. J. and Horuk, R. (2002). Chemokines, chemokine receptors and small-molecule antagonists: recent developments. Trends in Pharmacological Sciences, 23 (10), pp.459–467. [Online]. Available at: doi:10.1016/S0165-6147(02)02064-3.

Oppermann, M. (2004). Chemokine receptor CCR5: insights into structure, function, and regulation. Cellular Signalling, 16 (11), pp.1201–1210. [Online]. Available at: doi:10.1016/j.cellsig.2004.04.007.

Park, E. K. *et al*. (2007). Optimized THP-1 differentiation is required for the detection of responses to weak stimuli. Inflammation Research, 56 (1), pp.45–50. [Online]. Available at: doi:10.1007/s00011-007-6115-5.

Patterson, S. J. *et al*. (2016). T regulatory cell chemokine production mediates pathogenic T cell attraction and suppression. The Journal of Clinical Investigation, 126 (3), pp.1039–1051. [Online]. Available at: doi:10.1172/JCI83987.

Pencik, J. *et al*. (2015). STAT3 regulated ARF expression suppresses prostate cancer metastasis. Nature Communications, 6, p.7736. [Online]. Available at: doi:10.1038/ncomms8736.

Pencik, J. *et al*. (2023). STAT3/LKB1 controls metastatic prostate cancer by regulating mTORC1/CREB pathway. Molecular Cancer, 22 (1), p.133. [Online]. Available at: doi:10.1186/s12943-023-01825-8.

Prediger, E. (2024). How to design primers and probes for PCR and qPCR | IDT. [Online]. Available at: https://eu.idtdna.com/pages/education/decoded/article/designing-pcr-primers-and-probes [Accessed 12 July 2024].

Qi, B. *et al*. (2020). Advances of CCR5 antagonists: From small molecules to macromolecules. European Journal of Medicinal Chemistry, 208, p.112819. [Online]. Available at: doi:10.1016/j.ejmech.2020.112819.

Qi, C. *et al*. (2016). HEK293T Cells Are Heterozygous for CCR5 Delta 32 Mutation. PloS One, 11 (4), p.e0152975. [Online]. Available at: doi:10.1371/journal.pone.0152975.

Rogers-Broadway, K.-R. and Karteris, E. (2015). Amplification efficiency and thermal stability of qPCR instrumentation: Current landscape and future perspectives. Experimental and Therapeutic Medicine, 10 (4), pp.1261–1264. [Online]. Available at: doi:10.3892/etm.2015.2712.

Rose-John, S. *et al*. (2006). Interleukin-6 biology is coordinated by membrane-bound and soluble receptors: role in inflammation and cancer. Journal of Leukocyte Biology, 80 (2), pp.227–236. [Online]. Available at: doi:10.1189/jlb.1105674.

Rose-John, S. *et al*. (2023). Targeting IL-6 trans-signalling: past, present and future prospects. Nature Reviews Immunology, 23 (10), pp.666–681. [Online]. Available at: doi:10.1038/s41577-023-00856-y.

Sakellakis, M., Jacqueline Flores, L. and Ramachandran, S. (2022). Patterns of indolence in prostate cancer (Review). Experimental and Therapeutic Medicine, 23 (5), p.351. [Online]. Available at: doi:10.3892/etm.2022.11278.

Sampson, N. *et al*. (2013). In vitro model systems to study androgen receptor signaling in prostate cancer. Endocrine-Related Cancer, 20 (2), pp.R49-64. [Online]. Available at: doi:10.1530/ERC-12-0401.

Samson, M. *et al*. (1997). The Second Extracellular Loop of CCR5 Is the Major Determinant of Ligand Specificity*. Journal of Biological Chemistry, 272 (40), pp.24934–24941. [Online]. Available at: doi:10.1074/jbc.272.40.24934.

Sasaki, S. *et al*. (2016). Essential roles of the interaction between cancer cell-derived chemokine, CCL4, and intra-bone CCR5-expressing fibroblasts in breast cancer bone metastasis. Cancer Letters, 378 (1), pp.23–32. [Online]. Available at: doi:10.1016/j.canlet.2016.05.005.

Schaefer, T. S., Sanders, L. K. and Nathans, D. (1995). Cooperative transcriptional activity of Jun and Stat3 beta, a short form of Stat3. Proceedings of the National Academy of Sciences of the United States of America, 92 (20), p.9097. [Online]. Available at: doi:10.1073/pnas.92.20.9097.

Scurci, I. *et al*. (2021). CCR5 tyrosine sulfation heterogeneity generates cell surface receptor subpopulations with different ligand binding properties. Biochimica Et Biophysica Acta. General Subjects, 1865 (1), p.129753. [Online]. Available at: doi:10.1016/j.bbagen.2020.129753.

Seim, I. *et al*. (2017). Whole-Genome Sequence of the Metastatic PC3 and LNCaP Human Prostate Cancer Cell Lines. G3 Genes|Genomes|Genetics, 7 (6), pp.1731–1741. [Online]. Available at: doi:10.1534/g3.117.039909.

Shariat, S. F. *et al*. (2001). Plasma levels of interleukin-6 and its soluble receptor are associated with prostate cancer progression and metastasis. Urology, 58 (6), pp.1008–1015. [Online]. Available at: doi:10.1016/S0090-4295(01)01405-4.

Sharrard, R. M. and Maitland, N. J. (2007). Regulation of Protein Kinase B activity by PTEN and SHIP2 in human prostate-derived cell lines. Cellular Signalling, 19 (1), pp.129–138. [Online]. Available at: doi:10.1016/j.cellsig.2006.05.029.

Shaw, R. J. (2009). LKB1 and AMP-activated protein kinase control of mTOR signalling and growth. Acta Physiologica (Oxford, England), 196 (1), pp.65–80. [Online]. Available at: doi:10.1111/j.1748-1716.2009.01972.x.

Shen, M. M. and Abate-Shen, C. (2010). Molecular genetics of prostate cancer: new prospects for old challenges. *Genes & Development*, 24 (18), pp.1967–2000. [Online]. Available at: doi:10.1101/gad.1965810.

Shen, X. *et al*. (2021). Correlation between the Expression of Interleukin-6, STAT3, E-Cadherin and N-Cadherin Protein and Invasiveness in Nonfunctional Pituitary Adenomas. Journal of Neurological Surgery. Part B, Skull Base, 82 (Suppl 3), pp.e59–e69. [Online]. Available at: doi:10.1055/s-0039-1700499.

Shin, S. Y. *et al*. (2017). C-C motif chemokine receptor 1 (CCR1) is a target of the EGF-AKT-mTOR-STAT3 signaling axis in breast cancer cells. Oncotarget, 8 (55), pp.94591–94605. [Online]. Available at: doi:10.18632/oncotarget.21813.

Sicoli, D. *et al*. (2014). CCR5 receptor antagonists block metastasis to bone of v-Src-oncogene-transformed metastatic prostate cancer cell lines. Cancer research, 74 (23), p.7103. [Online]. Available at: doi:10.1158/0008-5472.CAN-14-0612.

Sigma-Aldrich. (No date). Universal SYBR Green qPCR Protocol. [Online]. Available at: https://www.sigmaaldrich.com/GB/en/technical-documents/protocol/genomics/qpcr/sybr-green-qpcr [Accessed 12 July 2024].

Signoret, N. *et al*. (2000). Endocytosis and Recycling of the HIV Coreceptor Ccr5. The Journal of Cell Biology, 151 (6), pp.1281–1294.

Signoret, N. *et al*. (2005). Agonist-induced endocytosis of CC chemokine receptor 5 is clathrin dependent. Molecular Biology of the Cell, 16 (2), pp.902–917. [Online]. Available at: doi:10.1091/mbc.e04-08-0687.

Sung, H. *et al*. (2021). Global Cancer Statistics 2020: GLOBOCAN Estimates of Incidence and Mortality Worldwide for 36 Cancers in 185 Countries. CA: a cancer journal for clinicians, 71 (3), pp.209–249. [Online]. Available at: doi:10.3322/caac.21660.

Tai, S. *et al*. (2011). PC3 is a cell line characteristic of prostatic small cell carcinoma. The Prostate, 71 (15), pp.1668–1679. [Online]. Available at: doi:10.1002/pros.21383.

Tang, Q., Jiang, J. and Liu, J. (2015). CCR5 Blockade Suppresses Melanoma Development Through Inhibition of IL-6-Stat3 Pathway via Upregulation of SOCS3. Inflammation, 38 (6), pp.2049–2056. [Online]. Available at: doi:10.1007/s10753-015-0186-1.

Taylor, S. C. *et al*. (2019). The Ultimate qPCR Experiment: Producing Publication Quality, Reproducible Data the First Time. Trends in Biotechnology, 37 (7), pp.761–774. [Online]. Available at: doi:10.1016/j.tibtech.2018.12.002.

ThermoFisher. (2022a). PCR Primer Design Tips - Behind the Bench. [Online]. Available at: https://www.thermofisher.com/blog/behindthebench/pcr-primer-design-tips/ [Accessed 12 July 2024].

ThermoFisher. (2022b). Trust your SYBR Green qPCR Data. [Online]. Behind the Bench. Available at: https://www.thermofisher.com/blog/behindthebench/trust-your-sybr-green-qpcr-data/ [Accessed 17 July 2024].

ThermoFisher. (No date). TaqMan vs SYBR Chemistry - UK. [Online]. Available at: https://www.thermofisher.com/uk/en/home/life-science/pcr/real-time-pcr/real-time-pcr-learning-center/real-time-pcr-basics/taqman-vs-sybr-chemistry-real-time-pcr.html [Accessed 17 July 2024].

Tufail, A. *et al*. (2024). New insight into a simple high-yielding method for the production of fully folded and functional recombinant human CCL5. Scientific Reports, 14 (1), p.24188. [Online]. Available at: doi:10.1038/s41598-024-75327-y.

Tuttle, D. L. *et al*. (1998). Expression of CCR5 increases during monocyte differentiation and directly mediates macrophage susceptibility to infection by human immunodeficiency virus type 1. Journal of Virology, 72 (6), pp.4962–4969. [Online]. Available at: doi:10.1128/JVI.72.6.4962-4969.1998.

Urata, S. *et al*. (2018). C-C motif ligand 5 promotes migration of prostate cancer cells in the prostate cancer bone metastasis microenvironment. Cancer Science, 109 (3), pp.724–731. [Online]. Available at: doi:10.1111/cas.13494.

Vaday, G. G. *et al*. (2006). Expression of CCL5 (RANTES) and CCR5 in prostate cancer. The Prostate, 66 (2), pp.124–134. [Online]. Available at: doi:10.1002/pros.20306.

Velasco-Velázquez, M. *et al*. (2012). CCR5 antagonist blocks metastasis of basal breast cancer cells. Cancer Research, 72 (15), pp.3839–3850. [Online]. Available at: doi:10.1158/0008-5472.CAN-11-3917.

Venkatesan, S. *et al*. (2002). Reduced Cell Surface Expression of CCR5 in CCR5Δ32 Heterozygotes Is Mediated by Gene Dosage, Rather Than by Receptor Sequestration*. Journal of Biological Chemistry, 277 (3), pp.2287–2301. [Online]. Available at: doi:10.1074/jbc.M108321200.

Voeltzke, K. *et al*. (2022). EIF4EBP1 is transcriptionally upregulated by MYCN and associates with poor prognosis in neuroblastoma. Cell Death Discovery, 8 (1), pp.1–12. [Online]. Available at: doi:10.1038/s41420-022-00963-0.

Wang, L. *et al*. (2024). JAK/STAT signaling pathway affects CCR5 expression in human CD4+ T cells. Science Advances, 10 (12), p.eadl0368. [Online]. Available at: doi:10.1126/sciadv.adl0368.

Wang, Y.-W. *et al*. (2015). High expression of cAMP responsive element binding protein 1 (CREB1) is associated with metastasis, tumor stage and poor outcome in gastric cancer. *Oncotarget*, 6 (12), pp.10646–10657. [Online]. Available at: doi:10.18632/oncotarget.3392

Weber, R. *et al*. (2020). IL-6 regulates CCR5 expression and immunosuppressive capacity of MDSC in murine melanoma. Journal for ImmunoTherapy of Cancer, 8 (2), p.e000949. [Online]. Available at: doi:10.1136/jitc-2020-000949.

Wen, Z., Zhong, Z. and Darnell, J. E. (1995). Maximal activation of transcription by statl and stat3 requires both tyrosine and serine phosphorylation. Cell, 82 (2), pp.241–250. [Online]. Available at: doi:10.1016/0092-8674(95)90311-9.

Wyce, A. *et al*. (2013). Inhibition of BET bromodomain proteins as a therapeutic approach in prostate cancer. Oncotarget, 4 (12), pp.2419–2429. [Online]. Available at: doi:10.18632/oncotarget.1572.

Xiong, H. *et al*. (2012). Roles of STAT3 and ZEB1 proteins in E-cadherin down-regulation and human colorectal cancer epithelial-mesenchymal transition. The Journal of Biological Chemistry, 287 (8), pp.5819–5832. [Online]. Available at: doi:10.1074/jbc.M111.295964.

Xiong, Z. *et al*. (2024). Cancer-associated fibroblasts promote enzalutamide resistance and PD-L1 expression in prostate cancer through CCL5-CCR5 paracrine axis. iScience, 27 (5), p.109674. [Online]. Available at: doi:10.1016/j.isci.2024.109674.

Xu, M. *et al*. (2021). Role of the CCL2-CCR2 signalling axis in cancer: Mechanisms and therapeutic targeting. Cell Proliferation, 54 (10), p.e13115. [Online]. Available at: doi:10.1111/cpr.13115.

Ye, J. *et al*. (2012). Primer-BLAST: a tool to design target-specific primers for polymerase chain reaction. BMC bioinformatics, 13, p.134. [Online]. Available at: doi:10.1186/1471-2105-13-134.

Zhao, D. *et al*. (2017). Synthetic essentiality of chromatin remodelling factor CHD1 in PTEN-deficient cancer. Nature, 542 (7642), pp.484–488. [Online]. Available at: doi:10.1038/nature21357.

Zhao, J. *et al*. (1998). Chemokine receptor CCR5 functionally couples to inhibitory G proteins and undergoes desensitization. Journal of Cellular Biochemistry, 71 (1), pp.36–45. [Online]. Available at: doi:10.1002/(SICI)1097-4644(19981001)71:1<36::AID-JCB4>3.0.CO;2-2.

Zhao, R. *et al*. (2018). Endothelial cells promote metastasis of prostate cancer by enhancing autophagy. Journal of Experimental & Clinical Cancer Research : CR, 37, p.221. [Online]. Available at: doi:10.1186/s13046-018-0884-2.

Zlotnik, A. and Yoshie, O. (2000). Chemokines: A New Classification System and Their Role in Immunity. Immunity, 12 (2), pp.121–127. [Online]. Available at: doi:10.1016/S1074-7613(00)80165-X.